Department of Environmental Chemistry

Faculty of Organic Agricultural Sciences

University of Kassel

Amount, composition and turnover of organic matter in topsoils and subsoils under mature beech forest

Dissertation

Submitted to the Faculty of Organic Agricultural Sciences

of the University of Kassel

to fulfill the requirements for the degree

"Doktor der Naturwissenschaften" (Dr. rer. nat)

by

Svendja Vormstein

Witzenhausen, Mai 2017

This work has been accepted by the Faculty of Organic Agricultural Sciences of the University of Kassel as a thesis for acquiring the academic degree "Doktor der Naturwissenschaften" (Dr. rer. nat).

First Supervisor: Prof. Dr. Bernard Ludwig
Second Supervisor: Prof. Dr. Rainer Georg Jörgensen

Defense day: 12th September 2017

Preface

This thesis is submitted to the Faculty of Organic Agricultural Sciences of the University of Kassel to fulfill the requirements for the degree "Doktor der Naturwissenschaften" (Dr. rer. nat.). The work was prepared within the Research Group 1806 `The forgotten Part of Carbon Cycling: Organic Matter Storage and Turnover in Subsoils (SUBSOM)´ funded by the Deutsche Forschungsgemeinschaft (DFG). The dissertation is based on three scientific papers as first or co-author which are published in or in preparation for submission to international refereed journals. The manuscripts are included in chapters 2, 3 and 4. A general introduction of the research topic as well as the objectives of this thesis are given in Chapter 1. Chapter 5 comprises a general conclusion covering the three papers, followed by an outlook on future research needs in chapter 6.

The following papers are included in this thesis:

Chapter 2:

Vormstein, S., Kaiser, M., Piepho, H.-P., Joergensen, R.G., Ludwig, B., (2017): Effects of fine root characteristics of beech on carbon turnover in the topsoil and subsoil of a sandy Cambisol. European Journal of Soil Science, 68, 177-188.

Chapter 3:

Vormstein, S., Kaiser, M., Piepho, H.-P., Ludwig, B., (2017): Amount and composition of organic matter associated with aggregate size and density fractions in relation to depth and mineral characteristics of five different forest soils. (in preparation for submission).

Chapter 4:

Ludwig, B., Vormstein, S., Niebuhr, J., Heinze, S., Marschner, B., Vohland, M., (2017): Estimation accuracies of near infrared spectroscopy for general soil properties and enzyme activities for two forest sites along three transects. Geoderma 288, 37-46.

Table of contents

List of tables

List of figures

List of abbreviations

Al	Aluminum
$AlCl_3$	Aluminum chloride
Al_{dith}	Dithionite-soluble aluminum
Al_{ex}	Exchangeable Al
Al_{ox}	Oxalate-soluble aluminum
B/A	Numerical parameter consisting of "band A" (added heights of the absorption maxima in the "aliphatic" region) and "band B" (maximum signal height at the region for the hydrophilic C=O functional groups) of the FTIR spectra
B/A*OC	B/A ratios scaled with the OC content
C	Carbon
C_{max}	Calibrated maximum mineralizable amount of native C under the experimental conditions
C_{max1} / C_{max2}	Fast / slow calibrated maximum mineralizable amount of substrate C under the experimental conditions
C_{mic}	Microbial biomass C
Ca	Calcium
Ca_{ex}	Exchangeable Ca
$CaCl_2$	Calcium chloride
CEC	Cation exchange capacity
CO_2	Carbon dioxide
DER	Order of derivative
DFG	Deutsche Forschungsgemeinschaft
DRIFT	Diffuse reflectance infrared spectroscopy
Fe	Iron
Fe_{dith}	Dithionite-soluble iron
Fe_{ox}	Oxalate-soluble iron
flF	Free light fraction
FTIR	Fourier transform infrared
GA	Genetic algorithm
HF	Heavy Fraction
HPLC	High performance liquid chromatography
IQR	Interquartile range of laboratory results
k	Calibrated rate constant

K	Potassium
K_2SO_4	Potassium sulfate
k_{EC}, k_{EN}	Extractable portion of total C (k_{EC}) and N (k_{EN}) from the microbial biomass
LOO	Leave-one-out
Mg	Magnesium
Mg_{ex}	Exchangeable Mg
MIXED	Mixed models
MLR	Multiple linear regression
n	Number of samples
N	Nitrogen
N_{mic}	Microbial biomass N
N_{min}	Inorganic, mineralized N (sum of NO^{3-} and NH^{4+})
Na	Sodium
NaOH	Sodium hydroxide solution
NIR	Near infrared
NIRS	Near infrared spectroscopy
NH^{4+}	Ammonium
NO^{3-}	Nitrate
n.s.	Not significant
OC	Organic carbon
olF	Occluded light fraction
OM	Organic matter
P	Phosphorus
p	Probability value for significance
Pg	Petagram (10^{15} g)
PG	Polynomial degree
PLS	Partial least squares
r	Correlation coefficient
RPD	Ratio of prediction to deviation
RPIQ	Ratio of performance to inter-quartile distance
$RPIQ_{CV}$	RPIQ for cross-validation
$RPIQ_V$	RPIQ for validation
S	Sulphur
SD	Standard deviation
SECV	Standard error of cross-validation

SEP	Standard error of prediction
SOC	Soil organic carbon
SOM	Soil organic matter
t	Time
SPT	Sodium polytungstate
Vis	Visible
vis-NIRS	Visible and near infrared spectroscopy
VR	Variance ratio
VR_{CV}	VR for cross-validations
VR_{V}	VR for validation

Summary

Two-third of the terrestrial carbon (C) is stored in soils, and 70 % of the total soil organic carbon (SOC) in forest soils. Although the SOC contents in subsoil (i.e., soil compartment below the Ah/Ap horizon) are considerable lower than in topsoil, up to 63 % of the total SOC can be found in a soil depth of 30 – 100 cm and even in depths between 100 and 200 cm up to 40 % of the total SOC can be found. Based on the observed higher average age of the OC stored in subsoil compared to the OC in topsoil, subsoil OC can be considered as more stable against microbial decomposition. This leads to the assumption that subsoil provides a C sink and is of major importance in the global C cycle. However, only in the recent years the organic matter (OM) stored in subsoil received more attention. Due to differences in environmental conditions, soil mineral characteristics and OM quality between top- and subsoil, the rate of mineralization and the mechanisms of OC stabilization in subsoil cannot be deduced from topsoil. For that reason there is still a lack of knowledge, especially for forest soils, regarding the mechanisms of OC mineralization as well as stabilization in different soil depths.

The function of soil to act as a sink for CO_2 is affected by the decomposition intensity of dead fine roots, which are an important source for OC in subsoils, entering the mineral soil at different depths. The size of these organic particles is assumed to be an important factor influencing the decomposition rate. Smaller particles might be better protected against microbial decomposition by occlusion in aggregates or mineral coatings, but show also less structural resistant against microbial decomposition. These effects can influence the mineralization rates in different directions leading to contrary results in the literature. As a further factor, potentially influencing the mineralization rate of dead fine roots their distribution (e.g., homogeneously or heterogeneously) with varying contacts to the soil matrix is also discussed contradictory in literature. Some studies found no differences for the mineralization rates between homogeneously and heterogeneously distributed organic particles such as residues from roots and aboveground plant material. Other studies reported reduced mineralization rates for homogeneously distributed organic particles due to a potential greater protection through a higher particle-to-mineral surface contact or smaller mineralization rates for heterogeneously distributed OM. The potential explanations for the latter were a higher protection due to a reduced contact to the mineral soil or limited supply of nutrients. However, both OM characteristics and its distribution change with increasing soil depth. Therefore, it can be assumed that their effect on the decomposition is also changing with increasing soil depth.

Beside the substrate characteristics, soil mineral characteristics exert a great influence on OM mineralization and stabilization. Due to associations of OM with minerals or by occlusion within aggregates, OM can be protected against microbial decomposition. The capability of soils to provide such stabilization mechanisms depends on soil mineral characteristic such as the content of clay, iron and aluminum oxides or polyvalent cations. The proportion of OM which is either free and physically unprotected or occluded within aggregates to the total SOC content decreases with increasing soil depth, whereas the proportion of mineral associated OM, considered as stabilized against decomposition, increases. These organo-mineral complexes are considered as the basic units of soil aggregates, which could extend towards larger aggregates, whereas micro-aggregates (<250 μm) are more stable against disturbance like bioturbation or erosion than macro-aggregates (>250 μm). Due to changing soil mineral characteristics and a changing influence of disturbance with increasing soil depth, the type and relative importance of OM stabilization mechanisms are thought to be different between topsoil and subsoil.

Near infrared spectroscopy (vis-NIRS) could be a useful tool for the estimation of a large number of soil properties, especially for studies with large data sets (e.g., long term field experiments with regular monitoring), even if the estimation accuracies are depending on soil mineral characteristics and are less accurate than the results obtained by wet-chemical analysis. For the decomposition of OM soil enzymes are of particular importance, however, the estimation of their activities by laboratory methods is elaborate and time-consuming. Therefore, the application of vis-NIRS could be an alternative for the estimation of enzyme activities, whereby the usefulness is discussed controversially. A combination of a variable selection method, keeping only those variables that contain relevant information, with partial least-squares (GA-PLS) regression provide promising and improved estimation accuracies compared to standard procedures (e.g., PLS regression).

In the first study the effects of concentration, spatial distribution and size of fine beech roots on their rates of decomposition in topsoil and subsoil were analyzed. To determine the CO_2 emissions, a long term incubation experiment for ten different treatments (i.e. variations in size, application rate and spatial distribution of fine roots) with undisturbed (intact soil columns) and disturbed (soil sieved <2 mm) samples from topsoil and subsoil of a sandy Cambisol was conducted. At the end of the incubation experiment subsamples were taken and several soil properties (e.g., total C, microbial biomass C, nutrients) were determined. The rate of root application affected the mineralization at both soil depths, whereas the spatial distribution had an effect in all topsoil treatments but in subsoil only for the larger roots. This hints to interactions between the root characteristics influencing the mineralization

rate. Also the availability of macronutrients seems to exert control on the root decomposition because positive correlations between the contents of calcium and potassium and the microbial biomass C was found, which in turn affected the C turnover. The results of this study indicate that not only root characteristics but also the content of macronutrients has to be taken into account for the clarification of the decomposition kinetics of roots in different soil depths.

To enhance the knowledge about the influence of soil mineral characteristics on different OM stabilization mechanisms in relation to soil depth, five pedogenetically different sites under mature beech forest were sampled horizontally and analyzed within the second study. These samples were separated into four aggregate size and three density fractions which were quantified and further characterized by infrared spectroscopy. Additionally, the microbial biomass C contents and the cumulative basal respiration over the course of 14 days were determined. Independent of the soil type, the relative proportion of the OC, which can be considered as stabilized, is increasing with an increase in soil depth. Contrary to an enhanced OM stabilization also an increase in the relative proportion of the bulk SOC that was respired within two weeks with increasing soil depth was found. Therefore, it can be assumed that the OM in subsoil compared to the topsoil is stronger separated into a labile and a stable pool. This study underlined the importance of forest subsoils for the long term C stabilization independent from the soil type. Furthermore, the data point to the importance of subsoil OM to maintain the microbial activity as well as the nutrient cycle in subsoil horizons.

In the third study the estimation accuracies and the usefulness of visible near infrared spectroscopy (vis-NIRS) for general soil properties (e.g., SOC, N, pH, texture) and nine enzyme activities were determined. Therefore, soil samples of two pedogenetically different sites (i.e. sandy soil and loess soil) were taken in a regular sampling grid along three transects. The samples of two transects of each site represent the calibration sample and the samples of the third transect the independent validation sample. To determine the usefulness of vis-NIRS for the estimation of soil properties as well as enzyme activities two different chemometric methods (PLS and GA-PLS), where GA-PLS may improve the estimation accuracies, were applied on the data obtained by the absorbance spectra of each sample and compared with the results of laboratory analyses. The study confirmed the usefulness of vis-NIRS for an estimation of SOC and N contents in independent transects of a field scale, whereas the estimation accuracy of pH and texture was variable and depending on the range of measured data. However, the approach of GA-PLS markedly improved estimation accuracies of the main soil properties compared to PLS, but generally not in the validation transects. Only few enzyme activities could be estimated in independent validation, but there

was no benefit of the application of vis-NIRS for a direct estimation of their activities compared to laboratory methods.

Overall, the findings of this thesis indicate that the influence of substrate quality as well as soil mineral characteristics on C mineralization and stabilization, respectively, was more pronounced in subsoil compared to topsoil.

Zusammenfassung

Zwei Drittel des gesamten terrestrischen Kohlenstoffs ist in Böden gespeichert, wobei 70 % des im Boden gespeicherten Kohlstoffs in Waldböden zu finden ist. Obwohl die Kohlenstoffgehalte im Unterboden (d.h. unterhalb des Ah/Ap – Horizonts) deutlich geringer sind als im Oberboden, kann bis zu 63 % des gesamten Kohlenstoffvorrats in einer Bodentiefe von 30 – 100 cm gefunden werden und bis zu 40 % zwischen 100 – 200 cm. Aufgrund einer höheren durchschnittlichen Verweilzeit des Unterboden-Kohlenstoffs im Vergleich zum Oberboden-Kohlenstoff, kann der Kohlenstoff im Unterboden als stabiler gegen mikrobielle Zersetzung angesehen werden als der Kohlenstoff im Oberboden. Das führt zu der Annahme, dass Unterböden eine Kohlenstoffsenke sein können und somit von großer Bedeutung im globalen Kohlenstoffkreislauf sind. Allerdings fand die organische Substanz, die in Unterböden gespeichert ist, erst in den letzten Jahren vermehrt Beachtung. Da im Unterboden andere Umgebungsbedingungen vorherrschen als im Oberboden und sich ebenfalls die Mineraleigenschaften sowie die Eigenschaften der organischen Bodensubstanz unterscheiden, können weder die Mineralisierungsraten noch die Kohlenstoff-Stabilisierungsmechanismen vom Oberboden auf den Unterboden übertragen werden. Aus diesem Grund bestehen, besonders bei Waldböden, noch immer große Wissenslücken bei den Mechanismen, die die Kohlenstoffmineralisierung genauso wie die -stabilisierung in verschiedenen Bodentiefen steuern.

Die Fähigkeit von Böden als Senke für Kohlenstoffdioxid (CO_2) zu fungieren ist erheblich durch die Abbaurate von toten Feinwurzeln beeinflusst, die eine wichtige Kohlenstoffquelle im Unterboden darstellen und in unterschiedlichen Tiefen in den Boden eindringen. Es wird angenommen, dass die Größe dieser organischen Partikel die Abbaurate beeinflusst. Auf der einen Seite könnten kleinere Partikel durch Einschluss in Aggregate oder durch Beschichtung mit Mineralpartikeln besser gegen mikrobielle Zersetzung geschützt sein, auf der anderen Seite aber strukturell schwächer geschützt sein gegen Zersetzung als größere organische Partikel. Beide Varianten würden die Mineralisationsrate entweder positiv oder negativ beeinflussen, wobei in der Literatur gegensätzliche Ergebnisse zu finden sind. Die Verteilung der organischen Bodensubstanz, die durch unterschiedlichen Kontakt zur Bodenmatrix Einfluss auf die Mineralisierung haben könnte, wird in der Literatur ebenfalls kontrovers diskutiert. In einigen Studien zeigten sich keine Unterschiede zwischen den Mineralisierungsraten von homogen und heterogen verteilter organischer Substanz. Andere Ergebnisse zeigten, vermutlich aufgrund eines größeren Schutzes durch einen höheren Partikel-zu-Mineral-Oberflächenkontakt, eine verringerte Mineralisierungsrate von homogen

verteilten Partikeln. Wiederum andere Studien fanden geringere Mineralisierungsraten für heterogen verteilte organische Substanz. Potenzielle Begründungen hierfür lagen in einem höheren Schutz durch einen geringeren Kontakt zum Mineralboden oder aber in einer Unterversorgung mit Nährstoffen, die für mikrobielle Aktivität notwendig sind. Ein weiterer wichtiger Faktor ist die Menge an reaktiven C=O Gruppen (Carbonyl und Carboxyl) in der organischen Substanz. Diese C=O Gruppen sind für die Bildung von organisch-mineralischen Verbindungen sowie von Aggregaten und somit für die Kohlenstoffstabilisierung von großer Bedeutung. Allerdings ändern sich sowohl die Eigenschaften als auch die Verteilung von organischer Bodensubstanz mit zunehmender Bodentiefe, weshalb davon ausgegangen werden kann, dass sich auch die Einflüsse auf den Abbau der organischen Substanz ändern.

Neben den Eigenschaften der organischen Bodensubstanz haben auch die Mineraleigenschaften des Bodens einen großen Einfluss auf die Mineralisierung bzw. Stabilisierung von organischer Substanz. Durch Verbindungen zwischen Bodenmineralen und organischer Substanz oder deren Einschluss in Aggregate, kann organisches Material vor mikrobieller Zersetzung geschützt werden. Das Ausmaß der Kohlenstoffstabilisierung mittels dieser Mechanismen, hängt von den Mineraleigenschaften des Bodens, wie dem Gehalt an Ton, Eisen- und Aluminiumoxiden oder mehrwertigen Kationen, ab. Der Anteil der organischen Substanz der entweder frei und ungeschützt oder in Aggregaten eingeschlossen ist, nimmt an der Gesamtmenge des Bodenkohlenstoffs mit steigender Bodentiefe ab. Der Anteil der organischen Substanz der eine Verbindung mit Mineralien eingegangen ist und somit als stabilisiert angesehen werden kann, nimmt hingegen mit steigender Bodentiefe zu. Diese organisch-mineralischen Verbindungen dienen als Ursprung für die Bildung von Bodenaggregaten und können sich zu größeren Aggregaten weiterentwickeln, wobei Mikroaggregate (<250 µm) stabiler gegen Störung wie z.B. Bioturbation oder Erosion sind als Makroaggregate (>250 µm). Aufgrund sich ändernder Mineraleigenschaften und sich ändernder Einflüsse durch Störung mit zunehmender Bodentiefe wird angenommen, dass sich ebenfalls Art und Stellenwert der Stabilisierungsmechanismen zwischen Oberboden und Unterboden unterscheiden.

Die Nahinfrarotspektroskopie könnte ein nützliches Instrument für die Abschätzung einer großen Anzahl an Bodeneigenschaften sein, besonders für Studien mit einer großen Probenanzahl (z.B. Langzeitfeldexperimente mit regelmäßiger Kontrolle), auch wenn die Schätzgenauigkeit von den Mineraleigenschaften des Bodens abhängt und ungenauer ist als die Ergebnisse die man durch nasschemische Analysen erhält. Für die Zersetzung von organischer Substanz sind Bodenenzyme von besonderer Bedeutung, allerdings ist die

Bestimmung ihrer Aktivität mittels Labormethoden aufwändig und zeitintensiv. Daher könnte die Nahinfrarotspektroskopie eine gute Alternative zur Bestimmung der Enzymaktivitäten sein, wobei deren Eignung kontrovers diskutiert wird. Eine Kombination (GA-PLS) aus einer Methode, die nur diejenigen Variablen bei behält die relevante Informationen enthalten (GA), und der PLS (partial least-squares) Regression bietet vielversprechende Ergebnisse und verbesserte Schätzgenauigkeiten im Vergleich zu Standardverfahren (z.B. nur die PLS Regression).

In der ersten Studie wurde der Einfluss von Menge, räumlicher Verteilung und Größe von Buchenfeinwurzeln auf ihre Zersetzungsrate im Oberboden und Unterboden untersucht. Um die CO_2 Emissionen zu ermitteln wurde ein Langzeitinkubationsexperiment für zehn unterschiedliche Varianten (d.h. Unterschiede in Wurzelgröße, Menge und räumlicher Verteilung) in ungestörten (intakten Bodensäulen) und gestörten (Boden gesiebt <2 mm) Proben sowohl vom Ober- als auch vom Unterboden einer sandigen Braunerde durchgeführt. Am Ende des Inkubationsexperimentes wurden an Teilproben verschiedene Bodeneigenschaften (z.B. Gesamt-Kohlenstoffgehalt, Gehalt an mikrobiellem Kohlenstoff oder Nährstoffen) bestimmt. Die Menge der Wurzelzugabe beeinflusste die Mineralisierung in beiden Bodentiefen, wohingegen die räumliche Verteilung einen Einfluss in allen Oberbodenvarianten hatte, im Unterboden allerdings nur auf die Varianten mit großen Wurzeln. Das deutet darauf hin, dass Interaktionen zwischen den einzelnen Wurzeleigenschaften die Mineralisierung beeinflussen. Da positive Korrelationen zwischen der mikrobiellen Biomasse, die den Kohlenstoffumsatz beeinflusst, und den Gehalten an Calcium und Kalium gefunden wurden, muss auch die Verfügbarkeit von Makronährstoffen berücksichtigt werden. Die Ergebnisse dieser Studie deuten darauf hin, dass nicht nur die Wurzeleigenschaften sondern auch die Menge an Makronährstoffen bei der Aufklärung der Zersetzungskinetik in verschiedenen Bodentiefen berücksichtigt werden müssen.

Um einen größeren Einblick über den Einfluss der Mineraleigenschaften des Bodens auf verschiedene Kohlenstoff-Stabilisierungsmechanismen in Bezug auf die Bodentiefe zu erhalten, wurden in der zweiten Studie fünf pedogenetisch unterschiedliche Standorte unter voll entwickeltem Buchenwald horizontweise beprobt. Diese Proben wurden in vier Aggregat- und drei Dichtefraktionen aufgetrennt, welche anschließend quantifiziert und mittels Infrarotspektroskopie charakterisiert wurden. Zusätzlich wurde der Gehalt an mikrobiellem Kohlenstoff sowie die kumulative Basalatmung mittels eines zweiwöchigen Inkubationsexperiments ermittelt. Unabhängig vom Bodentyp nahm der relative Anteil des organischen Kohlenstoffs, der als stabilisiert angesehen werden kann, mit zunehmender Bodentiefe zu. Dabei scheinen Aluminiumoxide für die Stabilisierung von organischer

Substanz von zunehmender Bedeutung zu sein. Des Weiteren offenbaren die Infrarotanalysen eine höhere Menge an C=O Gruppen innerhalb der organischen Substanz in der schweren Fraktion (assoziiert mit der Mineralphase) im Vergleich zu der organischen Substanz innerhalb der anderen Fraktionen. Zudem nahm der Gehalt von C=O Gruppen mit zunehmender Bodentiefe zu. Das deutet darauf hin, dass das organische Material innerhalb der schweren Fraktion und mit zunehmender Bodentiefe mikrobiell stärker zersetzt ist. Im Gegensatz zu der erhöhten Stabilisierung mit zunehmender Bodentiefe wurde auch ein Anstieg des relativen Anteils des gesamten organischen Kohlenstoffs des Bodens, der innerhalb von 14 Tagen veratmet wurde, mit zunehmender Bodentiefe gefunden. Daher kann angenommen werden, dass die organische Substanz im Unterboden im Vergleich zum Oberboden stärker in einen labilen und einen stabilen Pool unterteilt ist. Diese Studie verdeutlicht die Bedeutung von Waldunterböden für die langfristige Kohlenstoffspeicherung, unabhängig von Bodentyp und somit von Bodeneigenschaften. Darüber hinaus deuten die Daten auf die Bedeutung des Unterboden-Kohlenstoffs zur Aufrechterhaltung der mikrobiellen Aktivität sowie des Nährstoffkreislaufs in den Unterbodenhorizonten hin.

In der dritten Studie wurden die Schätzgenauigkeiten und die Eignung der Nahinfrarotspektroskopie zur Bestimmung allgemeiner Bodeneigenschaften (z.B. Kohlenstoff- und Stickstoffgehalt, pH, Textur) und neun Enzymaktivitäten untersucht. Dafür wurden zwei pedogenetisch unterschiedliche Standorte (ein sandiger und ein Löss-Standort) mittels eines gleichmäßigen Beprobungsrasters entlang dreier Transekte beprobt. Die Proben zweier Transekte jedes Standortes stellen den Kalibrierungs-Probensatz dar und die Proben des jeweils dritten Transektes den unabhängigen Validierungs-Probensatz. Um die Eignung der Nahinfrarotspektroskopie für die Abschätzung von Bodeneigenschaften sowie von Enzymaktivitäten zu ermitteln, wurden zur Auswertung zwei verschiedene chemometrische Methoden (PLS und GA-PLS) auf die Daten, die durch die Spektren jeder Probe erhalten wurden, angewendet und mit den Ergebnissen der Laboranalysen verglichen. Hierbei könnte die GA-PLS die Schätzgenauigkeiten verbessern. Die Ergebnisse dieser Studie bestätigen die Eignung der Nahinfrarotspektroskopie für die Abschätzung des Kohlenstoff- und Stickstoffgehaltes in unabhängigen Transekten auf Feldebene, wohingegen die Schätzgenauigkeiten von pH und Textur variabel und abhängig von der Bandbreite der gemessenen Daten waren. Allerdings verbesserte die Herangehensweise mittels GA-PLS im Vergleich zur PLS die Schätzgenauigkeiten der allgemeinen Bodeneigenschaften deutlich, aber im Allgemeinen nicht in den Validierungstransekten. Nur wenige Enzymaktivitäten konnten in der unabhängigen Validierung abgeschätzt werden. Zudem gab es keinen Vorteil

bei der Anwendung der Nahinfrarotspektroskopie für eine direkte Abschätzung ihrer Aktivitäten im Vergleich zu Labormethoden.

Insgesamt deuten die Ergebnisse dieser Arbeit auf einen größeren Einfluss der Substrateigenschaften sowie Bodeneigenschaften im Unterboden im Vergleich zum Oberboden sowohl auf die Kohlenstoffmineralisierung als auch auf die Kohlenstoffstabilisierung hin.

1   General Introduction

1.1   SOC in subsoil

The global soil organic carbon (SOC) stock (2000 Pg) preserves nearly two-third of the terrestrial C and is thus the largest and most important terrestrial pool of organic carbon (OC) in the global C cycle (Janzen, 2004; Batjes, 1996). Forest soils are of large importance as they comprise approximately 70 % of the global SOC (Vancampenhout et al., 2012). Despite considerably lower SOC contents in subsoil (i.e., soil compartment below the A horizon) compared to topsoil, between 30 and 63 % of the total SOC is stored within a soil depth of 30 – 100 cm and up to 40 % of the total SOC can be found in a depth of 100 – 200 cm (Angst et al., 2016; Batjes, 1996). Thus, subsoil horizons provide a large reservoir for the SOC storage, which is still considerably larger than other terrestrial C-pools (e.g., biomass and atmosphere) (Janzen et al., 2004; Jobbágy and Jackson, 2000) and can either be source or sink for CO_2 (Rumpel and Kögel-Knabner, 2011; Rumpel et al., 2004), which is of increasing interest regarding the discussion of climate change. Several studies have shown that the radiocarbon age of SOC is increasing with increasing soil depth, indicating that OC in subsoil is more stable against degradation and has therefore a higher residence time than topsoil OC (e.g., Rumpel and Kögel-Knabner, 2011; Eusterhues et al., 2003; Rumpel et al., 2002). This leads to the assumption that subsoil provides a C sink and is hence of large importance regarding the climate change concerns.

The environmental conditions (e.g., soil temperature, soil moisture, nutrient availability), soil characteristics (e.g., texture, Fe- and Al-oxides, content of polyvalent cations) as well as OM quality (e.g., size, distribution, composition) influencing the carbon mineralization and stabilization mechanisms differ widely between topsoil and subsoil (e.g., Rumpel and Kögel-Knabner, 2011; Rasse et al., 2006; Rumpel et al., 2004). Hence, the dynamics of OC in subsoil horizons cannot be deduced from that in the topsoil. While the composition and the mechanisms of mineralization and stabilization of soil OM have been well investigated and evaluated for topsoils, these information are limited for subsoils (Rumpel and Kögel-Knabner, 2011; Sanaullah et al., 2011) and especially scarce for forest subsoils (Vancampenhout et al., 2012).

1.2   Factors controlling carbon stabilization in soil

1.2.1   Organic matter quality and distribution

The ability of forest soils to store organic C and to act as a sink for CO_2 is affected by the decomposition intensity of plant fine roots (diameter <2 mm) entering the mineral soil at

different depths. Dead fine roots are assumed to be an important source for the organic C stored in subsoils (Rasse et al., 2005). Factors that generally affect the rates of microbial decomposition of OM are environmental conditions and the OM quality as well as its distribution (Prieto et al., 2016; Solly et al., 2014; Giacomini et al., 2007; Rasse et al., 2005). Since the environmental conditions change with increasing soil depth they presumably become less favorable for the microbial decomposition (e.g., Santos et al., 2016). OM quality and distribution also changes with increasing soil depth (Rasse et al., 2006). Thus the factors controlling the decomposition of OM in subsoil are very different from those in topsoil (e.g., Rumpel and Kögel-Knabner, 2011; von Lützow et al., 2006; Rumpel et al., 2004).

The particle size of the OM is considered as an important factor influencing the decomposition rate. Smaller particles might be more capable to associate to organo-mineral complexes or for occlusion within aggregates and could thus be better protected against microbial decomposition (e.g., Rovira and Vallejo, 2002) resulting in a decreased mineralization rate. On the other hand smaller particles are assumed to provide less structural resistance against microbial decomposition than larger and more intact ones (Loecke and Robertson, 2009; Rovira and Vallejo, 2002), which could lead to an enhanced mineralization. Furthermore, it is assumed that an altering size of the residues might change their chemical composition (e.g., C/N ratio). Additionally, soil type and pedological processes has to be considered because of their influence on the chemical composition of SOM (Rumpel and Kögel-Knabner, 2011; Rumpel et al., 2002).

Organic matter in subsoil horizons is distributed more heterogeneously than in topsoil (e.g. Rumpel and Kögel-Knabner , 2011; Salomé et al., 2010; Chabbi et al., 2009). In several studies the effect of the OM distribution in soil was investigated, however, the results were contrary. Breland (1994) reported a reduced rate of decomposition for a homogenized distribution compared to a localized application and attributed the results to a greater particle-to-mineral surface contact with thus a higher protection against microbial decomposition. Contrary, Loecke and Robertson (2009) as well as Magid et al., (2006) found no differences between homogeneously and heterogeneously distributed residues or smaller mineralization rates for the heterogeneously than for the homogeneously distributed residues. A less protection by minerals of homogeneously distributed residues or a larger demand and limited supply of nutrients required to maintain the microbial activity in the localized treatments were potential explanations.

1.2.2 *Soil mineral characteristic*

The association of OM with mineral compounds and the occlusion within aggregates leading to a reduced access for microorganisms were shown to be important factors for the preservation of OC in soil (Schmidt et al., 2011; Kögel-Knabner et al., 2008; von Lützow et al., 2008). The capability of soils to protect OM against biological decomposition by the formation of organo-mineral associations depends on soil mineral characteristics such as content of reactive Fe- and Al-oxides, polyvalent cations, and layer silicates (Mikutta et al., 2006; Eusterhues et al., 2005; Baldock and Skjemstat, 2000), which in turn are mainly affected by the soil type and soil horizon specific processes. To assess the interaction between OM and the mineral phase, schemes of density fractionation offer a useful tool (Cerli et al., 2012; John et al., 2005). These procedures separate the bulk soil OM into the free light fraction (flF), the aggregate occluded light fraction (olF), and the mineral-associated OM (heavy fraction: HF) (Schrumpf et al., 2013; Cerli et al., 2012; Schrumpf et al., 2011). The OM associated with the olF is more degraded, smaller in size and, better protected against microbial decomposition by occlusion in aggregates, than the physically unprotected flF (Schrumpf et al., 2013; Cerli et al., 2012; Wagai et al., 2009). The proportions of both light fractions to the bulk soil OC declines with increasing soil depth (Angst et al., 2016; Kögel-Knabner et al., 2008), whereas the proportion of the C associated with the HF, considered as stabilized against microbial decomposition, increases with soil depth (Schrumpf et al., 2013). Organo-mineral complexes are considered to act as basic units for the formation of soil aggregates (Lehmann et al., 2007; Christensen, 2001), which could extend towards larger aggregates, depending on the availability of organic (e.g., microbial and plant debris, fungal hyphae, roots) and inorganic (oxides, cations) binding agents (Tisdall and Oades, 1982). Through disturbance (e.g., bioturbation, rain-drop impact, erosion) aggregates can be destroyed which leads to an enhanced microbial decomposition, resulting in an elevated release of CO_2 (e.g., Smith et al., 2016; Grave et al., 2015). However, micro-aggregates (<250 µm) are more stable than macro-aggregates (>250 µm) and thus the OM associated to smaller aggregates is more stabilized against microbial decomposition (Cambardella and Elliott, 1993; Tisdall and Oades, 1982). An additional separation of water-stable aggregate size fractions by a wet-sieving procedure from soil provides further information about the relevance of aggregate formation at different scales for the OM storage and stabilization. Both soil mineral characteristics and the influence of disturbance change with increasing soil depth. This leads to the assumption that type and relative importance of these OM stabilization mechanisms are different between top- and subsoils.

1.3 Near infrared spectroscopy – estimation accuracies of soil properties and enzyme activities

For the estimation of a large number of physical (e.g., particle size, aggregation, soil water), chemical (e.g., soil organic C (SOC), OM, macro- and micronutrients, pH) and biological (e.g., microbial biomass, respiration, enzymatic activities, microbial groups) soil properties, the application of visible and near infrared spectroscopy (vis-NIRS) (range: 800 – 2500 nm for near infrared (NIR) and 400 – 2500 nm for visible and NIR (vis-NIR)) has been suggested to be a useful tool (Soriano-Disla et al., 2014). Although the accuracies of vis-NIR estimations are less accurate compared to results obtained by wet-chemical analysis, vis-NIRS may still be sufficient and even important for many research goals, especially for studies requiring a high sample number, such as long-term field experiments with a regular monitoring of soil properties. However, vis-NIRS is not be reliable for the estimations of soil properties in sandy soils, due to comparably featureless spectra of sand fractions in combination with a high reflectance, a relatively small total surface area of sand particles, and possible nonlinear effects resulting from unproportionally high absorbance by the dark OM (Stenberg, 2010). Therefore, soil properties for the entire range of soil texture could not be estimated by vis-NIRS satisfactorily.

Soil enzymes are very important for OM decomposition and nutrient cycling (Bandick and Dick, 1999; Dick, 1994), but the laboratory-based determination of their activities is elaborate and time-consuming. Thus, an estimation of enzyme activities by the application of vis-NIRS could be beneficial, provided that specific spectral effects exist for different enzymes. However, the usefulness of vis-NIRS for the estimation of enzyme activities is discussed controversially. Several studies (e.g., Soriano-Disla et al., 2014; Dick et al., 2013; Zornoza et al., 2008) summarized that vis-NIRS is a useful tool for the estimation of biological properties also including enzyme activities. Standard procedures for vis-NIR estimations are multiple linear regressions using distinct wavelengths (related to C\\H, C\\O and N\\H vibrations) and full spectrum partial least-squares (PLS) regression. However, recent studies (Shi et al., 2014; Vohland and Emmerling, 2011) showed promising results and improved estimation accuracies after the application of a PLS regression combined with a variable selection procedures, keeping only those variables that contain relevant information, such as a genetic algorithm (GA).

1.4 Objectives

The detailed understanding of factors and mechanisms controlling the C dynamics in subsoil is important for terrestrial ecosystem services such as mitigation of climate change. Summarizing the information above, especially the current knowledge about the mineralization and stabilization processes of OM in forest subsoil is scarce. Therefore, this thesis focuses on a better understanding of the decomposition of dead fine roots serving as an important subsoil C source and the mechanisms controlling the OM storage as a function of soil mineral characteristics and soil depth. Furthermore, the estimation accuracies of vis-NIRS for general soil properties and enzyme activities were clarified for two different procedures.

1.4.1 Objectives of the first study: Investigation of the effects of concentration, distribution, and size of fine beech roots on their rate of decomposition

A long-term incubation experiment with disturbed and undisturbed samples from topsoil and subsoil and different fine beech root characteristics was carried out to determine the CO_2 emission rates from soil (Figure 1.1). At the end of the incubation experiment soil samples, representative for the different treatments, were analyzed for total C and N, microbial biomass C and N, ergosterol, macronutrients and mineral N. Additionally, correlation analyses provided the opportunity to detect effects of the above mentioned factors on the root decomposition. This study aimed to elucidate the effects of (i) concentration, (ii) size and (iii) distribution on the decomposition of fine beech roots in subsoil compared to topsoil.

Root size	1-2 cm		<2 mm	
Root amount (dry mass)	2 g kg^{-1}	8 g kg^{-1}	2 g kg^{-1}	8 g kg^{-1}
Disturbance ↓ Root distribution	Minimal ↓	Maximal ↓	Minimal ↓	Maximal ↓
	Localized	Homogeneous	Localized	Homogeneous

Figure 1.1: Factorial design of the treatments incubated in the first study.

1.4.2 Objectives of the second study: Investigation of the influence of soil mineral characteristics on organic matter associated with aggregate size and density fractions

Soil samples (Figure 1.2) were taken horizon specific from five pedogenetic different sites under mature beech forest. All samples were fractionated into four aggregate size and three density fractions, which are indicative for different degrees of OM stabilization. These fractions were quantified and then characterized by FTIR spectroscopy, providing additional information about the amount of functional groups, which are involved in the formation of organo-mineral associations and aggregates. Additionally, several soil characteristics (e.g., contents of Fe- and Al-oxides, polyvalent cations, microbial biomass C) and the cumulative basal respiration over the course of 14 days were determined. The objectives of this study were (i) to analyze the relative importance of the formation of orgnano-mineral associations and aggregates for SOM stabilization against microbial decomposition in relation to soil depth and type and (ii) to clarify the influence of soil mineral characteristics on the amount and composition of OM associated to the different fractions.

Figure 1.2: Overview of the different soil samples used in the second study.

1.4.3 Objectives of the third study: Determination of the estimation accuracies of near infrared spectroscopy for general soil properties and enzyme activities

Soil samples of two sites, different in soil mineral characteristics, were taken in a regular sampling grid along three transects, each starting in close distance to a beech tree (Figure 1.3). Main soil properties (e.g., texture, pH, contents of SOC and N) and several enzyme activities were determined and absorbance spectra in the vis-NIR range were recorded for each soil sample. On the data two different chemometric methods, a standard

procedure (PLS regression) and an optimised method (GA-PLS regression), were applied. The aim of this study was (i) to determine the estimation accuracies of vis-NIRS for soil properties as well as enzyme activities with PLS and GA-PLS for both above mentioned sites and (ii) to clarify if the spectral predictions of the enzyme activities are based on specific spectral effects features being strong enough to markedly impact the measured vis-NIR signals or on correlations with spectrally sensitive soil properties.
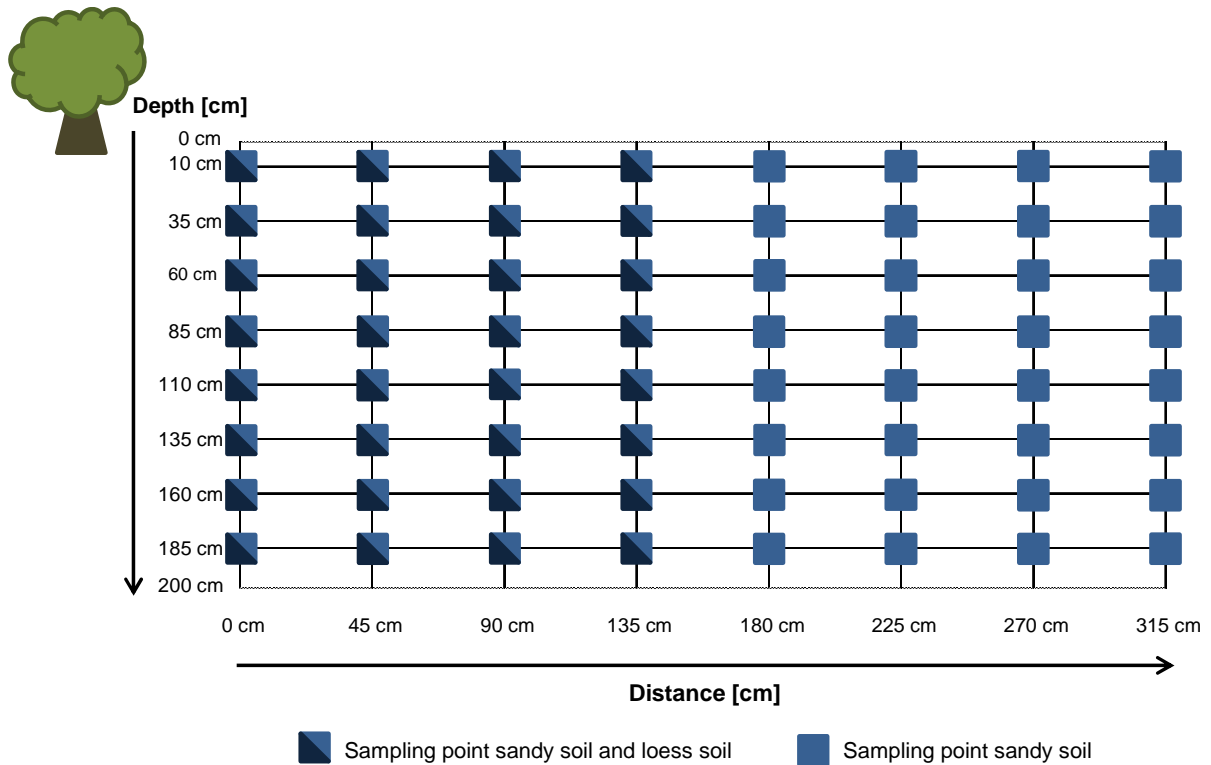
Figure 1.3: Scheme of the grid sampling design applied to three transects at the study sites for the third study.

2 Effects of fine root characteristics of beech on carbon turnover in the topsoil and subsoil of a sandy Cambisol

Svendja Vormstein[a], Michael Kaiser[a*], Hans-Peter Piepho[b], Rainer Georg Joergensen[c], Bernard Ludwig[a]

[a] *Department of Environmental Chemistry, University of Kassel, Nordbahnhofstr. 1a, 37213, Witzenhausen, Germany*

[b] *Biostatistics Unit, Institute of Crop Science, University of Hohenheim, Fruwirthstr. 23, 70599, Stuttgart, Germany*

[c] *Department of Soil Biology and Plant Nutrition, University of Kassel, Nordbahnhofstr. 1a, 37213, Witzenhausen, Germany*

* Correspondence: M. Kaiser, E-mail: michael.kaiser@uni-kassel.de

2.1 Summary

Fine roots that enter mineral soil at different depths are a major source of organic carbon stored in forest soil. Little is known about the key factors that govern the mineralization kinetics of fine roots in topsoil compared with subsoil. Therefore, we analysed the effects of concentration, spatial distribution and size of fine beech roots on their rates of decomposition in the topsoil and subsoil of a sandy Cambisol. Undisturbed (intact soil columns) and disturbed (soil sieved <2 mm) samples from the topsoil (2 – 10 cm) and subsoil (145 – 153 cm) were incubated for 365 days to determine the carbon dioxide emissions. The treatments included applications of fine roots that varied in size (length: <2 mm and 1 – 2 cm), different rates of application (2 and 8 g kg^{-1}) and spatial distribution (homogeneous and locally concentrated, i.e. localized). The mineralization was affected significantly at both depths by the rate of application (large rate > small rate) and in the topsoil by distribution (localized > homogeneous). The spatial distribution of large roots, but not smaller ones, affected rates of emission in subsoil but not in topsoil. Correlation analyses suggest an effect of the calcium and potassium supply on the microbial biomass and on the turnover of roots if these are locally concentrated. The data of this study suggest that in sandy soil the availability of macronutrients has to be considered complementary to root characteristics such as concentration, size and distribution to elucidate their decomposition kinetics throughout the soil profile.

2.2 Highlights

- Analysis of effects of characteristics of fine beech roots on organic matter decomposition in top- and subsoil.

- The rate of decomposition in the topsoil was larger if the fine roots were locally concentrated.

- The rate of mineralization of fine beech roots in the subsoil increased with increasing root size.

- Soil microbial biomass carbon is affected by the supply of calcium and potassium if the fine beech roots are locally concentrated.

2.3 Introduction

The global soil organic carbon (SOC) stock is about 1.6 times larger than the amount stored in biomass and the atmosphere (Janzen, 2004). Forest soil is of particular importance; it contributes about 70 % of global SOC storage (Vancampenhout et al., 2012), which includes the topsoil and the subsoil (i.e. below 30 cm soil depth). Batjes (1996) reported for a global soil dataset that within the first 100 cm, 30 – 63 % of the SOC is stored below a depth of 30 cm.

It is known that the ability of forest soil to store organic C and act as a sink for CO_2 is affected by the rate of decomposition of fine roots (diameter <2 mm) that enter the mineral soil at different depths. The factors that control this process, however, are less well understood (Rumpel and Kögel-Knabner, 2011). Factors that generally affect the rates of microbial decomposition of fine roots are soil moisture, soil temperature and nutrient content together with the quality of root litter (e.g., C/N ratio, nutrient concentration) (Prieto et al., 2016; Solly et al., 2014). The decomposition of fine roots was also shown to be affected by the fine-root order (McCormack et al., 2015). It is assumed that with increasing soil depth, the environmental conditions for the microbial decomposition of fine roots in terms of oxygen and nutrient supply become less favourable (e.g., Santos et al., 2016). Despite the general agreement about the importance of root-derived C for the SOC of subsoil (Rasse et al., 2005), effects of the characteristics of fine roots on decomposition in the subsoil compared with the topsoil are, however, poorly understood, especially for trees.

Hertel et al. (2013) found fine root necromasses at 12 sites in beech forest stands of about 200 – 800 g m^{-2} at 0 – 30 cm soil depth, which corresponds to a concentration between about 0.56 and 2.2 g fine roots per kg soil assuming a bulk soil density of 1.2 g cm^{-3}. Leuschner and Hertel (2003) reported on data for 14 beech forest stands that

suggest a maximum concentration of about 6 g fine roots per kg^{-1} soil at 0 – 40 cm depth. To account for potentially larger concentrations in the uppermost topsoil (0 – 10 cm) and in localized concentrations, we included in our analyses a maximum application rate of 8 g fine roots per kg soil for comparison with an application rate of 2 g kg^{-1}. To compare top- and subsoil organic matter (OM) dynamics we applied the same rates of fine roots to samples from both sampling depths.

The size (i.e. length) of root- or litter-derived residues has an important effect on decomposition rates because smaller particles are assumed to provide less structural resistance (i.e. larger surface to mass ratio) to microbial degradation than larger and more intact ones. On the other hand, smaller particles might be protected better than larger ones by occlusion in aggregates or mineral coatings (e.g., Rovira and Vallejo, 2002). Furthermore, the composition (e.g., C/N ratio) might change with the size of residues, which in turn should affect decomposition processes, especially in the short term (i.e. <10 years). The size effect, however, seems also to depend on the magnitude of differences in the root size because Toenshoff et al. (2014) did not observe an effect for residues from poplar roots in a silty loamy soil that were <1 and 1 – 5 mm in size. Vestergaard et al. (2001) reported similar results by analyzing the decomposition of residues of <2 and 4 – 5 mm from maize (*Zea mays* L.) leaves and barley (*Hordeum vulgare* L.) straw in a sandy loam soil. Furthermore, the effect of size on plant residue decomposition can be transient and change over time, as Iqbal et al. (2014) showed in an incubation experiment over 301 days. To test for the effect of size, we analyzed a wider range in size (i.e. length) than that analyzed by Vestergaard et al. (2001) and Toenshoff et al. (2014) and compared roots of <2 mm with those of 1 – 2 cm. Our incubation experiment over 365 days was adapted from Iqbal et al. (2014) to account for potential changes in the decomposition dynamics over the course of 1 year.

The interrelated destruction of the soil structure, aggregates and pore network because of disturbances from, for example, land-use change, rain-drop impact and erosion, wind throw, clear cut deforestation or bioturbation affects the decomposition of OM in soil. Such destructive events cause a flush of CO_2 release from enhanced microbial decomposition of the soil OM (e.g., Smith et al., 2016; Grave et al., 2015). This accelerated microbial decay is explained by, among other factors, the destruction of soil aggregates that provide different degrees of protection, but also by an increase in the contact between OM and microorganisms with intense mixing. The intensity of disturbances can be expected to decrease with increasing soil depth, which might contribute to greater stabilization of OM in the subsoil than topsoil (e.g., Mathieu et al., 2015). However, the effect of disturbance on decomposition dynamicsi in the subsoil is scarcely investigated compared with the topsoil. To

mimic disturbance, we sieved the soil to <2 mm, which destroys macro-aggregates, and distributed the added fine roots homogeneously to reduce the possibility of spatial disconnection between the decomposer community and substrate.

A homogeneous distribution of residues from white clover (*Trifolium repens* L.) in a loamy soil reduced the rate of decomposition more than with localized application in litterbags (Breland, 1994). This was attributed to the greater shoot particle-to-mineral surface contact and protection against microbial decay with a homogeneous distribution of residues. Other studies, however, have reported rates of decomposition for plant residues from clover (*Trifolium pretense* L.), maize (*Zea mays* L.) and rape (*Brassica napus* L.) applied to the soil in locally concentrated layers and patches that are similar to or smaller than those for homogeneously distributed material (Loecke and Robertson, 2009; Magid et al., 2006). Potential explanations for the contrasting results were that there was less protection of homogeneously distributed residues by minerals because of the large sand content in the soil analyzed (Loecke and Robertson, 2009) or there was a larger demand and limited supply of nutrients required to maintain the microbial activity in the localized treatments (Magid et al., 2006).

To the best of our knowledge, studies to elucidate the effects of (i) concentration, (ii) size and (iii) distribution or disturbance or both on the decomposition of tree roots at different soil depths are absent. Therefore, we analyzed the effects of these factors on the decomposition of fine beech roots in both sandy top- and subsoil. We hypothesized that the rate of decomposition of fine beech roots would increase with a decrease in root size (<2 mm and 1 – 2 cm) because of less structural resistance, and that decomposition would be greater for localized rather than for homogeneously distributed roots because of less particle-to-mineral surface contact. We also expected generally larger rates of root decomposition in the topsoil than subsoil because of more favourable conditions for the decomposer community.

2.4 Materials and methods

2.4.1 Study site and sampling

The study site (Grinderwald, 52°34′22″N 9°18′51″E) is 40 km northwest of Hannover in Lower Saxony (Germany) in a beech forest established in 1916 in the form of a plantation after clear cutting. The mean annual precipitation is 718 mm and the mean annual temperature is 8.7°C (http://www.worldclim.org/download). The soil type is a Dystric Cambisol (IUSS, 2006) developed from fluvial and aeolian sandy deposits from the Saale glacial period (347 000 to 128 000 years before present). The bulk densities are 1.4 g cm^{-3} in

the topsoil (2 – 10 cm) and 1.6 g cm^{-3} in the subsoil (145 – 153 cm). The particle-size distribution of the topsoil was 69.5 % (±2.2 %) sand, 27.2 % (±2.1 %) silt and 3.3 % (±0.2 %) clay, and that of the subsoil was 95.4 % (±1.1 %) sand, 3.2 % (±1.2 %) silt and 1.4 % (±0.3 %) clay (numbers in parentheses are standard errors). The pH of the topsoil was 3.4 (±0.03) and the pH of the subsoil was 4.3 (±0.01).

Three soil pits were excavated in September 2013 and five undisturbed soil cores were taken from each pit, from 2 – 10 cm and 145 – 153 cm depths, by inserting Plexiglas columns with an inner diameter of 15 cm and a height of 12.5 cm into the soil. Afterwards, the columns were dug out with a spade and any protruding soil and root materials were carefully removed with a sharp blade. Composite soil samples were also taken from both soil depths of each soil pit, then thoroughly mixed for each pit and soil depth separately and sieved to <2 mm. The soil cores and samples were kept in a climate chamber at 10°C until the start of the incubation experiment in January 2014.

Fine roots with a diameter <2 mm were sampled from the tangle of beech roots below the litter horizon that were removed when the soil pits were excavated. Root samples from each soil pit were mixed to obtain one composite sample. The fine roots were washed and freed from mineral and non-root-derived organic material. After drying at 40°C, all roots were cut with scissors into pieces of 1 – 2 cm length. A subsample of the 1 – 2 cm roots was chopped with a cutting mill into pieces of <2 mm length. The fine roots contained 51.8 % C and 1 % N determined by dry combustion (Elementar Vario El, Hanau, Germany).

2.4.2 Factorial design

To analyze the effect of the spatial distribution and accessibility of roots together with their concentration and size on the C turnover in topsoil compared with subsoil, an incubation experiment was carried out for 10 different treatments for the soil samples taken from 2 – 10 cm and 145 – 153 cm depths.

The treatments were:

- two control treatments per soil depth (minimally and maximally disturbed soil samples without addition of roots),

- four treatments with additions of 2 g roots kg^{-1} soil per soil depth [addition of roots of <2 mm or 1 – 2 cm to minimally disturbed soil (i.e. soil columns and localized roots) or maximally disturbed soil (i.e. after mixing and sieving the soil and a homogeneous distribution of roots)], and

- four treatments with additions of 8 g roots kg^{-1} soil per soil depth (again, root sizes were <2 mm or 1 – 2 cm and soil disturbance was minimal or maximal).

Each treatment was carried out with soil from each pit, thus we had three field replicates per soil depth. An exception was the subsoil treatment with maximally disturbed soil and an application of 2 g kg^{-1} roots of 1 – 2 cm, which could be evaluated with n = 2 only because of technical problems in the incubation experiment for one column that impeded the evaluation of CO_2 data from that column.

2.4.3 *Preparation of minimally and maximally disturbed soil columns*

To enable incorporation of the roots into the minimally disturbed, intact soil columns in a similar spatial pattern, a circular template of card with a diameter of 15 cm was placed on the top of the soil surface in the column. The template had five positions marked (i.e. holes with a diameter of 2.5 cm); one was in the middle of the template and the others were at right angles to each other and had a distance of 5 cm from their centres to the centre of the hole in the middle. Stainless steel cylinders (length 10 cm, inner diameter 2.5 cm) were driven into the sample at the predefined, marked holes and the soil material within each cylinder was removed with a spatula. Subsequently, the cylinders were removed and all the soil removed was homogenized to produce one sample. From this sample, 75 % of the soil was mixed with roots of 1 – 2 cm or <2 mm length for the treatments with 2 g roots kg^{-1} soil. The amount of roots required was based on the mass of soil in the core. For the 8 g roots kg^{-1}, 50 % of the soil removed was mixed with the required amount of roots. The soil and root mixture was subdivided into five equal aliquots, which were placed into the empty holes in the soil column under slight pressure to create the domain of locally concentrated roots. The remaining space between the surface of the surrounding soil and that of the re-filled soil and root mixture was levelled with soil material. The control treatments (without any addition of roots) were treated in the same way, except that the soil removed was totally refilled after homogenization.

The same type of Plexiglas columns used for sampling the minimally disturbed soil were filled with the same mass of homogenized and sieved soil material as for the undisturbed soil columns to prepare the maximally disturbed samples. The disturbed soil material (<2 mm) was mixed thoroughly with roots of 1 – 2 cm and <2 mm length at concentrations of 2 and 8 g root kg^{-1} soil, respectively, for 90 minutes in an overhead shaker. The mixture was gradually placed into the columns under slight pressure with a Styrofoam plate. After the filling was completed, the soil was compressed slightly. For the control treatments, homogenized and sieved soil material was placed into the columns and compressed without the addition of roots.

2.4.4 Incubation experiment

The soil in all columns was adjusted to 50 % of the water-holding capacity with deionized water. The microcosms used for the incubation experiment consisted of columns containing soil, Plexiglas lids and ceramic plates at the bottom. Two plug valves were embedded in the lid to enable the microcosms to be connected by flexible tubes to a gas chromatograph. The microcosms were airtight after being sealed and were incubated at 10°C for 1 year. The headspaces (4.5 cm distance between soil and lid) of the microcosms were flushed continuously with fresh air at a rate of $4 - 15$ ml minute^{-1} and the gas samples were obtained by an automatic sampling system and analyzed with the gas chromatograph (Shimadzu Gas Chromatograph GC-14A, Duisburg, Germany) for their CO_2 concentration every 6 hours. Water content was monitored by weighing the cylinders regularly and balanced, if necessary, by the addition of deionized water to maintain constant water content. Cumulative CO_2 emissions are shown in Figures 2.1 and 2.2. Emissions in each microcosm are likely to be correlated with one another and the errors are unlikely to be independent.

2.4.5 Soil analyses

At the end of the incubation experiment, the minimally and maximally disturbed soil columns were sampled with stainless steel cylinders at the five sampling points used to apply the roots to the minimally disturbed columns. In addition, for the minimally disturbed samples, undisturbed soil from around the localized material was sampled. This sampling design resulted in three categories of samples: (i) homogenized bulk soil material from the maximally disturbed columns (homogenized), (ii) undisturbed bulk soil from the minimally disturbed columns around the hot spots (surrounding) and (iii) the locally concentrated material incorporated into the undisturbed columns at the beginning of the incubation (localized). The homogenized, surrounding and localized materials from the five sampling points were mixed separately for each column into one sample that was used to determine chemical, physical and biological soil characteristics.

The pH of all samples (i.e. homogenized, surrounding and localized) was measured after the incubation with a glass electrode (pH electrode BlueLine 14 pH, Schott Instruments, Mainz, Germany) in 0.01 m $CaCl_2$ (25 ml $CaCl_2$ to 10 g soil). Particle-size distribution was determined on bulk soil samples from the controls of the homogenized and minimally disturbed columns by wet sieving and the pipette method. Total C and N concentrations of all samples were determined after the incubation by dry combustion (Elementar Vario El, Hanau, Germany); total soil C represents the SOC because carbonates were absent.

Microbial biomass C and N concentrations of all samples were determined after the incubation by the chloroform-fumigation extraction method (Brookes et al., 1985; Vance et al., 1987). Microbial biomass C was calculated as EC / k_{EC}, where EC = (organic C extracted from fumigated soils) - (organic C extracted from non-fumigated soils) and k_{EC} = 0.45 (Wu et al., 1990). Microbial biomass N was calculated as EN / k_{EN}, where EN = (total N extracted from fumigated soils) - (total N extracted from non-fumigated soils) and k_{EN} = 0.54 (Brookes et al., 1985; Joergensen and Mueller, 1996). The fungal cell-membrane component ergosterol was extracted with 100 ml ethanol from 2 g of each sample after the incubation (Djajakirana et al., 1996). Ergosterol was determined by reversed-phase HPLC (high performance liquid chromatography, column: Spherisorb ODS II 5 µm (C18), Phenomenex Inc., Torrance, CA, USA) with 100 % methanol as the mobile phase and detected at 282 nm (Dionex D170 S, Dionex-Thermo Fisher Scientific Inc., Waltham, MA, USA). Inorganic, mineralized N (N_{min}, the sum of NO_3^- and NH_4^+) was determined in K_2SO_4 extracts of the non-fumigated samples by a continuous flow analyzer (Evolution II auto-analyzer, Alliance Instruments, Salzburg, Austria). The concentrations of available macronutrients important for maintaining microbial life, that is, calcium (Ca), potassium (K), phosphorus (P) and sulphur (S) (Madigan *et al.*, 2012; Lichstein, 1960;Guirard, 1958) were determined for all samples after incubation by applying the Mehlich-3 multi-element extraction method according to Wolf and Beegle (1995) with ion chromatography (850 Professional IC, Metrohm, Herisau, Switzerland, for K, and Varian VISTA RL CCD Simultaneous ICP-AES, Varian Inc., Melbourne, Australia, for Ca, P and S).

2.4.6 *Modelling the CO_2 emission data*

Models with first-order kinetics were used to evaluate the CO_2 emission data. Based on the CO_2 emission data of the topsoil control treatment, a one-pool model was calibrated to describe the mineralization of the native organic C (Figure 2.1 a) by non-linear least squares regression with the statistical software R version 3.2.2 (R Development Core Team, 2015).

The model was:

$$\text{Cumulative } CO_2 - C \text{ emission} = C_{max} \{1 - \exp(kt)\}, \qquad (1)$$

where C_{max} is the calibrated maximum mineralizable amount of native C under the experimental conditions (485 mg kg^{-1}), k is the calibrated rate constant (2.34 × 10^{-3} day^{-1}) and t is the time.

To describe the mineralization of root C, a two-pool model was calibrated based on the CO_2 emission data of the homogenized subsoil with 2 g roots (<2 mm) per kg soil (Figure 2.2 b), which was enabled by the absence of native organic C in the subsoil (Figure 2.2 a).

The model was:

$$\text{Cumulative } CO_2 - C \text{ emission} = C_{max1} \{1 - \exp(k_1 t)\} + C_{max2} \{1 - \exp(k_2 t)\}, \qquad (2)$$

where C_{max1} is the fast calibrated maximum mineralizable amount of substrate C under the experimental conditions (23.1 mg kg^{-1}) and C_{max2} the slow calibrated maximum mineralizable amount of substrate C (77.6 mg kg^{-1}). The respective rate constants, k_1 and k_2, are 7.65×10^{-2} day^{-1} and 2.30×10^{-3} day^{-1} and t is the time. The models were validated for the other treatments as follows:

- The two-pool model was validated for the remaining three subsoil treatments with additions of 2 g roots per kg soil (homogenized subsoil and root size of 1 – 2 cm and both root additions (sizes <2 mm and 1 – 2 cm) to minimally disturbed subsoil).
- For the combination of native C (one-pool model) and substrate (two-pool model), a three-pool model (with the parameters given above) was validated for all four topsoil treatments with additions of 2 g roots per kg soil (both homogenized and minimally disturbed soil, root sizes <2 mm and 1 – 2 cm).
- The two-pool model was also validated for the four subsoil treatments with additions of 8 g roots per kg soil. The only modification was that C_{max1} and C_{max2} were quadrupled, resulting in 92.4 and 310.3 mg kg^{-1}.
- The three-pool model described above was also validated for the four topsoil treatments with additions of 8 g roots per kg soil. Again, the only modification was a quadrupling of C_{max1} and C_{max2} to 92.4 and 310.3 mg kg^{-1}.

For the validation treatments, the model approach enabled us to test the basic assumptions that root mineralization is controlled by substrate characteristics, that root size and distribution do not affect C mineralization, that mineralization of the root and of soil organic C behave additively (i.e. priming effects are negligible) and that root C mineralization increases in proportion to the increase in the amount of roots. These assumptions are confirmed if the validated CO_2 data fit the measured data.

2.4.7 Statistical analysis

All statistical analyses were carried out separately for each soil depth with the statistical software packages SAS (SAS Institute Inc., 2014) and R.

For treatments with the addition of roots, a fixed effects model was fitted to study the main effects of root distribution (levels: roots locally concentrated and homogeneously distributed), amount of roots added (levels: 2 and 8 g roots kg^{-1}), root size (levels: <2 mm and 1 – 2 cm) and their interactions and the main effect of soil pit (levels: soil profiles 1 – 3) on cumulative CO_2 emissions with the mixed models (MIXED) procedure of SAS for the final cumulative CO_2 emissions. All effects given above were treated as fixed effects and pits were treated as blocks. Studentized residuals (residuals divided by an estimate of their standard deviation) were inspected for homoscedasticity and normality.

For the topsoil, a logarithmic (log_{10}) transformation of the final cumulative CO_2 emissions was required to achieve normality and homoscedasticity. For the subsoil, significant interactions between rate of root addition and root size, and between root distribution and root size, were observed (Table 1). For these cases, the means of the respective factor levels were compared at levels of the interacting factor by the SLICE statement of the MIXED procedure (Tables 1 and 2). The SLICE statement tests for the simple main effects of factor A for factor B, which are calculated by extracting the appropriate rows from the coefficient matrix for the A×B least squares means and by using them to form an *F* test.

Pearson product-moment correlations (for normally distributed data) and Spearman rank correlation analyses (for non-normally distributed data) were computed for the pairs: cumulative CO_2 emission and microbial biomass C, microbial biomass C and N_{min}, microbial biomass C and available Ca, and microbial biomass C and available K, for the treatments with maximally and minimally disturbed soil (sampled either from localized material or surrounding material) at both depths (data are given in Table 2.3). For the correlation analyses, the data of the individual field replicates were considered. Significant ($P \leq 0.05$) relations only are reported.

2.5 Results

2.5.1 Rates of emission of CO_2

Differences in the decomposition of fine beech roots were deduced from the cumulative CO_2 emissions measured constantly for about 1 year. This long-term incubation

should account for potential changes in the structure of the microbial community because of adaption to a heterogeneous and varying nutrient supply.

For the topsoil samples with 2 g of roots per kg soil, we detected cumulative rates of emission of between 330 and 460 mg CO_2-C per kg soil (Figure 2.1 b, c). Compared with the smaller rates of application, we detected cumulative emission rates that were about twice as large for treatments with application rates of 8 g of roots per kg soil (Figure 2.1 d, e).
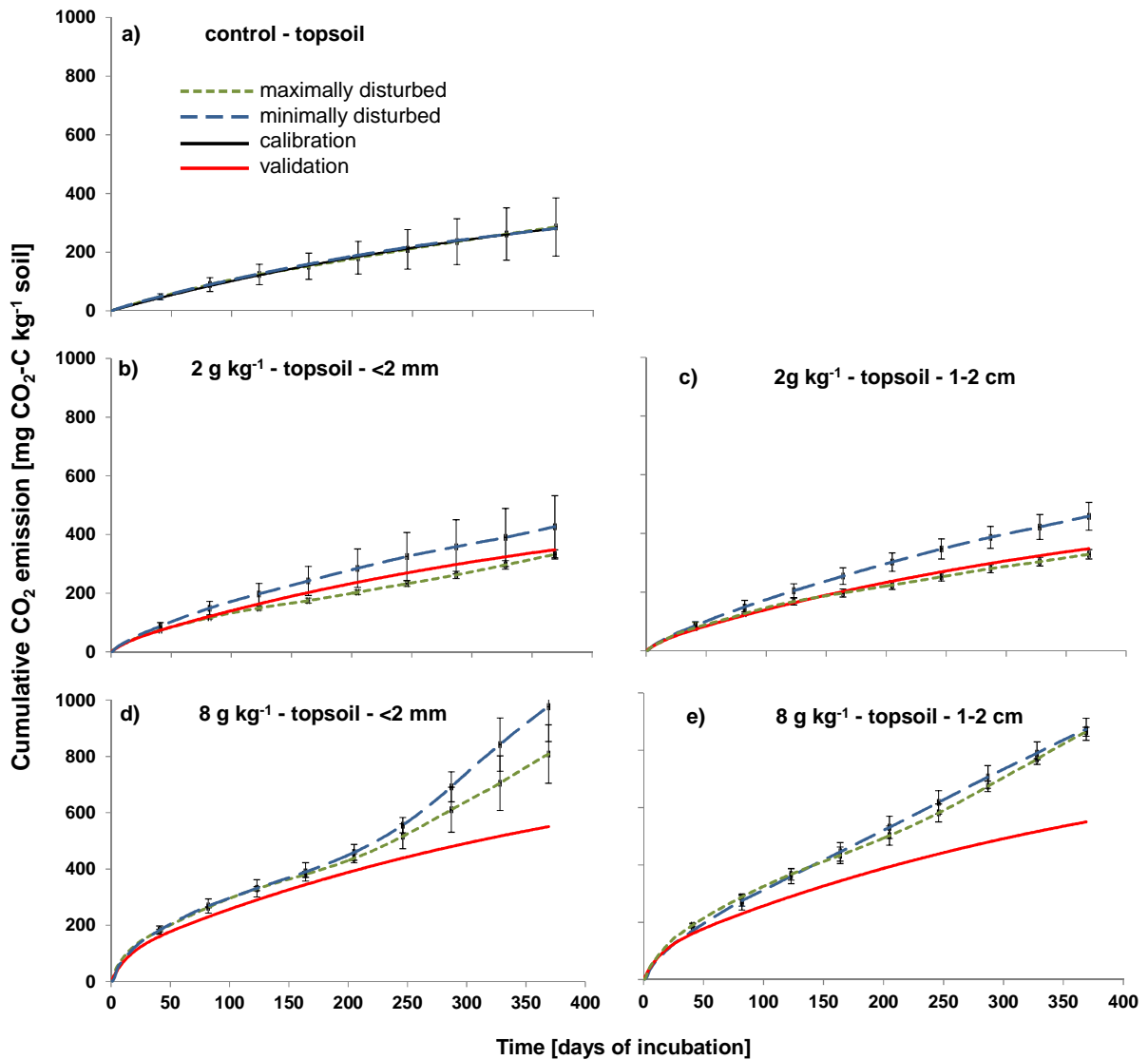
Figure 2.1: Cumulative rates of CO_2 emissions from the minimally and maximally disturbed topsoil treatments, including: (a) the control and (b, c) the application of < 2 mm and 1 – 2 cm large roots at rates of 2 g roots per kg soil, respectively, and (d, e) 8 g roots per kg soil, respectively, homogenously distributed (maximally disturbed, dotted line) and locally concentrated (minimally disturbed, dashed line). The measured data are means from the three replicated field samples and the error bars represent the standard errors for selected dates. The data derived from the calibration and validation of the first-order model are depicted as solid lines.

The subsoil samples with 2 g of roots per kg soil had emission rates of 70 – 170 mg CO_2-C per kg soil (Figure 2.2 b, c). The subsoil samples with the larger rate of application of 8 g of roots <2 mm per kg soil emitted 280 and 310 mg CO_2-C per kg soil (Figure 2.2 d). Rates of emission were twice as large for the same rate of application of large roots of 1 – 2 cm; they were 550 and 680 mg CO_2-C per kg soil (Figure 2.2 e).
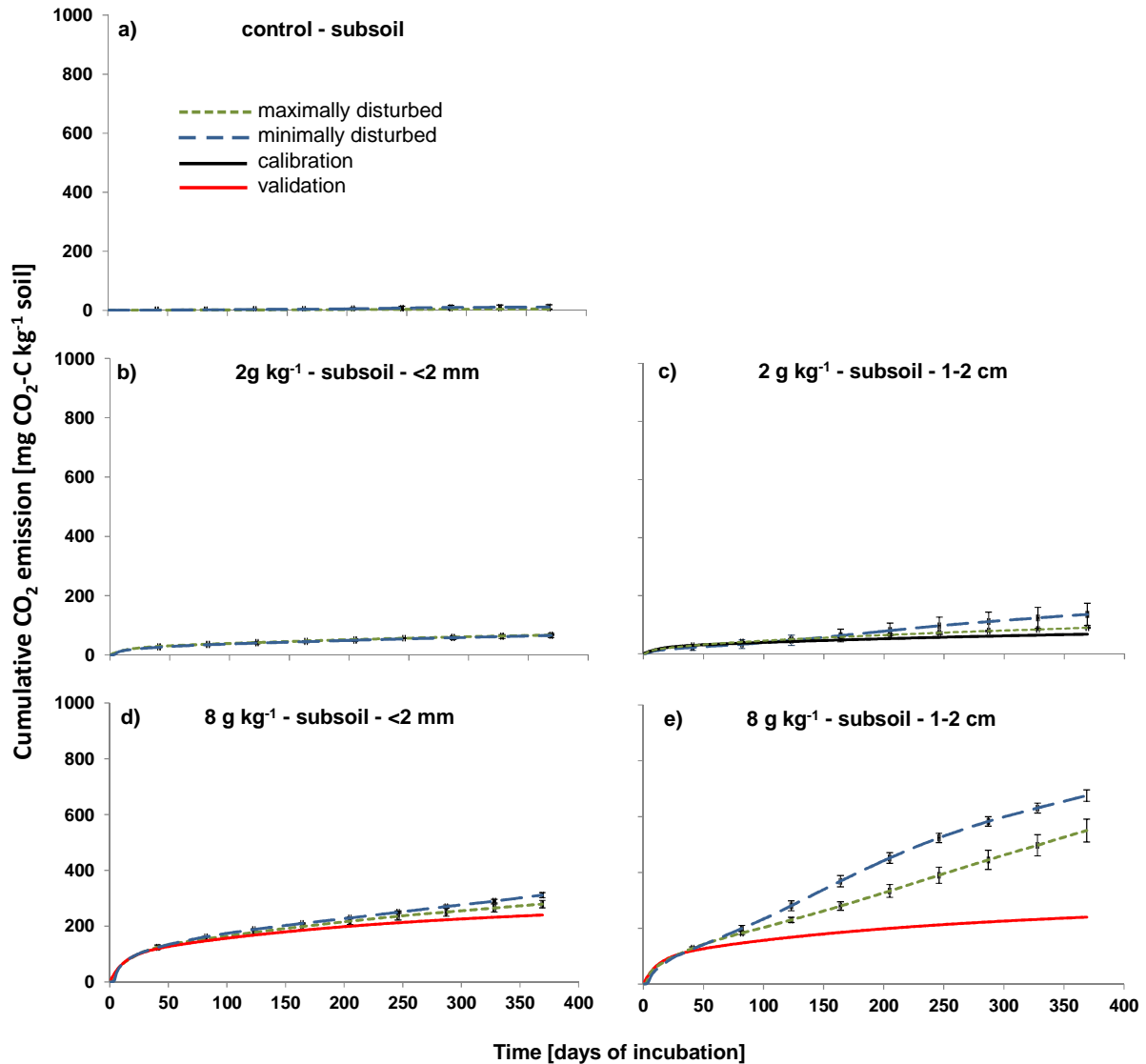
Figure 2.2: Cumulative CO_2 emissions of the minimally and maximally disturbed subsoil treatments, including the control (a) and the application of <2 mm and 1 – 2 cm large roots at rates of 2 g roots per kg soil (b, c, respectively) and 8 g roots per kg soil (d, e, respectively), homogenously distributed (maximally disturbed, dotted line) and locally concentrated (minimally disturbed, dashed line). The measured data are means from the three replicated field samples and the error bars represent the standard errors for selected dates. The data derived from the calibration and validation of the first-order model are depicted as solid lines.

Results of fixed-effects models for the effects of pit, root distribution, rate of root C addition and root size on the log-transformed cumulative CO_2 emissions (topsoil) or cumulative CO_2 emissions (subsoil) are shown in Tables 2.1 and 2.2. For the topsoil treatments we detected a significant positive effect from the rate of root C addition ($F = 115$, $P < 0.0001$, Table 2.1) and root distribution ($F = 5.22$, $P = 0.04$) on the log-transformed cumulative CO_2 emissions Table 2.1).

Table 2.1: Results of the fixed-effects models for the effects of site (Pit), root distribution (Distribution), rate of root addition (Rate) and root size (Size) on the cumulative CO_2 emissions (subsoil) or log10-transformed cumulative CO_2 emissions (topsoil).

Source	Degrees of freedom	Mean square	F ratio	P
Topsoil: tests for fixed effects				
Pit	2	0.00944	1.36	0.29
Distribution	1	0.0363	5.22	0.04
Rate	1	0.801	115.0	<0.0001
Size	1	0.000615	0.09	0.77
Distribution x rate	1	0.00744	1.07	0.32
Distribution x size	1	0.000188	0.03	0.87
Rate x size	1	0.00106	0.15	0.70
Distribution x rate x size	1	0.00699	0.96	0.34
Residual	14	0.00696		
Subsoil: tests for fixed effects				
Pit	2	698	0.65	0.54
Distribution	1	2.08×10^4	19.5	0.0007
Rate	1	7.01×10^5	658.0	<0.0001
Size	1	2.06×10^5	194.0	<0.0001
Distribution x rate	1	1.83×10^3	1.72	0.21
Distribution x size	1	1.17×10^4	11.0	0.006
Rate x size	1	8.84×10^4	82.9	<0.0001
Distribution x rate x size	1	5.19	0	0.95
Residual	13	1.07×10^3		
Subsoil: tests for segment effects				
Distribution x size				
Large roots	1	2.96×10^4	28.0	0.0001
Small roots	1	691	0.65	0.44
Homogeneously distributed roots	1	6.42×10^4	60.2	<0.0001
Roots locally concentrated	1	1.48×10^5	139.0	<0.0001
Rate x size				
Large roots	1	6.04×10^5	566.0	<0.0001
Small roots	1	1.56×10^5	147.0	<0.0001
Rate: 8 g kg^{-1}	1	3.03×10^5	284.0	<0.0001
Rate: 2 g kg^{-1}	1	1.15×10^4	10.8	0.006

In the subsoil, there were significant effects of rate, distribution and root size together with the interactions of root size and distribution, and of root size and rate (Table 2.1). Subsequent tests for the segment effects indicated that for all factors of the interactions investigated, significant effects were found, except for root distribution if small roots were applied ($F = 0.65$, $P = 0.44$, Table 2.1).

Table 2.2: Mean values of final cumulative CO_2 emissions and their lower and upper confidence limits for the different treatments.

Treatments	Mean	Lower confidence limit	Upper confidence limit
		[mg CO_2-C kg^{-1} soil]	
Topsoil			
Distribution: homogeneously distributed roots	523	464	589
Distribution: roots in local concentration	625	555	704
Rate: 2 g roots kg^{-1}	375	333	423
Rate: 8 g roots kg^{-1}	871	773	981
Subsoil			
Large roots, homogeneously distributed	320	291	348
Large roots, locally concentrated	426	394	459
Small roots, homogeneously distributed	173	145	202
Small roots, locally concentrated	189	160	217
Large roots, 2 g roots kg^{-1}	133	100	166
Large roots, 8 g roots kg^{-1}	613	584	642
Small roots, 2 g roots kg^{-1}	67	38	96
Small roots, 8 g roots kg^{-1}	295	266	324

For the topsoil, predicted marginal means and confidence limits were back-transformed and may be interpreted as medians and confidence limits of the medians (Piepho, 2009).

2.5.2 *Soil organic carbon, total N and microbial biomass*

To determine the distribution of microorganisms and nutrients in different soil compartments and their potential effect on the decomposition dynamics, we analyzed separately the homogenized and localized material together with the soil surrounding the local substrate concentrations.

For the homogenized topsoil material, the SOC concentrations ranged from 12.7 to 16.4 g kg^{-1} and total N concentrations from 0.51 to 0.62 g kg^{-1} (Table 2.3), with similar concentrations for the surrounding material of the minimally disturbed topsoil. Compared with those, the localized material had larger SOC (13.0 – 41.9 g kg^{-1}) and total N concentrations (0.49 – 1.27 g kg^{-1}) (Table 2.3). The SOC and total N concentrations of the respective subsoil samples were generally smaller than those of the topsoil (Table 2.3).

Table 2.3: Soil chemical and biological characteristics of the homogenized material (Homogenized) derived from the maximally disturbed top- and subsoil treatments and of the localized (Localized) and surrounding material (Surrounding) derived from minimally disturbed top- and subsoil treatments with the root application rates (Rate) of 2 and 8 g roots per kg soil (2 and 8 g kg^{-1}) and the Control (no application) for the root sizes (Size) of <2 mm and 1 – 2 cm.

Rate	Size	Soil material	C		N		C_{mic}		N_{mic}		Ergosterol		N_{min}		Ca		K	
			[g kg^{-1} soil]						[mg kg^{-1} soil]									
Topsoil																		
Control	-	Homogenized	12.7	(1.3)	0.51	(0.04)	48.3	(11.4)	7.4	(0.4)	0.58	(0.17)	22.1	(1.2)	46.2	(3.9)	12.6	(1.8)
		Localized	13.0	(1.2)	0.49	(0.02)	111.6	(7.9)	19.0	(2.0)	0.54	(0.09)	18.9	(3.9)	63.7	(20.0)	23.8	(4.9)
		Surrounding	13.7	(1.7)	0.52	(0.05)	86.5	(21.8)	12.9	(1.9)	0.55	(0.17)	19.3	(4.3)	59.5	(16.6)	21.4	(1.7)
2 g kg^{-1}	<2 mm	Homogenized	13.5	(1.3)	0.54	(0.04)	81.5	(13.9)	14.8	(3.7)	0.67	(0.15)	21.2	(2.0)	52.5	(4.1)	22.1	(4.1)
		Localized	22.1	(2.9)	0.72	(0.08)	124.9	(28.4)	22.7	(5.1)	1.62	(0.27)	20.9	(6.6)	82.9	(6.2)	21.5	(1.9)
		Surrounding	15.4	(2.8)	0.56	(0.07)	109.2	(35.4)	20.2	(6.8)	0.85	(0.25)	19.1	(5.8)	62.6	(3.7)	18.6	(0.6)
	1-2 cm	Homogenized	13.9	(1.2)	0.55	(0.03)	70.9	(11.0)	12.4	(2.8)	0.59	(0.11)	23.0	(1.3)	45.8	(5.7)	20.0	(0.5)
		Localized	20.8	(1.7)	0.71	(0.11)	135.6	(16.4)	23.8	(5.2)	1.13	(0.21)	19.2	(5.7)	68.9	(17.5)	21.7	(4.4)
		Surrounding	14.5	(2.2)	0.56	(0.11)	97.7	(10.0)	21.0	(5.0)	0.49	(0.14)	21.0	(7.5)	52.5	(25.9)	25.4	(4.4)
8 g kg^{-1}	<2 mm	Homogenized	16.3	(1.0)	0.62	(0.03)	120.1	(13.1)	16.8	(0.5)	0.97	(0.16)	15.3	(1.2)	73.0	(6.6)	23.3	(3.3)
		Localized	39.6	(0.5)	1.27	(0.05)	360.0	(65.6)	53.2	(5.9)	3.75	(0.26)	19.0	(8.2)	187.5	(34.0)	33.8	(4.0)
		Surrounding	13.7	(1.1)	0.52	(0.05)	89.0	(10.3)	16.0	(1.0)	0.54	(0.03)	13.7	(7.2)	79.6	(18.3)	25.0	(1.7)
	1-2 cm	Homogenized	16.4	(0.8)	0.61	(0.03)	102.8	(6.8)	14.8	(1.9)	0.85	(0.20)	21.8	(1.7)	58.9	(8.9)	22.7	(2.8)
		Localized	41.9	(6.0)	1.23	(0.13)	307.3	(32.0)	48.2	(7.5)	1.22	(0.21)	21.2	(3.2)	117.4	(20.9)	31.2	(4.9)
		Surrounding	13.9	(2.4)	0.53	(0.06)	91.1	(7.2)	17.9	(1.9)	0.61	(0.15)	17.9	(3.5)	74.2	(18.0)	24.7	(4.9)
Subsoil																		
Control	-	Homogenized	0.6	(0.1)	0.05	(0)	2.4	(0.9)	0.4	(0.3)	0	(0)	0.7	(0.37)	8.4	(1.1)	13.9	(2.0)
		Localized	0.4	(0.1)	nd	-	2.9	(0)	0.3	(0.2)	0	(0)	0.3	(0.14)	4.8	(4.8)	11.3	(2.0)
		Surrounding	0.5	(0.0)	nd	-	2.8	(1.8)	0.5	(0.3)	0	(0)	0.2	(0.09)	5.2	(5.2)	12.3	(5.2)
2 g kg^{-1}	<2 mm	Homogenized	1.4	(0.1)	0.05	(0)	1.7	(0.5)	1.9	(0.6)	0.08	(0.01)	0.4	(0.01)	21.8	(3.4)	7.2	(1.8)
		Localized	6.2	(0.1)	0.16	(0)	27.3	(4.2)	3.9	(1.2)	0.86	(0.05)	0.4	(0.02)	38.9	(5.4)	9.9	(2.0)
		Surrounding	0.7	(0.2)	nd	-	4.6	(1.6)	0.8	(0.1)	0.03	(0)	0.3	(0.02)	13.0	(2.3)	8.4	(2.3)
	1-2 cm	Homogenized	1.8	(0.4)	0.06	(0.01)	17.7	(3.0)	2.5	(0.7)	0.10	(0.01)	0.2	(0.09)	27.7	(12.3)	19.2	(5.6)
		Localized	5.1	(0.7)	0.13	(0.02)	72.8	(9.5)	8.8	(1.6)	0.12	(0.06)	0.2	(0.02)	14.2	(3.6)	13.7	(2.5)
		Surrounding	0.4	(0.1)	nd	-	8.7	(4.2)	1.2	(0.5)	0.02	(0.01)	0.2	(0.03)	4.3	(4.3)	15.9	(4.1)
8 g kg^{-1}	<2 mm	Homogenized	4.0	(0.0)	0.11	(0)	21.6	(4.5)	3.1	(0.2)	0.41	(0.03)	0.3	(0.03)	34.6	(5.2)	18.2	(4.2)
		Localized	32.2	(2.0)	0.76	(0.05)	188.4	(14.5)	24.4	(1.2)	5.41	(0.55)	0.2	(0.01)	177.0	(13.6)	27.2	(3.2)
		Surrounding	0.9	(0.0)	0.05	(0)	5.1	(1.2)	1.0	(0.2)	0.08	(0.01)	0.2	(0.02)	7.3	(5.9)	15.6	(1.0)
	1-2 cm	Homogenized	5.0	(0.3)	0.13	(0.01)	26.7	(4.3)	3.4	(0.6)	0.21	(0.02)	0.4	(0.06)	22.1	(5.5)	23.3	(3.9)
		Localized	30.5	(3.9)	0.77	(0)	202.7	(5.5)	29.0	(2.0)	0.73	(0.26)	2.1	(1.72)	68.8	(6.7)	27.3	(4.3)
		Surrounding	0.9	(0.4)	0.07	(0)	6.4	(6.0)	1.6	(0.6)	0.06	(0.03)	1.2	(0.82)	6.2	(5.1)	18.6	(2.9)

The data are mean values of fhe replicated field samples and the standard errors are given in parentheses.
nd, below detection limit.

For the homogenized topsoil, the microbial biomass C and N concentrations were smallest for the control treatments and largest for the treatments with 8 g of roots <2 mm (Table 2.3). A similar range was detected for microbial biomass C and N concentrations in the surrounding material. The locally concentrated material in the topsoil had the smallest microbial biomass C and N concentrations for the control treatments and the largest for treatments with 8 g of roots <2 mm kg^{-1} soil (Table 2.3). The homogenized, surrounding and localized material of the subsoil samples had smaller microbial biomass C and N concentrations than the respective topsoil materials. The ergosterol concentrations of the topsoil samples differed between 0.49 and 3.75 mg kg^{-1} and those of the subsoil samples between 0.00 and 5.41 mg kg^{-1} (Table 2.3).

The data given in Table 2.3 were evaluated further by correlation analyses, which revealed significant relations between the cumulative CO_2 emissions and C_{mic} concentrations for the homogenized and localized material of the top- and subsoil (Table 2.4, Figure 2.3).

Table 2.4: Coefficients of correlation (significant at P ≤ 0.05) between the cumulative CO_2 emission rates (CO_2) and concentrations of microbial biomass C (C_{mic}) (n = 12), and between C_{mic} and concentrations of ergosterol, mineral N (N_{min}) and available Ca and K (n = 12), determined separately for the homogenized, the localized and the surrounding material of the maximally and minimally disturbed topsoil and subsoil treatments.

Correlated variables	Homogenized material		Localized material		Surrounding material	
	Topsoil	Subsoil	Topsoil	Subsoil	Topsoil	Subsoil
CO_2 and C_{mic}	0.63[a]	0.82[b]	0.93[b]	0.84[b]	n.s.	n.s.
C_{mic} and ergosterol	0.76[b]	n.s.	n.s.	n.s.	n.s.	n.s.
C_{mic} and N_{min}	n.s.	n.s	n.s.	n.s.	0.62[a]	n.s.
C_{mic} and Ca	0.80[b]	n.s.	0.90[b]	0.63[b]	n.s.	n.s.
C_{mic} and K	n.s.	0.88[b]	0.70[a]	0.80[a]	n.s.	n.s.

[a]These *r* values are Spearmans`s rank order correlation coefficients.
[b]These *r* values are Pearson`s product-moment correlation coefficients.
n.s., not significant.
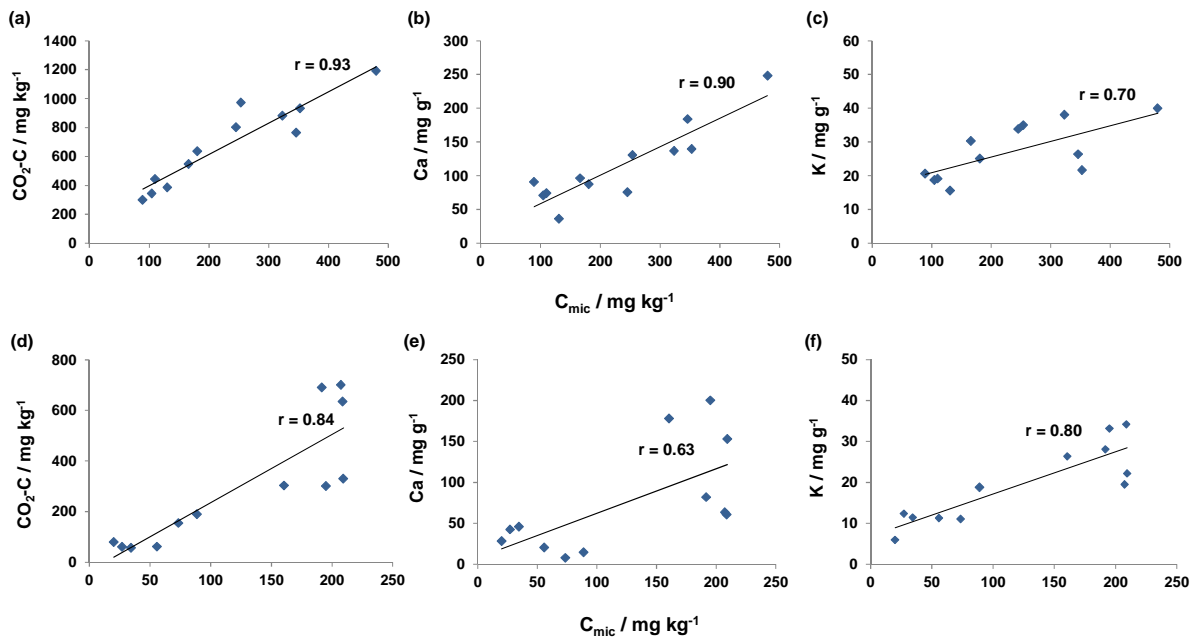
Figure 2.3: Microbial biomass C of the localized material from the minimally disturbed topsoil correlated with: (a) cumulative CO_2 emissions (minimally disturbed topsoil), (b) Ca concentrations (localized material from the minimally disturbed topsoil) and (c) K concentrations (localized material from the minimally disturbed topsoil). Microbial biomass C of the localized material from the minimally disturbed subsoils correlated with: (d) cumulative CO_2 emissions (minimally disturbed subsoils), (e) Ca concentrations (localized material from the minimally disturbed subsoils) and (f) K concentrations (localized material from the minimally disturbed subsoils).

2.5.3 Macronutrients

For the homogenized topsoil samples, NO_3^--N accounted for 90 – 93 % of N_{min}. For all other samples the contribution was less and accounted for 28 – 79 % of N_{min}. The N_{min} concentrations of the topsoil samples differed between 15.3 and 23.0 mg kg^{-1} for the homogenized material, between 13.7 and 21.0 mg kg^{-1} for the surrounding material and between 18.9 and 21.2 mg kg^{-1} for the localized material (Table 2.3). The N_{min} concentrations of the subsoil samples were distinctly smaller than those of the topsoil samples. For the homogenized topsoil samples, the concentration of Ca ranged from 46 to 73 mg kg^{-1}. The surrounding material had similar Ca concentrations, whereas those of the localized material were larger (63.7 – 187.5 mg kg^{-1}) (Table 2.3). The Ca concentrations of the subsoil samples were between 4.3 and 177.0 mg kg^{-1} for all samples (Table 2.3). The K concentrations of topsoil samples were between 12.6 and 23.3 mg kg^{-1} for the homogenized material, between 18.6 and 25.4 mg kg^{-1} for the surrounding material and between 21.5 and 33.8 mg kg^{-1} for the localized material. The K concentrations of the subsoil samples were smaller and ranged from 7.2 to 27.3 mg kg^{-1} (Table 2.3).

We found significant relations between concentrations of C_{mic}, Ca and K for the localized material of the top- and subsoil (Table 2.4, Figure 2.3).

2.6 Discussion

2.6.1 *Emissions of CO_2 from top- and subsoil increase with an increase in rate of root C addition*

Compared with the control soil, the concentration of fine beech roots had a larger effect on substrate decomposition and evolution of CO_2 in the subsoil than in the topsoil of the sandy soil studied. This can be explained by the fact that the added roots are the only source of substrate for microorganisms in the subsoil because the inherent bulk subsoil OC contents were below the detection limit. Therefore, the lack of alternative substrate sources or priming effects that might affect the differences for topsoil can be disregarded for the subsoil.

2.6.2 *Emissions of CO_2 from topsoil are not affected by the root size, but by the root distribution*

We detected no effect of root size, but the effect of root distribution on the topsoil log-transformed CO_2 emissions was significant (Table 2.1), which suggests larger rates of root decomposition if fine beech roots are localized rather than distributed homogeneously. The measured CO_2 data of the treatments with 2 g <2 mm or 1 – 2 cm roots per kg soil, however, were well described with our model approach and showed small or variable differences between the homogenized and localized samples irrespective of the root size (Figure 2.1 b, c). Overall, the data suggest that the size and distribution of fine beech roots with 2 g roots added per kg soil are of no (root size) or minor (distribution) importance for their mineralization in the sandy topsoil studied.

For the topsoil with 8 g <2 mm or 1 – 2 cm roots per kg soil, the CO_2 emissions were not described satisfactorily by the model approach (Figure 2.1 d, e). The modelled data underestimated the measured CO_2 emissions and the discrepancy increased with the duration of the incubation experiment. In particular, the continuing rise in the CO_2 emissions after 1 year of the incubation experiment was unexpected and might be related to priming effects that led to more intensive decomposition of native soil C with time. An additional factor might have been an adaptation of the soil microorganism community over time and transformation of the added root material into a more easily decomposable form because of ongoing microbial processing. The data suggest that for such 'self-catalysing' effects, a certain concentration of roots is necessary because we were unable to observe them with a root application rate that was four times smaller. Although the overall effect was significant,

the root distribution resulted in small or very variable differences in the rates of CO_2 emission after an application of 8 g roots per kg soil.

Loecke and Robertson (2009) found no differences in the cumulative rates of CO_2 emission after 39 days of decomposition for clover (*Trifolium pretense* L.) residues applied as patches or homogeneously at a rate of 4.5 g dry mass per kg soil, which is similar to the results for our topsoil treatments. Furthermore, Magid et al. (2006) detected no differences or only small differences in the cumulative CO_2 emissions from soil where maize (*Zea mays* L.) and rape (*Brassica napus* L.) residues were added homogeneously or as a layer at a rate of about 6.7 g dry mass per kg soil after 56 (maize) and 202 days (rape) of decomposition. The potentially improved protection of homogenously distributed plant residues against microbial decomposition by the greater litter particle-to-mineral surface contact seems to be of minor importance, especially in the more sandy substrate analyzed in our study (Loecke and Robertson, 2009; Magid et al., 2006).

2.6.3 Emissions of CO_2 from subsoil increase with increasing root size, but not all cases are affected by the root distribution

Emission rates of CO_2 for the homogenized and minimally disturbed (i.e. localized) subsoils with 8 g 1 – 2 cm roots per kg soil were twice as large as those where roots of <2 mm were added at the same rate. The largest cumulative CO_2 emission among the subsoil treatments was for the minimally disturbed samples with 8 g 1 – 2 cm roots per kg soil. This in turn led to the smallest difference in rate of CO_2 emission between the top- and subsoil among the treatments analyzed. This suggests that the intensive decomposition observed for the larger roots in the subsoil is affected mainly by root concentration because this effect was less pronounced for the smaller rate of root application.

A priming effect can be excluded for the subsoil because of the lack of native SOC. The larger rates of CO_2 emission for treatments with the larger roots after 1 year of incubation suggest more favourable conditions for the mineralization of 1 – 2 cm roots in the subsoil than for microbial utilization of the <2 mm roots, which is independent of the distribution. We found no distinct differences between the treatments with 1 – 2 cm or <2 mm roots in relation to soil pH, macronutrient concentrations (i.e. N_{min}, Ca, K, P and S), microbial biomass C or ergosterol concentrations. This suggests the absence of relations between nutrient dynamics and microbial abundance as well as activity. An alternative explanation might be a better pore-size distribution because of the addition of larger roots, which leads to more favourable conditions for soil microorganisms (Bodner et al., 2014). Additional pores might result from fungal hyphae that can push aside mineral or organic particles

(Emerson and McGarry, 2003; Bearden, 2001; Dorioz et al., 1993), or voids that remain after the decomposition of root residues. The newly created pores might then be stabilized because of binding agents exuded by fungal hyphae (e.g., De Gryze et al., 2006).

Loecke and Robertson (2009), for example, hypothesized that with decreasing size of plant residues the rate of mineralization increases because there is less structural resistance to microbial decay and improved contact between residues and microorganisms or extracellular enzymes. This was not confirmed, however, by the data from Iqbal et al. (2014) and Toenshoff et al. (2014), which accord with the results of our topsoil treatments. Nevertheless, the rates of CO_2 emission for the larger fine root residues were 1.3 – 2.6 times larger than those of the smaller roots for the subsoil with root additions of 2 and 8 g per kg soil, respectively, irrespective of their distribution, and have not been observed previously to the best of our knowledge. Therefore, the effect of the size of fine roots on the mineralization kinetic in subsoil needs further research.

2.6.4 Microbial biomass C is positively correlated with CO_2 emissions and soil Ca and K concentrations

For the homogenized top- and subsoil, we found positive correlations between the rates of CO_2 emission and concentrations of microbial biomass C (topsoil, r = 0.63; subsoil, r = 0.82) (Table 2.4). The positive correlations between rates of CO_2 emission and microbial biomass C concentrations measured for the localized material (topsoil, r = 0.93; subsoil, r = 0.84) in the minimally disturbed top- and subsoils were stronger than those for the homogenized roots. This suggests an increasing turnover of C with an increase in microbial biomass that is independent of soil depth. For the topsoil, this interaction seems to be of greater relevance if the roots are locally concentrated because the relation is stronger for these samples than for the homogenized ones.

For the localized material from the top- and subsoil, we found significant positive relations between the concentrations of microbial biomass C and of available Ca and K (Table 2.4). This suggests a strong positive effect of Ca and K supply on microbial biomass and the turnover of C at low soil pH, irrespective of soil depth. This is supported by a study from Silver and Miya (2001), who reported a strong positive effect of root Ca concentration on the decomposition of broadleaf fine roots. Calcium is considered to be crucial for the production of enzymes such as cellulase, whereas K is assumed to be important in the activation of enzymes in terms of functioning in microbial nutrition (Madigan et al., 2012; Williams, 1970; Lichstein, 1960; Guirard, 1958).

Interestingly, for most of the top- and subsoil treatments analyzed, we found no significant correlations between N_{min} concentrations and microbial biomass C (Table 2.4) or between N_{min} concentrations and emissions of CO_2 (not shown), which suggests that N limitation was less relevant for the processes examined. Concentrations of Ca and K, however, were shown to have greater explanatory power (Table 2.4), suggesting that these macronutrients are crucial to top- and subsoil C dynamics. The ergosterol concentrations showed almost no relation with the emissions of CO_2 and concentrations of microbial biomass C, similar to N_{min}. This suggests that fungi did not have a preferential effect on the turnover of C under the conditions analyzed, which corroborates the findings of Anderson and Domsch (1975), who showed that bacteria can account for up to 40 % of the decomposition of beech litter.

2.7 Conclusions

The rate of application of fine beech roots affected C mineralization at both sampling depths significantly ($P \leq 0.05$), whereas the distribution of roots had a significant (but small) effect in all topsoil treatments with roots but only in the subsoil with roots of 1 – 2 cm. For the subsoil, our data indicate significant effects of the rate of application, root size and root distribution, and of interactions between root size and distribution together with root size and rate of application.

The data suggest, independently of soil depth and root distribution, an increase in C turnover with an increase in microbial biomass, but for the topsoil this interaction was more evident if the roots were concentrated locally. Our data also suggest that the supply of Ca and K might have had an effect on microbial activity and C turnover that was independent of soil depth for the localized fine root concentrations. Therefore, the link between Ca and K supply and processes of microbial decomposition seems to be important for the plant nutrient and C dynamics in both the top- and subsoil only if the fine roots are not homogeneously distributed. The almost complete lack of positive relations between the rates of CO_2 emission and soil microbial biomass with concentrations of ergosterol suggests a less dominant role of fungi in the mineralization of fine beech roots under the conditions analyzed.

The decomposition of fine roots at different depths of the sandy soil studied seems to be controlled not only by direct effects such as root size and distribution, but also by indirect abiotic effects that affect the living conditions of the microbial community.

2.8 Acknowledgements

3 Amount and composition of organic matter associated with aggregate size and density fractions in relation to depth and mineral characteristics of five different forest soils

Svendja Vormstein[a], Michael Kaiser[a], Hans-Peter Piepho[b], Bernard Ludwig[a]

[a] *Department of Environmental Chemistry, University of Kassel, Nordbahnhofstr. 1a, 37213, Witzenhausen, Germany*

[b] *Biostatistics Unit, Institute of Crop Science, University of Hohenheim, Fruwirthstr. 23, 70599, Stuttgart, Germany*

3.1 Abstract

Forest soils store about 70 % of the global soil organic carbon and are, therefore, a major factor in the contribution of terrestrial ecosystems to mitigate climate change. Their capability to protect organic matter (OM) against microbial decomposition by the formation of aggregates and organo-mineral associations depends on soil mineral characteristics, which are affected by soil type and soil depth. Only little is known about the relative importance of different stabilization mechanisms for the OM storage in various depths of forest soils, which are characterized by distinct differences in soil mineral characteristics. Therefore, we sampled horizontally five pedogenetically different soils under mature beech forest down to the parent material. From these samples, we separated four aggregate size fractions and three density fractions, which were quantified and characterized by infrared spectroscopy. Additionally, we determined the contents of the microbial biomass C and the cumulative basal respiration over the course of 14 days for the bulk soil samples. The relative proportion of stabilized OC associated with the fraction <53 µm and with the heavy fraction is increasing with soil depth independent from the soil type. Also with increasing soil depth, the percentage of the bulk SOC that had been respired within 14 days as CO_2 tends to increase leading to the largest differences in the relative amounts of labile OM between the topsoil horizons (n = 5, 0 – 5/10 cm: 5 – 8 %) and the deepest analysed subsoil horizons (n = 2, 63/70 – 170/180 cm: 9 – 31 %). This indicates a stronger separation of the bulk soil OM into a labile and a stable pool on the cost of the intermediate OM pool in the subsoil as compared with the topsoil. The infrared analyses suggest an enrichment in C=O groups of the OM with increasing soil depth, which might result from a higher degree of microbial processing. Independent from soil type, our findings emphasize the importance of subsoils under mature

beech forest for the long-term C- sequestration and highlight at the same time the function of the OM stored in the subsoil to maintain microbial activity and to fuel the subsoil nutrient cycle.

3.2 Introduction

In terrestrial ecosystems, soils represent the largest pool of organic carbon (OC) and, consequently, of organic matter (OM). The global soil OC (SOC) stock (2000 Pg C) is about 1.6 times larger than that stored in the biomass (500 Pg C) and in the atmosphere (785 Pg C) (Janzen, 2004). While topsoils usually show distinctly higher SOC concentrations (g OC kg^{-1} soil) than subsoils (i.e., soil compartment below the Ah/Ap horizon), 30 to 63 % of the total SOC is stored in a soil depth of 30 – 100 cm and even in depths between 100 and 200 cm up to 40 % of the total SOC can be found (Angst et al., 2016; Batjes, 1996). Forest top- and subsoils account for approximately 70 % of the global SOC reasoning their large importance for terrestrial ecosystem services such as the mitigation of climate change (Vancampenhout et al., 2012). However, the dynamics of OC in the subsoil cannot be deduced from that in the topsoil because the soil environmental conditions differ widely from those in topsoils (e.g., Rumpel and Kögel-Knabner, 2011; Rasse et al., 2006; Rumpel et al., 2004). However, in contrast to forest topsoils there are much less information about the decomposition and stabilization of OM in subsoils (Vancampenhout et al., 2012; Rumpel and Kögel-Knabner, 2011).

The importance of temperature and water contents as key factors for the mineralization of organic inputs are quantitatively described in soil OM turnover models (Sanaullah et al., 2011; Gillabel et al., 2010; Fierer et al., 2003). In addition, the effect of oxygen has been understood in more detail and typical concentrations throughout the soil profile seem to be not limiting for OM decomposition (Salome et al., 2010). For the long-term (>100 years) climatically more important preservation of organic material, the association of OM with mineral compounds and the occlusion in aggregates were shown to be crucial (Schmidt et al., 2011).

Organo-mineral associations mainly result from interactions of the OM with polyvalent cations or with mineral surfaces via polyvalent cations or through a direct bond formation between OM and mainly Fe- or Al-oxides (Kleber et al., 2015; Mikutta et al., 2007; von Lützow et al., 2006). Furthermore, clay-, silt-, and sand-sized soil mineral particles that chemically interact with OM are considered as the basic units of soil aggregates (Lehmann et al., 2007; Christensen, 2001). These units are then thought to extend towards larger aggregates depending on the availability of inorganic binding agents (oxides, cations) and/or

organic binding agents (polysaccharides, organic acids, microbial and plant debris, roots, hyphae) (Tisdall and Oades, 1982). Therefore, the OM inside aggregates can exist as particulate, colloidal and molecular size classes and the stability of aggregate-protected OM tends to increase with decreasing aggregate size (Liao et al., 2006; John et al., 2005; Six et al., 2002; Balesdent, 1996; Skjemstad et al., 1993). Consequently, the capability of soils to protect OM against biological decomposition by the formation of aggregates and organo-mineral associations depends on mineral characteristics such as the content of reactive Fe- and Al-oxides, polyvalent cations, and layer silicates (Mikutta et al., 2006; Eusterhues et al., 2005; Baldock and Skjemstad, 2000) which in turn are mainly affected by the soil type and soil horizon specific pedogenetic processes. Furthermore, OM characteristics such as the compound size (particle, molecule) and the abundance of reactive oxygen containing functional groups (-COOH, -OH) exert large control on their ability to form organo-mineral associations and aggregates (e.g., Kleber et al., 2015).

Due to changing soil mineral characteristics with increasing soil depth, the main stabilization mechanisms are assumed to be different between top- and subsoils. For instance, aggregates larger than 53 µm are postulated to have stronger effects on OM stabilization in topsoils (Paul et al., 2001), whereas in subsoils organo-mineral associations and the formation of aggregates <53 µm seems to be more important (Rasse et al., 2006; Kaiser et al., 2002). This is also affected by changes in the characteristics of OM with soil depth. With increasing soil depth the total OM content and the relative amount of less decomposed plant derived organic particles is decreasing (Angst et al., 2016) whereby the relative amount of more microbially processed OM is increasing (Kaiser and Kalbitz, 2012). The microbially governed, ongoing oxidative breakdown (microbial processing) of organic inputs in aerated soils is generally associated with a decrease in size and an increase in the amounts of reactive functional groups (Kleber et al., 2015). This implies that with increasing soil depth the organic compounds should get smaller and more reactive towards charged mineral surface sites.

However, there is only little knowledge about the relative importance of different stabilization mechanisms in different depths of broadleaf forest soils especially across soil types with distinct differences in pedogenesis and, consequently, in mineral characteristics (Rumpel and Kögel-Knabner, 2011; Schrumpf et al., 2011). Such knowledge would allow for a more precise evaluation of the OM turnover with increasing soil depth and a better assessment of the contribution of forest subsoils to the long-term OC storage. To achieve this, separating aggregate size fractions as well as mineral–associated and aggregate

occluded OM from horizon specific soil material that was sampled from different soil types under mature broadleaf forest should be a useful experimental setting.

Density fractionation of soil offers a useful procedure to assess the interaction between OM and the mineral phase by separating the bulk soil OM into the free light fraction (fIF), the aggregate occluded light fraction (oIF), and the mineral-associated OM (heavy fraction: HF) (Schrumpf et al., 2013; Cerli et al., 2012; Schrumpf et al., 2011). The OM associated with the oLF and HF is more degraded, smaller in size, and more stabilized than the OM associated with the fIF (Schrumpf and Kaiser, 2015; Schrumpf et al., 2013; Wagai et al., 2009). It is also known that the contribution of fIF-OC and oIF-OC to the bulk SOC declines with soil depth (Angst et al., 2016) and that the stability of OM associated with HF is increasing with soil depth (Schrumpf et al., 2013). Complementary, the separation of water-stable aggregate size fractions (e.g., >250 µm, 53 – 250 µm, <53 µm) by a wet-sieving procedure from soil reveals more information about the relevance of aggregate formation at different scales for the OM storage and stabilization (i.e., increasing OM stability with decreasing aggregate size) in different soil depths. To clarify differences between these density and aggregate size fractions in the composition of the associated OM, FTIR analyses are a suitable tool to assess the amount of reactive C=O groups (carbonyl and carboxyl) that are involved in the formation of organo-mineral associations and aggregates (Kaiser et al., 2014; Kaiser et al., 2012).

The aim of the study was to clarify the relative importance of the formation of aggregates and organo-mineral associations for the OM storage in relation to soil depth and type. We also wanted to elucidate the effects of soil mineral characteristics on the amount and the composition of OM associated with density and aggregate size fractions. For this, we sampled material from soil horizons down to the parent material of five pedogenetically different soils under mature beech forest and similar climate. From these soil samples, we separated and quantified three density and four aggregate size fractions indicative for different degrees of OM stabilization, which were also characterized by FTIR spectroscopy providing information about their functional composition.

3.3 Materials and Methods

3.3.1 Study sites and soil sampling

We analyzed soil material from five different sites under matured beech forest and of different pedogenesis that were located in the near of Göttingen (Germany). Further details about parent material, soil classification, pedogenetic horizons and their depth distribution

are given in Table 3.1. In May 2014 three soil pits of each site were excavated and composite samples were taken horizon specific down to the parent material.

Table 3.1: Parent material (Soil), soil classification, soil horizon classification (Horizon) and depth ranges for soil sampling for the five investigated sites.

Soil	Soil classification[a]	Horizon[a]	Depth ranges for soil sampling [cm]	
			Upper	Lower
Shell Lime Stone	Eutric Cambisol	Ah	0	10
		BwAh	10	30-50
Basalt	Eutric Cambisol	Ah	0	10
		BwAh	10	40-60
		Bw	40-50	80
Red Sandstone	Dystric Cambisol	Ah	0	5-8
		BwAh / Bw *	5-8	43-50
		Bw	43-50	70-90
Tertiary Sand	Dystric Brunic Arenosol	AhE	0	7-10
		BwAh	7-10	20-30
		Bw	20-30	63-70
		2C	63-70	140-150
Loess	Haplic Luvisol / Eutric Cambisol *	Ah	0	5-10
		E / BwE *	5-10	45-50
		Bt / E2 / Bwt *	45-50	75-85
		C	80-85	170-180

*The differences in the classification of soil type and soil horizons within same sites result from the heterogeneity in the field

[a]Classification according to World Reference Base for Soil Resources (IUSS, 2006).

3.3.2 Physico-chemical soil characterization

A subsample of each field moist sample was sieved <2 mm to conduct following analyses. The soil texture was determined by wet sieving and the pipette method according to DIN ISO 1277 (2002). The pH values were measured in 0.01 M $CaCl_2$ (25 ml $CaCl_2$: 10 g soil) with a glass electrode (pH electrode BlueLine 14 pH, Schott Instruments, Mainz, Germany). For the determination of exchangeable Na^+, K^+, Ca^{2+}, Mg^{2+} and Al^{3+}, the soil (oven dry, 40°C) was slowly leached with 0.1 M barium chloride (soil : solution ratio 1 : 10). Cations were measured in the filtered extracts by the use of ion chromatography (850 Professional IC, 237 Metrohm, Herisau, Switzerland). The cation exchange capacity was calculated by the sum of the exchangeable cations (König and Fortmann, 1996) and all results were calculated on a soil dry mass. Contents of oxalate-soluble iron and aluminum were determined in slight modification according to DIN 19684-6 (1997). Briefly, 2.5 g field moist soil were extracted in 50 ml extraction solution (one part 0.1 M ammonium oxalate solution and 0.765 parts 0.1 M

oxalic acid) by horizontal shaking for two hours and afterwards filtrated. The filtrates were measured with an atomic absorption spectrometer (906 AA, GBC, Melbourne, Australia) and the results were calculated on soil dry mass. The measurements of dithionite-soluble iron and aluminum were done according to Mehra and Jackson (1960). Briefly, 2 g field moist soil were treated with a mixture composed of 40 ml 0.3 M Na-citrate solution and 10 ml 1 M sodium bicarbonate solution, heated to 70°C before 1 g Na-dithionite was added. After the reaction time of 2 hours with regularly stirring, the samples were left to cool and centrifuged at 3000 g (Multifuge 3 S-R, Heraeus, Hanau, Germany). This procedure was repeated up to three times until the soil was grey. The remaining soil was treated with 40 ml 0.1 M magnesium sulfate, stirred, centrifuged and added to the extraction solution. This solution was filled up with deionized water to 250 ml. Dithionite-soluble iron and aluminum were also measured using AAS (see above) and calculated on a soil dry mass.

The bulk soil, the aggregate size fractions and the heavy fraction were ball-milled, whereas the light fractions (see below for further details) and fractions with low yields were ground in an agate mortar by hand. Total C and N concentrations of all samples were analyzed by dry combustion (Elementar, Vario El, Hanau, Germany) whereby the total C content corresponds to the organic C (OC) content because no carbonates were detectable using a "Scheibler" apparatus. For the separated fractions, the OC contents (g OC kg^{-1} fraction) and the dry mass yield of each fraction (g fraction kg^{-1} soil) were used to calculate the OC content for each fraction in g OC kg^{-1} soil. The contents of microbial biomass C and N (C_{mic} and N_{mic}) were determined by the chloroform-fumigation-extraction method (Brookes et al., 1985; Vance et al., 1987). Microbial biomass C was calculated as EC / k_{EC}, where EC = (organic C extracted from fumigated soils) - (organic C extracted from non-fumigated soils) and k_{EC} = 0.45 (Wu et al., 1990). Microbial biomass N was calculated as EN / k_{EN}, where EN = (total N extracted from fumigated soils) - (total N extracted from non-fumigated soils) and k_{EN} = 0.54 (Brookes et al., 1985; Joergensen and Mueller, 1996). Soil respiration was determined as described by Heinze et al. (2011). Briefly, 60 g of field moist soil were adjusted to 50 % of the water holding capacity and incubated together with 5 ml of 0.5 M NaOH in a separate vessel, which was replaced after 7 days, in 1 l glass jars for two weeks at 22°C (Kühlbrutschrank ICP 750, Memmert, Schwabach, Germany). Each sample was incubated in three laboratory replicates. After the addition of 3 ml of 0.5 M $BaCl_2$ and three drops of phenolphthalein to the NaOH-solution the evolved CO_2 was determined by titration with 0.5 M HCl to pH 8.3 (Isermeyer, 1952).

3.3.3 Separation of aggregate size and density fractions

Water stable aggregates of all soil samples were fractionated using a wet-sieving method developed by Cambardella and Elliot (1993) and slightly modified by Jacobs et al. (2009). Briefly, 40 g of air-dried soil (<10 mm) were placed on a 1000 μm sieve and soaked in deionized water for 10 min to allow slacking. Floating organic particles were skimmed off separately. Afterwards the sieve was lifted out of the water until the water had run off. The sieve was re-submerged and lifted out again for 50 repetitions. The soil/water suspension passing the sieve was transferred onto the next smaller sieve and the fractionation procedure was continued as described above. The used mesh sizes were: 1000 μm for large water-stable macro-aggregates, 250 μm for small water-stable macro-aggregates and 53 μm for water-stable micro-aggregates. Each fraction also the soil/water suspension passing the 53 μm sieve (silt, clay and very small micro-aggregates) was recollected, vacuum-filtrated (<0.45 μm), dried at 40°C and weighed. Due to operator variability (Jacobs et al., 2010), the whole fractionating procedure was carried out by a single person after 25 – 30 test runs to ensure individual reproducibility.

Density fractionation (Jacobs et al., 2009; Golchin et al., 1994) was applied to all soil samples. We conducted a series of pre-tests to define the most suitable experimental setting with respect to the density cut offs used to separate the free light fraction (flF) and the occluded light fraction (olF) and the amount of ultrasonic energy applied to disperse aggregates before the olF was separated (Cerli et al., 2012). The tested densities of the sodium polytungstate solution (SPT) ranged between 1.6 and 2.0 g cm^{-3} for both the flF and the olF and the tested ultrasonic energies ranged between 200 and 800 J cm^{-3}. The power output of the ultrasonic device (Digital Sonifier 250, Converter model 102C, Branson Utrasonics, Danburry, USA) and sonication settings were determined according to North (1976). For all samples, the most suitable density cut off was 1.8 g cm^{-3} to separate the flF and the olF. The used ultrasonic energies varied between 200 J cm^{-3} for the Tertiary Sand, 400 J cm^{-3} for the Loess and the Red Sandstone, 600 J cm^{-3} for the Basalt, and 800 J cm^{-3} for the Shell Lime Stone. Briefly, 6 g field moist soil sieved <2 mm were placed in a 70 ml centrifugation tube and 30 ml of SPT were added. The tube was then gently shaken manually five times upside down. The suspension was then allowed to settle down for 30 min before it was centrifuged for 30 min at 4000 g. The supernatant with the floating particles was decanted and vacuum filtered (<0.45 μm) and, afterwards, washed with 2 l deionized water to obtain the flF. The remaining soil pellet was transferred into a 50 ml glass beaker, mixed with 30 ml SPT and subsequently sonicated with the energies given above to disperse the aggregates and release the occluded POM. During sonication, the samples were cooled

(<45°C) with crushed ice surrounding the beaker. After disaggregation, the suspension was transferred back in the 70 ml centrifugation tube, allowed to settle down for 30 min, centrifuged at 4000 g. The supernatant was decanted and the soil pellet was again mixed with 30 ml SPT, centrifuged and decanted, which was then repeated one more time. The decanted supernatants were combined, filtered and washed as described above to obtain the olF. The remaining soil pellet represents the HF. To clean the HF from the remaining SPT as complete as possible, the pellet suspended in 1.5 l deionized water. To precipitate the HF, 0.5 M AlCl$_3$ solution (2.5 ml to 1l suspension) was added. The water was siphoned off and the HF was also vacuum filtered and washed with 0.5 l deionized water. All fractions were dried at 40°C and weighed.

3.3.4 FTIR spectroscopic analyses

The composition of the OM associated with the aggregate size fractions and the heavy fraction was evaluated using diffuse reflectance infrared spectroscopy (DRIFT) (Tensor 27, BRUKER, Ettlingen, Germany). The FTIR spectra of each ball milled sample was recorded in the range of wave numbers from 850 to 4000 cm^{-1} at resolution of 4 cm^{-1} by performing 200 scans using the Easy Diff unit (Pike Technologies, Medison, USA). Using the subroutine from OPUS 7.5 software (Bruker, Ettlingen Germany), all spectra were smoothed once and then baseline corrected. The heights of the absorption maxima (wavenumbers 2904 – 2908 cm^{-1} and 2876 – 2836 cm^{-1}) in the "aliphatic" region (Capriel et al., 1995) were added (band "A") and related to the maximum signal height at 1645 – 1605 cm^{-1} (band "B") representing the hydrophilic C=O functional groups in soil OM (Ellerbrock and Gerke, 2013; Kaiser et al., 2014). Several parameters are related to the height of the absorption maxima of band "B": (i) the abundance of ionizable carboxyl groups and the resulting cation exchange capacity of the OM in the sample, (ii) the hydrophilicity and the polarity of the OM in the sample, and (iii) the abundance of proteinaceous material such as microbial debris. By relating the "C=O" region to the "aliphatic" region of the FTIR spectrum, we thus obtain a numerical parameter "B/A" that allows a semi-quantitative comparison of samples while being soil ecological meaningful.

3.3.5 Statistical analyses

All statistical analyses were conducted with the statistical software R (Version 3.3.2; R Development Core Team 2016). Multiple linear regression analyses with stepwise variable

selection were carried out for the response variables given below. In all cases, a fixed effect for the factor site (levels: Basalt, Red Sandstone, Loess, Shell Lime Stone and Tertiary Sand) was kept in the models. The other predictors (given below) were only considered in the final models in case of significant contributions. Residuals were inspected for normality (graphically and using the Shapiro-Wilk test) and homoscedasticity (graphically). Analyses were carried out separately for the topsoil (i.e. surface) horizons (five sites, n = 3 per site) and the first subsoil (i.e. subsurface) horizons (five sites, n = 3 per site) because these horizons were present in all of the analysed sites whereas the second and the third subsoil horizons were present only in four and two of the analysed sites.

3.4   Results

3.4.1   Physico-chemical soil characteristics

Soil texture varied widely, whereby the clay content covered a range from 3.8 (Tertiary Sand) to 39.9 % (Shell Lime Stone). All soils were acidic with a pH between 3.2 and 4.9. The contents of Fe_{ox} and Fe_{dith} for topsoils were lowest in the Tertiary Sand (1.1 and 4.6 g kg^{-1}) and highest in the Basalt topsoil (8.3 and 24.1 g kg^{-1}). For the subsoil samples the contents of Fe_{ox} and Fe_{dith} ranged from 0.1 and 2.9 g kg^{-1} (Tertiary Sand) to 7.0 and 24.5 g kg^{-1} (Basalt) (Table 3.2). The highest CEC was found in the Shell Lime Stone topsoil (139.8 µmol g^{-1}) and subsoil (122.5 µmol g^{-1}) and the lowest for the topsoil (44.4 µmol g^{-1}) and the subsoil (8.2 µmol g^{-1}) in the Tertiary Sand (Table 3.2).

The SOC contents ranged from 23.4 to 104.3 g kg^{-1} in the topsoils and from 0.4 and 23.2 g kg^{-1} in the subsoils. In accordance with the SOC contents, the lowest amount of microbial biomass C (C_{mic}) for the subsoils was found in the Tertiary Sand and the Loess (12 mg kg^{-1}) and the highest (233 mg kg^{-1}) in the Basalt (Table 3.2). The amounts of CO_2 which were respired within 14 days ranged from 109.2 to 302.5 g CO_2-C kg^{-1} (Loess and Basalt) for the topsoil samples and from 7.8 to 46.5 g CO_2-C kg^{-1} (Red Sandstone and Shell Lime Stone) for the subsoil samples (Table 3.2).

Table 3.2: Parent material (Soil), sampling depths (Depth), texture (Sand, Silt, Clay), pH, contents of oxalate- and dithionite-soluble iron (Fe_{ox}, Fe_{dith}) and aluminum (Al_{ox}, Al_{dith}), cation exchange capacity (CEC), contents of the bulk carbon (C) and nitrogen (N), CN-ratios, contents of the microbial biomass C (C_{mic}) as well as cumulative amounts of respired CO_2 after 7 and 14 days of the samples from the analyzed soil horizons of the five study sites. The presented data are mean values of the replicated field samples and the standard errors given in parentheses (n = 3, except Basalt 40/50 – 80 and Loess 80/85 – 170/180: n = 2).

Soil	Depth [cm]	Sand	Silt [%]	Clay	pH	Fe_{ox}	Fe_{dith} [g kg^{-1}]	Al_{ox}	Al_{dith}	CEC [mmol kg^{-1}]	C [g kg^{-1}]	N	CN - ratio	C_{mic} [mg kg^{-1}]	Basal respiration after 7 days [g CO$_2$-C kg^{-1}]	after 14 days
Shell Lime Stone	0-10	2.2 (0.40)	65.2 (3.61)	32.6 (3.23)	4.5 (0.14)	2.6 (0.59)	13.8 (1.97)	2.5 (0.32)	4.1 (0.44)	139.8 (16.2)	52.8 (4.75)	3.5 (0.26)	15 (0.47)	1149.1 (138.5)	96.6 (3.65)	177.8 (10.0)
	10-30/50	1.1 (0.39)	58.9 (4.23)	39.9 (4.00)	4.4 (0.18)	1.9 (0.29)	15.0 (1.33)	3.3 (0.72)	4.7 (0.63)	122.5 (37.4)	14.1 (1.90)	1.1 (0.19)	13 (0.56)	186.8 (72.3)	25.7 (4.43)	46.5 (6.3)
Basalt	0-10	4.3 (0.04)	77.2 (2.29)	18.5 (2.33)	3.5 (0.13)	8.3 (1.37)	24.1 (1.02)	3.3 (0.45)	5.0 (0.59)	104.4 (17.2)	104.3 (13.73)	6.6 (0.94)	16 (0.35)	2685.7 (968.4)	160.5 (15.41)	302.5 (32.3)
	10-40/60	6.1 (1.00)	72.4 (3.11)	21.5 (3.02)	4.2 (0.19)	7.0 (1.33)	24.5 (0.29)	3.0 (0.68)	4.5 (0.70)	52.6 (5.0)	23.2 (4.62)	1.8 (0.44)	13 (0.74)	233.0 (32.0)	22.3 (2.80)	41.2 (5.8)
	40/50-80	4.6 (0.06)	79.6 (3.66)	15.8 (3.60)	4.9 (0.16)	3.5 (0.15)	22.6 (6.53)	0.9 (0.10)	1.9 (0.18)	89.5 (26.2)	3.5 (0.02)	0.3 (0.00)	12 (0.09)	35.5 (6.2)	9.4 (0.07)	18.4 (0.4)
Red Sandstone	0-5/8	67.5 (0.48)	22.4 (0.87)	10.2 (0.82)	4.3 (0.21)	1.3 (0.05)	5.3 (0.10)	0.6 (0.02)	1.0 (0.07)	60.4 (6.5)	35.5 (3.59)	2.2 (0.20)	16 (0.21)	606.0 (86.1)	89.4 (5.26)	172.2 (4.9)
	5/8-43/50	67.3 (0.49)	23.6 (1.11)	9.0 (0.67)	4.1 (0.12)	1.4 (0.11)	5.4 (0.23)	1.2 (0.28)	1.4 (0.14)	24.2 (5.4)	6.5 (0.44)	0.4 (0.03)	16 (0.20)	129.0 (44.5)	11.0 (1.50)	18.2 (3.5)
	43/50-70/90	78.5 (4.87)	11.5 (1.06)	10.0 (3.82)	3.9 (0.01)	0.7 (0.41)	8.4 (0.78)	0.7 (0.16)	1.1 (0.14)	26.9 (7.9)	1.1 (0.14)	0.2 (0.03)	6 (0.06)	115.5 (82.8)	6.1 (0.70)	7.8 (1.8)
Tertiary Sand	0-7/10	78.2 (0.21)	16.1 (1.41)	5.7 (1.21)	3.2 (0.00)	1.1 (0.13)	4.6 (0.08)	0.7 (0.01)	1.3 (0.06)	44.4 (3.5)	70.0 (5.81)	3.6 (0.27)	20 (0.24)	1254.1 (132.5)	156.4 (32.56)	287.1 (55.0)
	7/10-20/30	80.5 (0.81)	13.3 (0.29)	6.2 (0.59)	3.7 (0.11)	2.0 (0.10)	5.1 (0.17)	1.4 (0.12)	1.9 (0.20)	28.2 (4.3)	17.7 (1.85)	0.8 (0.10)	21 (0.28)	130.8 (22.4)	18.2 (2.93)	30.7 (5.0)
	20/30-63/70	84.4 (0.88)	10.9 (1.62)	4.7 (0.84)	4.2 (0.01)	1.1 (0.12)	3.9 (0.15)	1.7 (0.12)	1.9 (0.09)	8.2 (0.6)	3.6 (0.80)	0.3 (0.05)	13 (0.67)	26.9 (7.2)	4.5 (0.71)	10.4 (3.8)
	63/70-140/150	92.6 (0.70)	3.6 (1.11)	3.8 (1.35)	4.0 (0.01)	0.1 (0.04)	2.9 (0.16)	0.3 (0.05)	0.7 (0.08)	8.9 (1.1)	0.4 (0.01)	0.0 (0.00)	9 (0.43)	12.0 (1.4)	2.0 (0.43)	8.5 (1.5)
Loess	0-5/10	9.2 (2.63)	75.0 (4.19)	15.8 (1.95)	4.1 (0.15)	2.2 (0.17)	6.8 (0.33)	1.1 (0.09)	1.8 (0.21)	52.7 (9.3)	23.4 (1.61)	1.6 (0.13)	14 (0.27)	521.8 (58.9)	55.8 (5.70)	109.2 (11.7)
	5/10-45/50	8.8 (2.06)	76.0 (2.40)	15.2 (1.15)	3.7 (0.03)	2.1 (0.15)	7.2 (0.55)	1.2 (0.11)	2.1 (0.10)	35.0 (4.1)	7.7 (0.18)	0.5 (0.02)	15 (0.66)	108.8 (14.9)	8.7 (3.77)	13.5 (3.9)
	45/50-75/85	5.7 (1.87)	73.7 (2.32)	20.6 (3.26)	3.9 (0.05)	2.2 (0.33)	8.2 (0.51)	1.2 (0.04)	2.3 (0.11)	50.5 (15.9)	3.2 (0.10)	0.2 (0.02)	13 (1.15)	24.6 (4.9)	5.1 (0.54)	8.0 (0.5)
	80/85-170/180	15.2 (4.73)	67.5 (4.44)	17.3 (0.29)	4.2 (0.08)	1.0 (0.09)	8.8 (0.84)	0.8 (0.14)	1.9 (0.11)	69.4 (4.4)	2.3 (0.90)	0.2 (0.01)	9 (2.76)	11.9 (3.3)	8.7 (0.97)	11.8 (1.5)

Amount and composition of organic matter associated with aggregate size and density fractions in relation to depth and mineral characteristics of five different forest soils

3.4.2 Aggregate size and density fractions

The majority of the topsoil SOC of the Shell Lime Stone and the Red Sandstone, respectively, was stored in the macro-aggregates >1000 µm (34.7 and 24.2 g OC kg^{-1}) (Table 3.3). Whereas the major part of SOC of the topsoils of the Basalt and the Tertiary Sand with 45.7 and 34.7 g OC kg^{-1}, representing 54 %, was stored in the macro-aggregates 1000 – 250 µm (Table 3.3). Except for the Shell Lime Stone, where 65 % of the OC of the depth 10 – 30/50 cm was stored in macro-aggregates (>1000 µm), the importance of macro-aggregates (>1000 µm and 1000 – 250 µm) decreased and the importance of micro-aggregates (250 – 53 µm) and of the silt- and clay-sized fraction (<53 µm) increased with increasing soil depth (Figure 3.1).

Table 3.3: Contents of organic carbon associated with aggregate size fractions and density fractions in different sampling depths of the five sites, mean values of the replicated field samples and standard errors given in parentheses (n = 3, except Basalt 40/50 – 80 and Loess 80/85 – 170/180: n = 2).

| Soil | Depth | Aggregate size fractions | | | | Density fractions | | | |
| | | > 1000 µm | 1000-250 µm | 250-53 µm | < 53 µm | fIF | | oIF | HF |
	[cm]	[g OC kg^{-1}]				[g OC kg^{-1}]			
Shell Lime Stone	0-10	34.67 (7.74)	10.80 (1.81)	1.92 (0.50)	0.58 (0.19)	1.85	(0.27)	18.27 (2.28)	27.93 (3.80)
	10-30/50	9.04 (3.26)	2.84 (1.09)	0.81 (0.26)	0.25 (0.08)	0.92	(0.10)	3.84 (0.30)	9.63 (1.59)
Basalt	0-10	24.41 (10.15)	45.65 (8.52)	15.44 (5.05)	1.86 (0.07)	36.70	(13.80)	26.38 (1.81)	35.20 (2.50)
	10-40/60	3.16 (1.07)	11.73 (1.23)	6.53 (2.19)	1.04 (0.33)	1.19	(0.38)	2.82 (0.39)	18.61 (4.32)
	40/50-80	0.39 (0.18)	1.22 (0.05)	1.43 (0.15)	0.51 (0.02)	0.27	(0.21)	0.19 (0.06)	3.07 (0.08)
Red Sandstone	0-5/8	24.17 (5.83)	10.44 (2.71)	2.71 (1.45)	0.22 (0.02)	5.30	(1.64)	12.39 (3.91)	14.92 (0.66)
	5/8-43/50	1.57 (0.37)	1.59 (0.20)	1.61 (0.11)	0.35 (0.04)	1.19	(0.13)	2.19 (0.12)	3.59 (0.10)
	43/50-70/90	0.24 (0.07)	0.13 (0.03)	0.41 (0.06)	0.20 (0.06)	0.14	(0.08)	0.09 (0.02)	0.78 (0.11)
Tertiary Sand	0-7/10	23.08 (4.50)	34.71 (8.70)	5.23 (0.81)	0.46 (0.13)	33.29	(2.27)	28.82 (6.28)	5.65 (0.60)
	7/10-20/30	1.65 (0.26)	14.32 (2.63)	2.28 (0.17)	0.22 (0.02)	4.10	(0.40)	3.85 (0.60)	9.42 (0.65)
	20/30-63/70	0.12 (0.04)	2.30 (0.47)	1.08 (0.30)	0.06 (0.01)	0.68	(0.40)	1.36 (0.50)	2.48 (0.57)
	63/70-140/150	0.02 (0.02)	0.10 (0.01)	0.23 (0.01)	0.05 (0.03)	0.00	(0.00)	0.00 (0.00)	0.28 (0.07)
Loess	0-5/10	9.07 (0.38)	9.28 (2.02)	1.99 (0.46)	0.80 (0.04)	0.78	(0.27)	6.49 (1.03)	14.07 (0.82)
	5/10-45/50	0.19 (0.03)	4.03 (0.28)	1.41 (0.13)	0.48 (0.03)	0.95	(0.02)	1.61 (0.07)	3.54 (1.09)
	45/50-75/85	0.03 (0.02)	0.48 (0.12)	1.12 (0.15)	0.33 (0.07)	0.57	(0.06)	0.92 (0.51)	2.09 (0.35)
	80/85-170/180	0.00 (0.00)	0.10 (0.03)	0.64 (0.06)	0.31 (0.03)	0.00	(0.00)	0.46 (0.07)	0.95 (0.01)

In the topsoil of the Basalt and of the Tertiary Sand 36.7 or 33.3 g OC kg^{-1} was found in the fIF representing 35 and 50 % of the SOC. In the Red Sandstone and the Tertiary Sand, 37 or 42 % of the total topsoil SOC was stored in the oIF (12.4 and 28.8 g OC kg^{-1}) (Table 3.3, Figure 3.1). The lowest amounts of fIF for the subsoils were found in the Tertiary Sand and the Loess (0 g OC kg^{-1}) and the highest in the first subsoil horizon of the Tertiary Sand (4.1 g kg^{-1}), representing 23.6 % of the total SOC of the corresponding horizon. For the oIF

the amounts in the subsoil horizons ranged between 0 and 3.9 g OC kg^{-1} (both Tertiary Sand), whereas the percentages ranged from 0 % (Tertiary Sand) to 31.5 % (Red Sandstone). In all sampled subsoil horizons more than 50 % of the total SOC was stored in the heavy fraction (HF), with growing importance with increasing soil depth (Figure 3.1). However, the SOC contents in the heavy fractions varied widely between 0.3 and 18.6 g OC kg^{-1} for the subsoil and between 5.7 and 35.2 g OC kg^{-1} for the topsoil samples (Table 3.3).

Amount and composition of organic matter associated with aggregate size and density fractions in relation to depth and mineral characteristics of five different forest soils
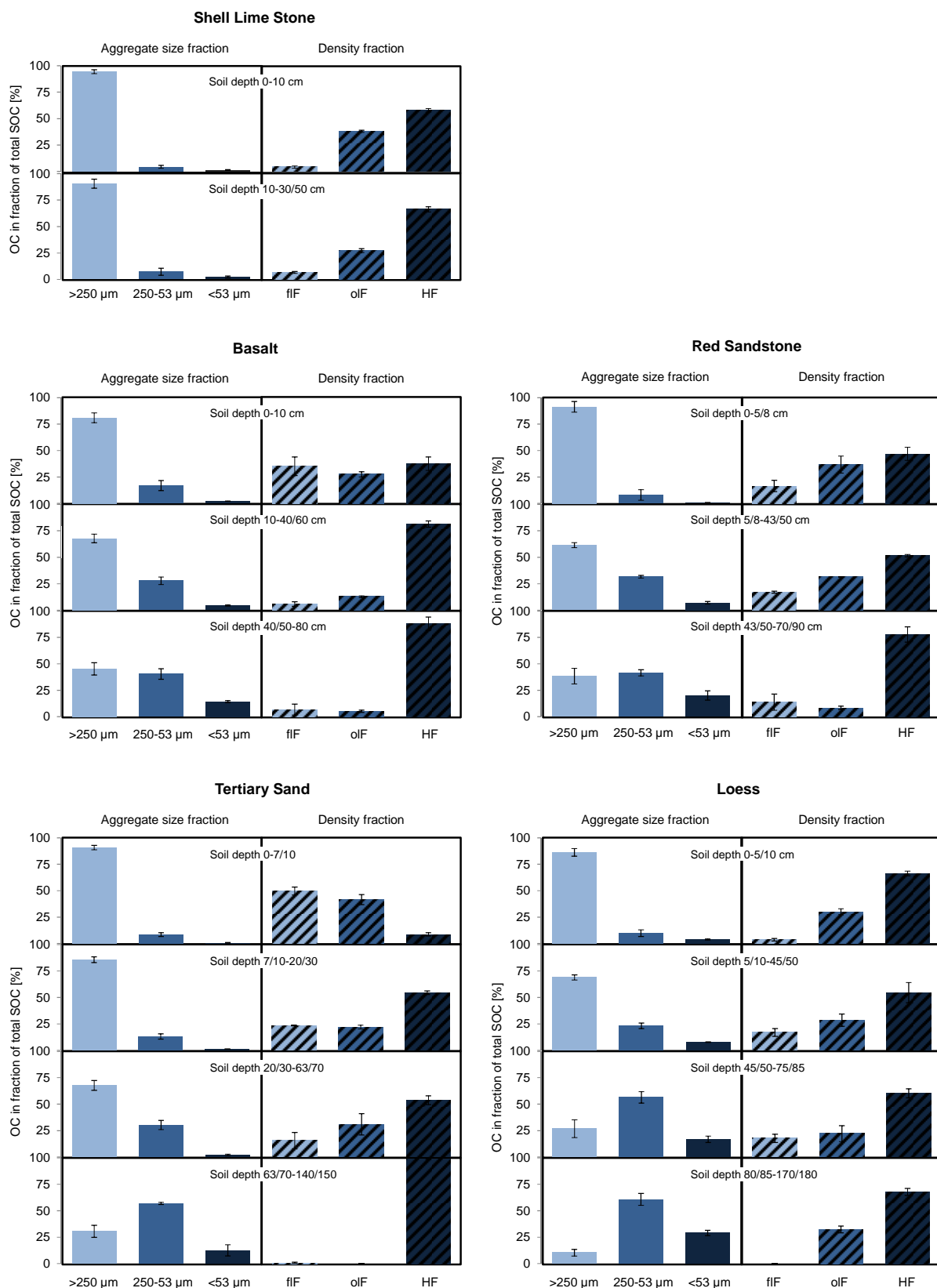
Figure 3.1: Distribution on a percentage basis of the soil organic carbon in the separated aggregate size fractions (macro-aggregates >250 µm, micro-aggregates 250 – 53 µm, fraction >53 µm; left box, unicolored) and in the density fractions (free light fraction – flF, occluded light fraction – olF, heavy fraction – HF; right box, striped) for each sampled soil horizon of the five sites. Given are the mean values (n = 3, except Basalt 40/50 – 80 and Loess 80/85 – 170/180 n = 2).

3.4.3 FTIR spectroscopic analyses

The B/A ratios for all fractions and sites were lowest in the topsoil ranging between 3.8 and 13.3 for both macro-aggregate fractions, between 4.7 and 34.5 for the micro-aggregates and the fraction <53 µm and between 8.2 and 52.8 for the HF. The B/A ratios increased with increasing soil depth and ranged for the subsoil horizons from 10.7 to 108.2 for the macro-aggregate fractions, from 9.4 to 175.6 for the micro-aggregates and the fraction <53 µm and from 22.3 to 162.3 for the HF (Figure 3.2).
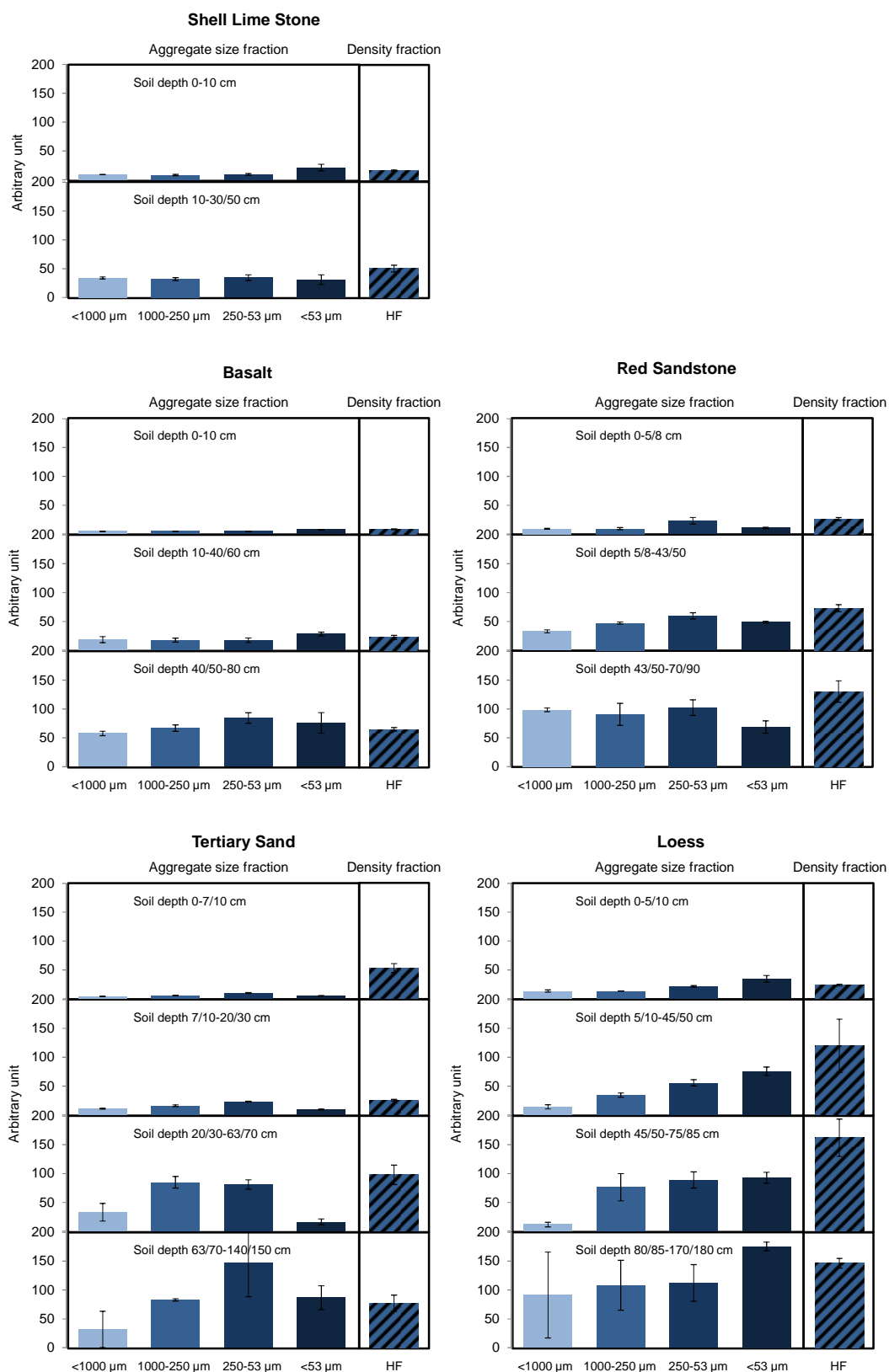
Figure 3.2: B/A ratios obtained of the FTIR spectroscopic analyses of the respective aggregate size fractions (>1000 µm, 1000 – 250 µm, 250 – 53 µm, <53 µm, unicolored) and the heavy fraction (striped) of each sampled soil horizon of the five investigated sites. Given are the mean values of the field replicates (n = 3, except Basalt 40/50-80 and Loess 80/85 – 170/180 n = 2).

3.4.4 Regression analyses

For the subsurface soil horizons, we aimed to describe SOC contents as a function of site and contents of Fe_{ox}, Al_{ox}, silt and clay. Stepwise model reductions resulted in a final model consisting of site and Fe_{ox} (Table 3.4, Figure 3.3). The same model was used for the surface soil horizons, where also Fe_{ox} was a significant predictor besides site (Table 3.4, Figure 3.3).

Table 3.4: Linear regressions for different target variables by additionally considering the sites. The equations are the results of stepwise model simplifications. Only regression terms with significant contributions were considered.

Response variable	Intercept	Site effect	Regression terms
		Topsoil	
SOC [g OC kg^{-1}]	37.47 g kg^{-1}	Red Sandstone: -12.67 g kg^{-1} Loess: -31.68 g kg^{-1} Shell Lime Stone: -5.62 g kg^{-1} Tertiary Sand: 23.68 g kg^{-1}	+8.01 * Fe_{ox}
Ln(C$_{mic}$) [ln(mg kg^{-1})]	5.64	Red Sandstone: 0.02 Loess: 0.13 Shell Lime Stone: 0.31 Tertiary Sand: 0.05	+0.02 * SOC
oIF [g OC kg^{-1}]	-5.33 g kg^{-1}	Red Sandstone: 6.93 g kg^{-1} Loess: 4.71 g kg^{-1} Shell Lime Stone: 7.54 g kg^{-1} Tertiary Sand: 12.86 g kg^{-1}	+0.30 * SOC
		Subsoil	
SOC [g OC kg^{-1}]	-1.37 g kg^{-1}	Red Sandstone: 3.09 g kg^{-1} Loess: 1.55 g kg^{-1} Shell Lime Stone: 8.79 g kg^{-1} Tertiary Sand: 12.21 g kg^{-1}	+3.51 * Fe_{ox}
C$_{mic}$ [mg kg^{-1}]	-56.40 mg kg^{-1}	Red Sandstone: 63.72 mg kg^{-1} Loess: -39.04 mg kg^{-1} Shell Lime Stone: -294.07 mg kg^{-1} Tertiary Sand: 103.35 mg kg^{-1}	+ 13.45 * clay
oIF [g OC kg^{-1}]	0.02 g kg^{-1}	Red Sandstone: 1.40 g kg^{-1} Loess: 0.66 g kg^{-1} Shell Lime Stone: 2.12 g kg^{-1} Tertiary Sand: 1.70 g kg^{-1}	+0.12 * SOC

The initial model for C_{mic} in the subsurface soil horizons consisted of site and the predictors SOC, silt, clay, Ca and Mg. Besides site, the final model after model simplification had clay as a significant predictor (Table 3.4, Figure 3.3). This model did not hold for the surface soil horizons. The optimal model for these horizons had log-transformed (ln) C_{mic} as response variable and site and SOC as significant predictors (Table 3.4, Figure 3.3).
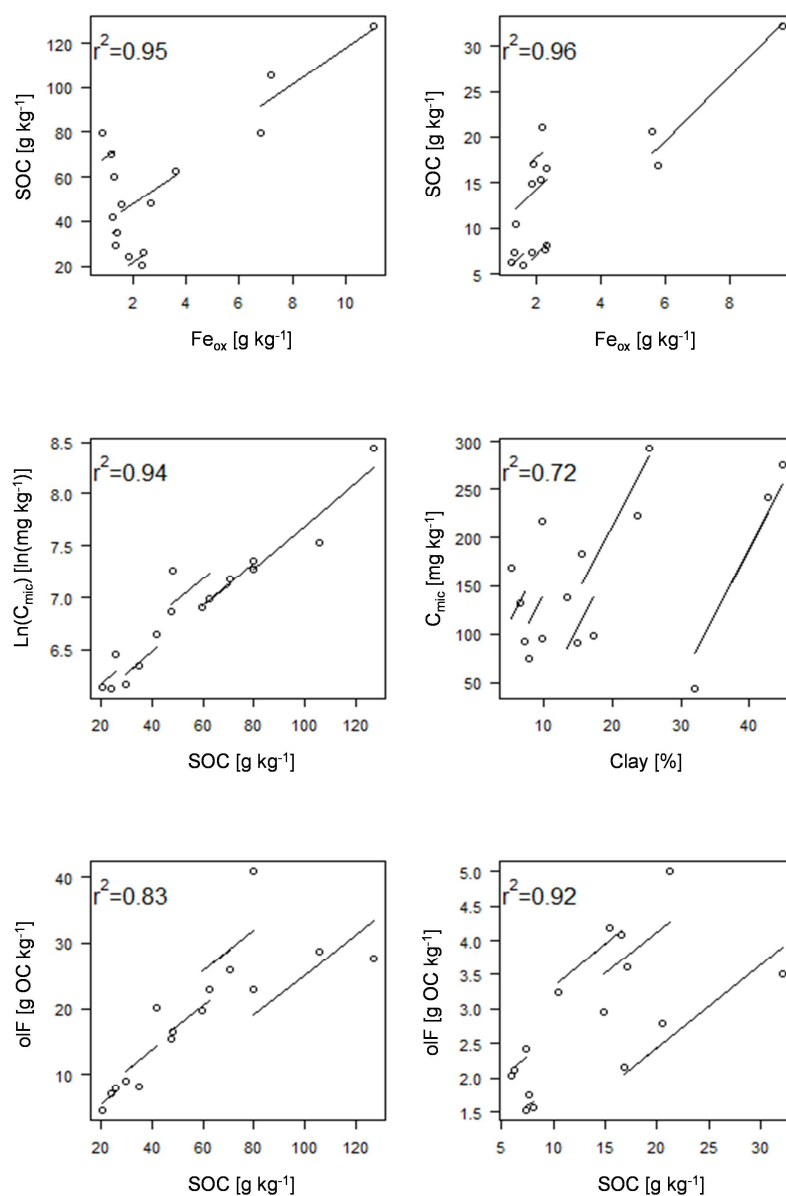
Figure 3.3: Experimental data (symbols) and results of linear regressions by additionally considering the factor site for the target variables SOC, C_{mic} and olF in the surface (left) and subsurface soil horizons (right).

We tested for the OC of the different aggregate size and density fractions (g OC kg^{-1} soil) as response variables significant predictors (such as SOC, silt, clay, Fe_{ox}, Al_{ox} and/or Ca) besides site. After stepwise variable selection, the final models for the surface and subsurface soil horizons revealed only the SOC as a significant predictor for the OC in the olF fraction (Table 3.4, Figure 3.3).

3.5 Discussion

3.5.1 General trends in OM dynamics as affected by soil depth and soil type

Irrespective of the soil type, the content of the bulk OC is decreasing with increasing soil depth confirming results from previous studies (e.g., Schrumpf et al., 2013; Rumpel et al., 2002). The depth specific total OC contents and the magnitude of the decrease in the OC content is, however, soil type specific. For the topsoil as well as for the subsoil, we found positive relationships between the contents of bulk SOC and Fe_{ox}. This points towards a site and depth independent positive effect of poorly crystalline Fe-oxides on the OC storage in acidic soils under mature beech forest thereby confirming results from previous studies (e.g., Zhao et al., 2016; Wiseman and Püttmann, 2006).

A general decrease with increasing soil depth can also be observed for the OC contents associated with most of the separated aggregate size and density fractions, which has been reported in the literature as well (e.g., Angst et al., 2016). This general pattern cannot be detected for the relative contributions of the OC associated with the separated fractions of the bulk SOC (see point 4.3.1). The same holds true for the composition of the OM because the relative C=O group amount of the OM associated with the different fractions is not constantly decreasing with an increase in the soil depth (see point 4.3.2).

We also observed a decrease in the cumulative CO_2-C emissions after 14 days and in the microbial biomass C (C_{mic}) contents with increasing soil depth irrespective of the soil type. Independent of the site, we detected for the topsoil a positive relationship between the contents of C_{mic} and the bulk SOC whereas for the subsoil the C_{mic} content was positively related to the clay content. Functioning as sources for nutrients and water, clay sized particles seems to be of increasing importance for the biomass of microorganisms in the substrate limited subsoil environment as compared with the topsoil. This would also mean that the clay content of the subsoil is not only positively affecting the OC stabilization but also the abundance of the OM decomposers.

In contrast to the CO_2-C emissions and the C_{mic} contents, the CO_2-C/SOC and CO_2-C/C_{mic} ratios generally show for the subsoil horizons of all study sites the reverse trend resulting in distinct differences between the topsoil horizons (depth range: $0 – 5/10$ cm) and the deepest subsoil horizons of the Loess and the Tertiary Sand (depth range: $63/70 – 170/180$ cm). For the topsoil horizon (n = 5), the means and standard errors of the CO_2-C/SOC and CO_2-C/C_{mic} ratios are 4.01 ($\pm$ 0.36) and 0.21 ($\pm$ 0.03). The mean values and standard errors for the first (n = 5), second (n = 4) and third (n = 2) subsoil horizon for the CO_2/SOC ratios are, respectively, 2.28 ($\pm$ 0.32), 4.70 ($\pm$ 1.33), 13.34 ($\pm$ 7.11) and these for

the CO_2/C_{mic} ratios are 0.23 (± 0.05), 0.37 (± 0.08), 0.96 (± 0.13). These data suggest an increase in the relative proportion of labile OM and a decrease in the microbial substrate use efficiency with increasing soil depth and confirm results from other studies (e.g., Wordell-Dietrich et al., 2016; Salomé et al., 2010; Agnelli et al., 2004; Joergensen et al., 2002).

Wordell-Dietrich et al. (2016) detected for a nutrient and OM poor Cambisol developed on Pleistocene fluvial and aeolian sandy deposits under mature beech forest that 0.7 % of the SOC in the deep subsoil (depth range: 130 – 160 cm) was respired over the course of 63 days. In contrast, only 0.2 % were respired from the SOC of the topsoil (depth range: 2 – 12 cm) and the shallow subsoil (depth range: 30 – 60 cm). This is generally confirmed by our data because we found for the topsoil horizon (n = 5, mean and standard error) that 6.6 % (± 0.62) of the SOC was respired within 14 days whereas 3.8 % (± 0.54), 7.5 % (± 1.91) and 21.2 % (± 12.6) of the SOC of the, respectively, first (n = 5), second (n = 4) and third (n = 2) subsoil horizon were respired.

However, is has to be taken into account that the standard errors for the mean CO_2-C/SOC ratio and, consequently, for the relative proportion of respired SOC are highest for the third subsoil horizon compared to the other soil horizons under study. This suggests a strong effect of the site specific conditions on the relative amount of labile OM in these deepest subsoil horizons. For the third subsoil horizon of the Loess (80/85 – 170/180 cm) and the Tertiary Sand (63/70 – 140/150 cm) we detected that 8.6 % and 33.8 %, respectively, of the SOC were respired. The Loess in this depth shows an about four times higher clay content and an about ten times higher Fe_{ox} content than the Tertiary Sand, which should have resulted in better protection of the OM by interactions with clays sized mineral particles such as poorly crystalline Fe-oxides in the third subsoil horizon of the Loess. However, for the Tertiary Sand and the Loess, the differences between the topsoil and the subsoil horizons in the contents of clay and Fe_{ox} or in the pH do not explain the detected differences in the relative proportion of the labile OM. One might speculate here, that a higher degree of specialisation of microorganisms, a higher amount of microbially processed dissolved OM (Kaiser and Kalbitz, 2012) and a lower microbial C use efficiency (Wordell-Dietrich et al., 2016) are contributing to the higher relative proportion of labile OM in third subsoil horizons compared to the topsoils of the Loess and Tertiary Sand. However, to further unravel this pattern, mechanistically and quantitatively, more extensive research is required.

3.5.2 Organic matter distribution and composition in the topsoil

3.5.2.1 Distribution of organic matter

In the analyzed A-horizons that covered a depth range from 0 to 5/10 cm, 81 to 94 % of the total OC is stored within both macro-aggregate fractions (>250 μm), indicating that macro-aggregates are of major importance for the OC storage in topsoils under mature beech forest. In contrast, only 4 to 17 % of the OC is stored in micro-aggregates (250 – 53 μm) and 0.5 to 4 % in the silt and clay sized fraction (<53 μm). Based on the inverse relationship between aggregate size and the stability of the associated OM (Liao et al., 2006; John et al., 2005; Tisdall and Oades, 1982), only a small proportion of the OC in the analyzed forest topsoils can be considered as effectively stabilized against microbial decomposition.

The proportion of the OC content associated with the fIF, which mainly represents non-aggregated plant particles, of the bulk SOC is highly variable and site specific and accounts for 4 % in the Shell Lime Stone and Loess and for 16 to 50 % in the three other soils. The data indicate that especially in the Basalt (35 %) and the Tertiary Sand (50 %) a large proportion of OM can be found in form of physically unprotected plant particles and is, therefore, easily susceptible to microbial decomposition (Gregorich et al., 2006). The proportion of OC associated with the oIF, which mainly represents aggregate occluded plant particles, shows a smaller range than the fIF (27 – 42 %) but also contributes largely to the SOC storage. The oIF was shown to be more stable than the fIF due the protection against microbial decomposition by occlusion in aggregates (Salomé et al., 2010; Rasmussen et al., 2005). Consequently, the effect of this fraction on the topsoil OC storage should be stronger and longer lasting than the effect of the fIF. This is corroborated by the relationship between the contents of the bulk SOC and the OC associated with the oIF, which could be detected site independently for the topsoil as well as for the subsoil. Similar to Schrumpf et al. (2013), we could not identify specific soil mineral characteristics explaining the differences in the OC concentrations associated with the oIF. This might be explained by the fact that the separated oIF integrates plant particles that are occluded within aggregates of different size, which are disrupted by the application of ultrasound during the fractionation. The released and separated oIF represents, therefore, a mixture of plant residues that are protected against microbial decomposition to different degrees, which is in turn governed by the contributors mainly controlling the aggregate formation at different scales.

The OC content associated with the HF ranged from 9 % for the Tertiary Sand to 38 and 47 % for the Basalt and Red Sandstone and to 58 % and 66 % for the Loess and Shell

Lime Stone. Considering the HF fraction as representative for OM that is protected against microbial decomposition by associations with the soil mineral phase (e.g., Hatton et al., 2012; Pronk et al., 2012; Sollins et al., 2009; Sollins et al., 2006) these relative proportions imply a much higher amount of stabilized OM compared to the data derived from the <53 µm fraction. Similar to the oIF, the HF recovers material that is part of aggregates of different size being disrupted during the density fractionation and those that are not occluded in aggregates. The HF is, consequently, a measure for the amount of OC associated with minerals independent from their location within the soil matrix and the size of the mineral particles (>1.8 g cm^{-3}) the OM is associated with.

3.5.2.2 Composition of organic matter

The relative C=O group amount of the OM is of major importance for the formation of organo-mineral complexes and aggregates because especially reactive carboxyl groups (i.e. -COO^{-}/H) are involved in ligand exchange reactions, co-precipitation and cation mediated interactions between organic and inorganic soil compounds, which can result in the formation of stable OM-mineral associations (Kleber et al., 2007; Mikutta et al., 2007; Mikutta et al., 2006). In the topsoil horizons, the relative C=O group amounts (i.e. B/A ratios) of both macro-aggregate fractions for all sites are similar indicating that the composition of the OM associated with the macro-aggregates is not largely varying among the different sites. Similar B/A ratios were found for the OM associated with the other fractions of the investigated sites with the following exceptions. Higher B/A ratios could be detected for the OM associated with the i) micro-aggregates (250 – 53 µm) of the Red Sandstone and the Loess, ii) the fraction <53 µm of the Shell Lime Stone and the Loess and iii) the HF of the Basalt, the Tertiary Sand and the Loess. This indicates that the OM recovered in these fractions is selectively enriched in C=O groups and more reactive towards the mineral phase than the OM separated with the other fractions.

3.5.3 Organic matter distribution and composition in the subsoil

3.5.3.1 Distribution of organic matter

Especially in the first subsoil horizon, the macro-aggregates (>1000 µm fraction + 1000 – 250 µm fraction), mostly representing less stabilized OM, account for 61 to 91 % of the bulk SOC thereby exerting a strong overall influence on the SOC storage in the depth range from 5/10 to 30/60 cm (respective range over all five sites). For all of the analyzed soils, we found a decreasing relative proportion of the OC associated with macro-aggregates

(>250 µm) of the bulk SOC with an increase in soil depth. This depth distribution shows the reverse trend compared to the CO_2-C/SOC data indicating that this fraction seems to be less relevant for the relative increase in easily available OM in the subsoil.

For the three subsoil horizons, between 7 and 61 % were stored in micro-aggregates and between 2 and 29 % were stored in the <53 µm fraction. Interestingly, the Loess showed for the second and third subsoil horizon the highest proportions of OC in both of the fractions. Consequently, the OM stabilization with increasing soil depth by aggregation processes seems to be strongly affected by the soil type. In contrast to the macro-aggregates (>250 µm), we detected a general increase in the relative proportion of the bulk SOC with increasing soil depth for the micro-aggregates and the <53 µm fraction. This suggests that the relative proportion of the stabilized OM is increasing with soil depth, which is corroborated by the depth distribution of the relative proportion of the HF (see below). In conjunction with the detected increase in the relative proportion of easily decomposable OM with soil depth, this suggests a stronger separation of the bulk soil OM into a labile and a stable pool with increasing soil depth and a decreasing importance of the intermediate pool for the OM storage and turnover.

For the Basalt, Red Sandstone and Tertiary Sand, the relative proportions of the OC content associated with the fIF of the bulk SOC are decreasing by trend with increasing soil depth confirming results from previous studies (Angst et al., 2016; John et al., 2005). For the Loess, however, we found a distinct increase from 4 % in the topsoil to 17 – 18 % in the first and second subsoil horizon (depth range: 5/10 – 75/85 cm). This might be derived from higher bioturbation and better conditions for root growth in the Loess subsoil compared to the other subsoils under study. Similar to the macro-aggregates, the depth distribution of the bulk SOC proportions of the fIF, representing free, easily available organic particles, is mostly reverse to the increase in the relative amount of easily decomposable OM with depth. Therefore, the main source of the respired subsoil OM is less explainable with the data from the OM fractions analyzed within this study and requires further research. For the fIF, a further separation into different particle size fractions might provide a more specific differentiation regarding the decomposability of the organic particles separated with this fraction.

The OM present in the subsoil in form of aggregate occluded organic particles as separated with the oIF accounted for 13 to 31 % of the bulk OC in the first subsoil horizons of the studied sites and for 0 to 32 % in the second and third subsoil horizons. In the third subsoil horizon (depth range: 80/85 – 170/180 cm) of the Loess profile, we found the highest relative proportion of the oIF of the bulk subsoil OC (32 %). Interestingly, we could not detect

any flF associated OC, which could mean that organic particles entering this subsoil horizon are immediately occluded within aggregates. This is in contrast to the third subsoil horizon of the Tertiary Sand (depth range: 63/70 – 140/150 cm) where no OM could be separated with the oIF. As explanations might serve a deeper rooting depth and stronger aggregation because of more reactive minerals in the Loess as compared with the Tertiary Sand.

Similar to the topsoils, a considerable higher proportion of OC might be considered as stabilized if considering the HF than the <53 µm fraction. Nevertheless, both fractions show generally increasing contributions to the total OC with an increase in soil depth (except for the HF of the Loess), which is in line with previous studies (e.g., Schrumpf et al., 2013). The OC associated with the HF thereby ranged from 52 to 81 % in the first subsoil horizons, from 54 to 88 % in the second and from 68 to 99 % in the third subsoil horizons of the investigated forest sites. Several studies showed slower specific mineralization rates with increasing contributions of OC associated with the HF to the bulk SOC (e.g., Schrumpf et al., 2013; Kalbitz et al., 2005), which indicates a greater stability against microbial decomposition of the soil OM, especially with increasing soil depth (Schrumpf et al., 2013). This assumption is corroborated by higher ^{14}C ages and therefore higher mean residence times for OM in the subsoil compared to the topsoil (Rumpel and Kögel-Knabner, 2011; Kögel-Knabner et al., 2008; Rumpel et al., 2002).

However, for the third subsoil horizon of the Tertiary Sand, we found 99 % of the OC associated with the HF suggesting that almost all of the OM in this horizon is associated with minerals. On the other hand, we detected for this horizon the highest relative amount of easily decomposable OM because about 33 % of the bulk SOC was respired during the two weeks incubation experiment as discussed above. This confirms studies reporting that fractions indicative for mineral-associated OM contain a certain proportion of fast cycling OM (Torn et al., 2013; Mikutta and Kaiser, 2011). Because we could barely detect any OM associated with the flF or the oIF, we assume the OM in this subsoil horizon to be mainly derived from microbially processed, dissolved OM (Kaiser and Kalbitz, 2012), which is weakly associated to the mineral phase because this is mainly consisting of less reactive sand size particles. Abiotic desorption processes as reported by Saidy et al. (2013) might then control the microbial decomposition of the mineral-associated OM.

3.5.3.2 Composition of organic matter

In general, the B/A ratios of the OM associated with the aggregate size fractions and the HF were increasing with an increase in soil depth suggesting a change in the composition of the OM with soil depth (Figure 3.2). The magnitude of the B/A ratio as a

measure for the relative C=O group content of the OM tends to vary as a function of the degree of microbial oxidative decomposition (adding oxygen containing functional groups to the processed substrate) and as a function of the concentration of amides (containing carbonyl groups) as derived from proteinaceous microbial debris (e.g., Kaiser et al., 2014). Therefore, the increase in the B/A ratio with soil depth suggests an increasing proportion of the bulk OM of microbially derived and increasingly microbially processed OM, which corroborates with previous findings (e.g., Kaiser and Kalbitz, 2012).

3.6   Conclusions

For the investigated forest topsoil under mature beech only a small portion of the OC can be considered as effectively stabilized against microbial decomposition because the majority of the topsoil OC is stored within macro-aggregates (>250 µm). In the analyzed forest subsoils, a higher proportion of the bulk SOC is stabilized against microbial decomposition because the relative amount of OM associated with highly stable aggregates (<53 µm) and/or the mineral phase (i.e. separated as HF) increased with increasing soil depth. Contrary to the enhanced OC stabilization with increasing soil depth, an additional increase in the relative proportion of labile OM with increasing soil depth was found, which suggests a stronger separation into a labile and a stable OM pool in the subsoil compared to the topsoil on the cost of the intermediate OM pool. For both the topsoil and the subsoil, the OM associated with the HF tends to have relatively higher C=O groups amounts as compared to the OM separated with the aggregate size fractions suggesting an enrichment of OM with a higher degree of microbial processing in the HF. The microbial imprint on the composition of the OM seems also to increase with increasing soil depth.

3.7   Acknowledgements

4 Estimation accuracies of near infrared spectroscopy for general soil properties and enzyme activities for two forest sites along three transects

Bernard Ludwig [a]*, Svendja Vormstein [a], Jana Niebuhr [b], Stefanie Heinze [b],
Bernd Marschner [b], Michael Vohland [c]

[a] *Department of Environmental Chemistry, University of Kassel, Nordbahnhofstr. 1a, 37213 Witzenhausen, Germany*

[b] *Soil Science and Soil Ecology, Ruhr-Universität Bochum, Universitätsstr. 150, 44801 Bochum, Germany*

[c] *Geoinformatics and Remote Sensing, Institute for Geography, Leipzig University, Johannisallee 19a, 04103 Leipzig, Germany*

* Correspondence: B. Ludwig, E-mail: bludwig@uni-kassel.de

4.1 Abstract

Visible and near infrared spectroscopy (vis-NIRS) is an established method for estimating the contents of soil organic carbon (SOC) and soil nitrogen (N). Recent studies have suggested that it may also be useful for estimating enzyme activities, however this potential has not been explored in detail. Objectives were to determine estimation accuracies of vis-NIRS for general soil properties (SOC, N, pH, texture) and nine enzyme activities for two forest sites, one on a sandy soil (Grinderwald) and the other on a loess soil (Rüdershausen). For each site, a calibration sample consisting of two transects sampled down to 185 cm (Grinderwald: 128 units, Rüdershausen: 64 units) and an independent validation sample consisting of one transect (Grinderwald: 64 units, Rüdershausen: 32 units) was obtained and their absorbance spectra recorded. Chemometric approaches included the standard partial least squares (PLS) regression and PLS regression with a genetic algorithm (GA-PLS) for variable selection, which may improve estimation accuracies. This study confirmed the marked usefulness of vis-NIRS for an estimation of SOC and N contents in independent transects of a field scale. Estimation accuracy of soil pH and texture in independent transects was variable and mainly dependent on the range of measured data. GA-PLS markedly improved estimation accuracies compared to PLS in the cross-validation, but generally not in the validation transects. Few enzyme activities could be estimated in independent validation, but there was almost no additional benefit of vis-NIRS for their

estimations compared to estimations using measured contents of main properties; however, these contents of main properties may also be estimated with vis-NIRS. Overall, for the studied sites, we do not see a benefit of vis-NIRS for a direct estimation of enzyme activities compared to laboratory methods, most likely due to a lack of sufficiently strong specific impacts on the measured spectral signals.

Keywords: Enzyme activities, General soil properties, Genetic algorithm, Multiple linear regression, RPD, RPIQ, Partial least squares regression

4.2   Introduction

The application of near infrared (NIR) spectroscopy (NIRS, 800 – 2500 nm, vis-NIRS, 400 – 2500 nm) has been suggested to be useful for the estimation of a large number of soil properties, including   physical (e.g., particle size,   aggregation and   soil water), chemical (e.g., soil organic C (SOC), organic matter, macro- and micronutrients and pH) and biological (e.g., microbial biomass, respiration, enzymatic activities and microbial groups; Soriano-Disla et al., 2014). The accuracies of vis-NIR estimations, although probably less accurate than data obtained by wet-chemical analysis, may still be sufficient for many research goals. Vis-NIRS may be especially important for studies which require large data sets, such as for long-term monitoring of soil properties.

Standard procedures such as multiple linear regressions using distinct wavelengths (related to C\\H, C\\O and N\\H vibrations) and full spectrum partial least-squares (PLS) regression have been applied in many soil studies and have well established that vis-NIRS is especially useful for estimating SOC, N, carbonates, and clay content. In the case of SOC, for example, absorbances responsible for the successful estimations are in the visible range due to the dark color of soil organic matter (Baumgardner et al., 1985). In the NIR region, absorbances in the ranges near 1730, 1760, 1900, 2050, 2220 and 2300 – 2350 nm are important for organic matter absorption (Stenberg, 2010; Viscarra Rossel and Behrens, 2010; Vohland and Emmerling, 2011). The usefulness in estimating soil texture has been reported because of absorbances in the NIR region related to different clay minerals (Clark, 1999; Soriano-Disla et al., 2014). Contents of sand – typically mainly consisting of quartz and feldspars, which are relatively featureless – may be assumed to be estimated mainly as a mirror image of clay (Wetterlind and Stenberg, 2010).

A usefulness of vis-NIRS for pH estimations using the above-mentioned standard procedures has also been described. However, the underlying mechanism is less clear and may be related to contents of organic acids and carbonates (Reeves, 2010) or merely to

co-variations of vis-NIRS to organics and minerals (Stenberg et al., 2010). However, vis-NIRS is not sufficiently reliable to estimate soil properties for the entire range of soil textures. Stenberg (2010) reported that vis-NIRS may not be reliable for estimations in sandy soils because of the comparably featureless spectra of sand fractions in combination with a high reflectance, a relatively small total surface area of sand particles, and possible nonlinear effects resulting from unproportionally high absorbance by the dark organic matter.

The reliability of any vis-NIRS estimation is not only affected by soil texture, but also by a soil`s mineralogical composition and therefore it should be mandatory to present in each study what the underlying population for the studied sample is (Ludwig et al., 2016); an issue which has been generally neglected in many studies and which hampers a critical appraisal of the usefulness and limitations of vis-NIRS for soil studies. Soil enzymes respond to changed soil management more rapidly than many other soil quality indicators. Moreover, they play an important role in organic matter decomposition and nutrient cycling (Dick, 1994; Bandick and Dick, 1999). Unfortunately, laboratory-based screening of enzyme activities is time-consuming and requires a number of chemicals. Application of vis-NIRS may thus be beneficial for an estimation of enzyme activities, provided that specific spectral effects exist for different enzymes. Overall, the usefulness of vis-NIRS for estimating enzyme activities may be a matter of controversy. Zornoza et al. (2008) reported for 393 soils obtained by sampling thirteen locations over three years (i.e. pseudo-replicates were present in the studied set) in SE Spain that many biological properties – including the activities of the enzymes acid phosphatase and β-glucosidase – were estimated by vis-NIRS with excellent accuracies. Similarly, Dick et al. (2013) reported for 184 diverse soils of Ohio, USA, that r^2 values, testing variation between concentrations as estimated by vis-NIRS and measured by chemical methods, were 0.91 for SOC, 0.92 for amino sugar N, and 0.82 for both soil β-glucosidase and β-glucosaminidase enzyme activities. The authors concluded that vis-NIRS clearly is able to measure multiple soil properties with a single spectral scan. Regarding the spectral basis for the estimations of enzyme activities, Reeves et al. (2000) suggested that indirect correlations with C or N may only partially explain the NIR results and that measures of biologically active N may be the basis for enzyme activity determinations. Overall, Soriano-Disla et al. (2014) summarized that vis-NIRS was successfully employed to estimate biological properties and suggested that results are likely due to a strong correlation between the biological properties and the quantity and quality of soil organic matter. Specific signature wavelengths may also be responsible for the estimates (Soriano-Disla et al., 2014).

Besides the classical PLS regression for an estimation of properties, variable selection procedures combined with PLS regression may be more useful (Leardi et al.,2002).

The aim of variable selection is to reduce the number of independent variables and to only keep those variables that contain relevant information, which results in improved statistical modelling (Wehrens, 2011). Several studies employed a combination of a variable selection method, such as a genetic algorithm (GA) with PLS regression (GA-PLS) for estimations of soil properties and the results were promising and showed improved estimation accuracies and reduced spectral variables compared with the full spectrum PLS regression (Vohland and Emmerling, 2011; Shi et al., 2014).

Objectives were to determine estimation accuracies of vis-NIRS for general soil properties (SOC, N, pH, texture) and nine enzyme activities with PLS and GA-PLS regressions for two forest sites, one on a sandy soil (Grinderwald) and the other on a loess soil (Rüdershausen) along three transects. For enzyme activities results are analyzed so as to elucidate whether spectral predictions are based on specific spectral features being strong enough to markedly impact the measured vis-NIR signals or rather due to correlations with spectrally sensitive general soil properties.

4.3 Materials and methods

4.3.1 Soils

Three transects from the site Grinderwald, a beech forest, Lower Saxony, Germany were sampled (sample Grinderwald, n = 64 per transect). The soil is a Dystric Cambisol (IUSS Working Group WRB, 2015) developed on glacio-fluviatile sandy deposits from the Saale glaciation (Cosack and Heinz, 1980). Each transect was established in the vicinity of a main tree (*Fagus sylvatica L.)* and had a depth of 2 m and a length of 3.15 m. Soils were taken from the depths 10, 35, 60, 85, 110, 135, 160 and 185 cm. In each depth, eight soils were taken in a distance of 45 cm from each other.

Additionally, three transects from the beech forest site Rüdershausen, Lower Saxony, Germany were sampled (sample Rüdershausen, n = 32 per transect). The soil is a Luvisol developed on loess. Again, each transect was established in the vicinity of a main tree. Soils were taken from the same depths as in the Grinderwald site, but at each depth only four soils at a distance of 45 cm from each other were sampled.

4.3.2 Laboratory analyses

A subunit of each sieved soil was dried over 3 days at 50°C for chemical analysis. Prior to the measurement of SOC and nitrogen, each soil was ground by a planet micromill (Fritsch Pulverisette 7) for 2 min and 700 rpm. SOC and N contents of the Grinderwald soils

were estimated by gas chromatography using a Vario EL analyzer (Elementar, Hanau, Germany), whereas the soils of Rüdershausen were measured by using an LECO TruMac, LECOelemental analyzer (LECO TruMac, St. Joseph, USA). The pH of subunits was detected in $CaCl_2$ with a ratio of soil to solution of 1:2.5. Texture was analyzed by laser particle measurements using an Analysette 22 (Fritsch, Idar-Oberstein, Germany). To enable a complete detection of sub-texture classes (fine sand, medium sand, coarse sand) each soil was separated by a 0.2 mm sieve into one part larger than 0.2 mm and another part smaller than 0.2 mm. Both subunits were measured for their texture percentages separately and afterwards calculated together for the complete texture description.

The activities of the enzymes α-glucosidase, β-xylosidase, N-acetyl-β-glucosaminidase, β-glucosidase, β-cellobiosidase, sulfatase, phosphatase, arginine-aminopeptidase and tyrosine-aminopeptidase were determined according to the method of Marx et al. (2001). For this purpose, subunits were stored at −20°C directly after sampling and were defrosted shortly before the measurement. One gram of each soil was weighed into beakers and 50 ml of ultrapure sterile water was added. After ultrasonication at 150 W for 1 min, each suspension was magnetically stirred for approx. 1 min. For each enzyme, three laboratory replicates of 50µl of each soil solution were pipetted into (Greiner 96 Flat Bottom Black Polystyrol) microplates, while stirring. To each laboratory replicate 50 µl of 0.1 M MES-buffer or 0.05 M TRIZMA-buffer (aminopeptidases) was added in order to reach the pH-optimum for every enzyme. After that, 100 µl of the corresponding 1 mM 4-methylumbelliferon or 7-amino-4-methylcoumarin (aminopeptidases) marked substrate solution was added to each well. Serial dilutions of methylumbelliferyl and aminomethylcoumarin were prepared for calibration. Next, the microplates were incubated for 190 min at 30°C. At 10, 40, 70, 100, 130, 160 and 190 min the fluorescence was measured using a Tecan infinite 200 microplate reader with 360 nm excitation and 465 nm emission wavelength. Enzyme activities in $nmol\ g^{-1}\ h^{-1}$ were then calculated from the development of the fluorescence over time.

Field-moist soils were filled into paper bags and freeze-dried for at least 3 d (Alpha 1–4, Christ GmbH, Osterode, Germany), then ground (<0.2 mm), filled into glass vials and stored in desiccators until vis-NIRS measurements were carried out. Each soil (≈10 g) was filled into a 5-cm-diameter cell with a quartz window. The absorbance spectra [log (1/reflectance)] of each soil were recorded in the vis-NIR range (400 – 2500 nm, 1050 data points) in 2-nm steps using a Foss NIRSystems 6500 spectrometer (Silver Spring, MD, USA). Each soil was refilled into the cell, a second spectrum was recorded and the average of the two spectra was calculated.

4.3.3 Mathematical treatments of the spectra

The statistical software R version 3.2.2 (R Development Core Team, 2015) including the prospectr package (miscellaneous functions for processing and sample selection of vis-NIR diffuse reflectance data) was used for the mathematical treatments of the spectra.

Two regions of the full spectra were removed: the beginning of the vis region which showed instrumental artefacts (Stevens et al., 2013) and the range with a detector change. Thus, in total each spectrum consisted of 992 data points with an increment of 2 nm (502 to 1092 and 1108 to 2498 nm, Figure 4.1). For the cross-validation equations described below, either a maximum of 992 data points or of 496 (resampling every second data point) was used.
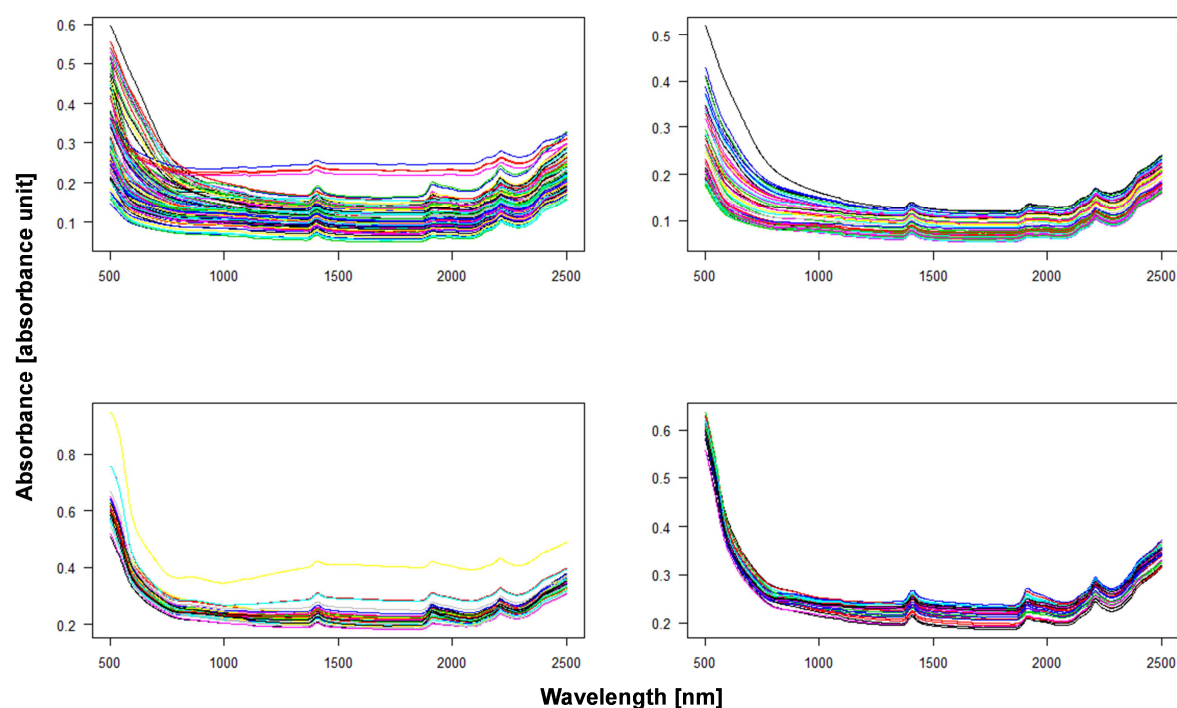
Figure 4.1: Near infrared absorbance spectra of the soils of the sample Grinderwald (top) and of the sample Rüdershausen (bottom). Panels on the left show the respective calibration samples (transects T1 and T2) and on the right the respective validation samples (transects T3).

Mathematical treatments included the use of the original spectra (i) with and (ii) without detrending and (iii–xxii) the use of the Savitzky-Golay algorithm with detrending: the polynomial (PG) degree ranged between 2 and 3, the order of derivative (DER) ranged from 1 to the order of the PG degree (PG-DER: 2-1, 2-2, 3-1, 3-2, 3-3) and the window size for smoothing was set to 5, 11, 17 or 23, resulting in 22 mathematical treatments for each of

the spectra with either 992 or 496 data points. Thus, in total 44 mathematical treatments were considered.

4.3.4 Differences between cross-validation and validation and the importance of such differences

Cross-validation is often used for estimating prediction errors and is a valid alternative to separate calibration and validation. However, one has to keep in mind that cross-validation may result in an over-optimistic performance and that the performance drops when one uses truly independent samples (Brown et al., 2005). Moreover, Hastie et al. (2009) emphasize: "Ideally, if we had enough data, we would set aside a validation set and use it to assess the performance of our prediction model". The importance of independent validation is also emphasized in other fields of NIRS, such as the medical field, where the use of three sets is recommended (European Medicines Agency, 2014): (i) a calibration set for creating the calibration model, (ii) a calibration test set for internal validation and optimisation of the model (cross-validation techniques may be applied instead, using the calibration set of samples), and (iii) an independent validation set for external validation of the model. The European Medicines Agency (2014) summarizes that a calibration set and an independent validation set of samples would be the minimum requirement.

We followed the recommendation by Brown et al. (2005) and Hastie et al. (2009) and used the transect T3 for independent validation. Our results are representative for the field scale. The mixing of units from sample T3 with units from sample T1 and T2 was strictly avoided, resulting in an independent validation. Nevertheless, an experimental design with more than three transects (e.g., five for calibration and one for independent validation) may have resulted in greater estimation accuracies of vis-NIRS.

4.3.5 PLS regression approaches

We used two different procedures to determine estimate accuracies of NIRS for soil main properties and enzyme activities: (i) standard PLS regression and (ii) GA-PLS using the statistical software R version 3.2.2 (R development Core Team, 2015) and different packages (each procedure is explained below).

In all calibrations (carried out as cross-validations), no outlier elimination was carried out. The maximum number of factors was set to 15 in all cases. For both procedures described below, data from transects T1 & T2 were used for a calibration and independent

validation was carried out using transect T3. The sites Grinderwald and Rüdershausen were evaluated separately.

4.3.5.1 Standard PLS regression

PLS regressions were carried out using the statistical software R version 3.2.2 and the pls package (partial least squares and principal component regression) using the kernel algorithm. The kernel algorithm is a fast and stable algorithm, which performs singular value decomposition on cross product matrix $X^T Y Y^T X$ rather than $X^T Y$ (Wehrens, 2011). A leave-one-out (LOO)-cross-validation was carried out to identify the best PLS model with an optimum of latent variables.

4.3.5.2 GA-PLS regression

Briefly, a genetic algorithm aims to find from a population of candidate solutions an optimum solution by variable selection. In analogy with natural selection in evolution the quality of each solution is called fitness. The higher the fitness (i.e., the smaller the standard error of cross-validation (SECV) of the respective regression model), the higher is the probability of reproduction. The ChemometricsWithR package (chemometrics with R-multivariate data analysis in the natural sciences and life sciences) was used. In this package, the initialization is carried out randomly, selection is a simple threshold selection, mutation swaps variables in or out of the subset and the cross-over type is uniform (Wehrens, 2011).

We set the number of iterations for each run to 200 and allowed 18 to 50 spectral data. We used the default mutation probability of 5 %. It cannot be guaranteed that an optimal solution can be found using a genetic algorithm (Wehrens, 2011). We therefore carried out 1500 calculations (500 per mathematical treatment) for each property. Three mathematical preprocessing approaches were tested: (i) the optimum treatment obtained for each property in the standard PLS regression, (ii) the use of the original absorbance spectra without detrending (992 data points), and (iii) use of the Savitzky-Golay algorithm with detrending (using the spectra with 992 data points): a polynomial degree of 3, a first order derivative and a window size for smoothing of 11. In the case that the optimum treatment obtained for each property in the standard PLS regression (i) was the same as (ii) or (iii) we used the original spectra with detrending as third mathematical pre-processing approach.

4.3.6 Ranking of cross-validation and validation results

We calculated RPIQ values (ratio of performance to inter-quartile distance, Bellon-Maurel et al., 2010) – the ratio of the interquartile range of laboratory results (IQR) and standard error of cross-validation (SECV) or standard error of prediction (SEP) as quality parameters for the cross-validations (RPIQ$_{CV}$) and validations (RPIQ$_V$).

For the ranking of RPIQ values, we used the ranking system by Saeys at el. (2005) (developed for RPD values (ratio of prediction to deviation, Saeys et al. (2005) – the ratio of standard deviation of laboratory results (SD) and SECV or SEP)) and by additionally considering that the IQR of a normal distribution equals 1.34896 × SD. Thus, the thresholds are "excellent" (RPIQ > 4.05), "good" (RPIQ between 4.05 and 3.37), "approximate quantitative" (RPIQ between 3.37 and 2.70) and "distinguishing between high and low values" (RPIQ between 2.70 and 2.02). However, it should be kept in mind that different ranking systems have been suggested in soil science (e.g., Chang et al., 2001) and that the usefulness of a model is defined in its specific context.

We also calculated 1−VR (variance ratio): $1 - SECV^2/SD^2$ or $1 - SEP^2/SD^2$ for the cross validations (1−VR$_{CV}$) and validations (1−VR$_V$), which has been suggested by the developers of WinISI software.

4.3.7 Statistical analysis: descriptive statistics of soil properties and multiple linear regressions without infrared data

Statistical analyses were carried out using the software R. Results of descriptive statistics are presented in Table 4.1. As expected – since contents of properties typically decrease markedly with depth and are thus not normally distributed – and as described before (e.g., Gobrecht et al., 2014), data for all properties were not normally distributed as indicated by Shapiro-Wilk tests (data not shown). The property data are generally right-skewed and markedly leptokurtic with few exceptions (Table 4.1). Neither a square-root (except for clay at Grinderwald) nor logarithmic transformation (data of properties with a minimum of 0 was increased by 0.1) resulted in normally distributed data, which emphasizes the need of using RPIQ instead of RPD values for ranking estimation accuracies of vis-NIRS for an estimation of soil properties. We calculated multiple linear regressions for the enzyme activities, the variables considered being those properties known to absorb in the vis-NIR region (e.g., Kuang et al., 2012; Soriano-Disla et al., 2014), namely pH and the contents of SOC, N, clay and silt. Only variables with significant contributions (p ≤ 0.05) were considered and the models with the lowest Akaike information criterion were chosen. Predictive qualities

of the multiple linear regression models were evaluated with the LOO-cross-validation procedure using the DAAG package (data analysis and graphics data and functions) for transects T1 and T2. Transects T3 were used for independent validation. The multiple linear regressions of enzyme activities with soil properties as predictors – and without infrared data – were carried out in order to compare obtained estimation accuracies with those of the vis-NIR based models to elucidate whether vis-NIR might provide an additional benefit.

Table 4.1: Descriptive statistics for the different properties and the results of the Shapiro-Wilk tests for the soil sample Grinderwald (transects T1 and T2, n = 127 for the main properties, n = 126 for the enzyme activities) and soil sample Rüdershausen (transects T1 and T2, n = 64, except for soil texture: n = 61).

| Property (unit) | Grinderwald | | | | | | | | Rüdershausen | | | | | | | |
| | Transect T1 & T2 | | | | | Transect T3 | | | Transect T1 & T2 | | | | | Transect T3 | | |
	Minimum	Maximum	Median	Skewness	Kurtosis	Minimum	Maximum	Median	Minimum	Maximum	Median	Skewness	Kurtosis	Minimum	Maximum	Median
pH (CaCl$_2$)	3.1	4.4	4.0	-0.9	3.2	3.1	4.3	4.1	3.5	4.3	3.9	0.0	1.8	3.6	4.1	3.9
SOC (%)	0.0	1.7	0.1	1.8	4.9	0.0	1.3	0.0	0.1	1.4	0.2	2.1	6.6	0.1	1.3	0.1
N (%)	0.0	0.1	0.0	1.8	6.2	0.0	0.1	0.0	0.0	0.1	0.0	2.0	6.3	0.0	0.1	0.0
Sand (%)	1.4	98.3	75.9	-1.2	4.4	46.7	98.5	94.3	0.0	10.8	2.4	1.0	2.6	0.0	7.7	1.8
Silt (%)	1.3	90.6	21.3	1.1	4.3	0.9	43.7	4.9	76.7	91.9	88.0	-0.8	3.2	84.8	91.2	87.5
Clay (%)	0.4	11.2	2.4	1.7	7.0	0.4	9.6	1.0	7.2	14.8	9.0	1.4	5.9	7.2	15.0	8.5
α-Glucosidase (nmol g^{-1} h^{-1})	0.0	8.5	1.1	1.2	3.5	0.0	12.4	2.5	0.0	35.6	6.0	2.3	11.1	0.0	24.6	6.0
β-Xylosidase (nmol g^{-1} h^{-1})	0.0	16.6	2.7	1.2	3.9	0.0	16.0	1.9	1.8	56.6	6.3	2.2	7.1	0.1	56.8	4.1
N-Acetyl-β-Glucosaminidase (nmol g^{-1} h^{-1})	0.0	60.1	2.8	2.1	7.5	0.0	78.3	5.6	0.0	206	7.7	4.7	28.5	1.3	328	5.7
β-Glucosidase (nmol g^{-1} h^{-1})	0.0	83.7	1.8	2.6	9.6	0.0	48.1	2.9	2.1	135	6.9	3.4	15.3	0.1	343	5.4
β-Cellobiosidase (nmol g^{-1} h^{-1})	0.0	55.8	1.0	5.1	37.2	0.0	4.9	1.4	0.0	12.9	3.3	1.3	4.9	0.1	26.8	2.9
Sulfatase (nmol g^{-1} h^{-1})	0.0	18.2	1.6	1.4	3.6	0.0	20.6	1.3	1.6	127	4.1	3.5	16.5	1.0	102	2.6
Phosphatase (nmol g^{-1} h^{-1})	0.0	514	28.3	1.9	6.3	0.0	410	13.3	47.9	795	112	2.3	7.9	68.4	743	137
Tyrosine-Aminopeptidase (nmol g^{-1} h^{-1})	0.0	28.2	2.1	2.2	7.0	0.0	25.6	2.4	0.0	80.2	5.3	2.6	9.6	0.0	70.4	5.0
Arginine-Aminopeptidase (nmol g^{-1} h^{-1})	0.0	84.9	7.8	2.6	10.1	0.0	35.5	5.2	0.0	74.3	12.9	1.6	5.8	0.0	137	10.0

4.4 Results and discussion

4.4.1 Estimations of main properties using vis-NIRS

Vis-NIRS estimations of the main properties SOC, N, pH and texture were generally successful in the cross-validation procedure (transects T1 & T2) for the Grinderwald and Rüdershausen sites with standard PLS regressions (Table 4.2). The estimation accuracies reported in Table 4.2 are similar to the accuracy summarized by Kuang et al. (2012) for a number of studies (apparently a mixture of cross-validation results (e.g., Viscarra Rossel and Behrens, 2010) and validation results (e.g., Shepherd and Walsh, 2002)). They reported for SOC (RPD range: 1.30 – 9.70), N (0.34 – 6.80) and clay (1.70 – 3.10) in general excellent estimation accuracies, for pH (0.57 – 2.39) in general good to approximate quantitative accuracies and for sand (0.87 – 3.40) and silt (1.09 – 3.07) in general approximate quantitative accuracies.

For Rüdershausen, the estimation accuracies obtained in the cross-validation procedures indicated excellent (pH, SOC) estimations, a distinction between high and low values (N, sand, silt) or no usable estimations (clay, Table 4.2). The poorer performance for soil texture of the loess site Rüdershausen compared to the sandy site Grinderwald is surprising, since sandy sites have been reported to be potentially less appropriate for NIRS estimations (e.g., Heinze et al., 2013). Overall, our data and the wide range of RPD values summarized by Kuang et al. (2012) for sand and silt indicate that for a given site poor to excellent estimations may occur.

Table 4.2: Statistics of cross-validation for the soil samples Grinderwald (transects T1 & T2) and Rüdershausen (transects T1 & T2) using the pls package in R (R-PLS) and validation statistics for the respective samples transect T3; shown are the mathematical treatments, the number of factors used in the PLS models, the standard error of cross-validation (SECV, the unit is given in the 1st column), 1 – the variance ratio for the cross-validation (1–VR_{CV}) and validation (1–VR_V), and the ratio of the interquartile range to SECV and SEP ($RPIQ_{CV}$ and $RPIQ_V$).

Property (unit)	Grinderwald Transects T1 & T2						Transect T3		Rüdershausen Transects T1 & T2						Transect T3	
	Math Treatment[e]	Data points	Factors	SECV	1 - VR_{CV}	$RPIQ_{CV}$	1 - VR_V	$RPIQ_V$	Math Treatment[e]	Data points	Factors	SECV	1 - VR_{CV}	$RPIQ_{CV}$	1 - VR_V	$RPIQ_V$
pH (CaCl$_2$)	0-0-0-y	992	15	0.08	0.93	4.89[a]	0.75	1.98	3-1-5-y	492	15	0.05	0.95	7.26[a]	-0.46	1.62
SOC (%)	3-1-5-y	492	13	0.04	0.99	6.24[a]	0.98	3.38[b]	3-3-17-y	480	15	0.03	0.99	6.41[a]	0.95	3.39[b]
N (%)	3-3-23-y	970	14	0.01	0.90	3.62[b]	0.88	3.10[c]	0-0-0-n	992	15	0.00	0.94	2.03[d]	0.91	3.53[b]
Sand (%)[a]	0-0-0-n	992	14	9.06	0.80	2.80[c]	0.84	4.67[a]	3-1-5-y	988	4	2.24	0.51	2.04[d]	-0.06	1.49
Silt (%)[a]	0-0-0-n	496	14	8.32	0.80	2.92[c]	0.84	4.85[a]	3-1-11-y	982	4	2.37	0.52	2.19[d]	0.42	2.14[d]
Clay (%)[a]	0-0-0-n	992	15	0.78	0.82	2.27[d]	0.61	2.10[d]	2-2-17-y	976	6	1.15	0.32	1.44	0.34	1.45
α-Glucosidase (nmol g^{-1} h^{-1})	2-1-17-y	976	6	1.61	0.41	1.93	0.04	1.19	3-3-17y	976	9	5.19	0.26	0.86	0.16	1.01
β-Xylosidase (nmol g^{-1} h^{-1})	0-0-0-n	992	10	1.82	0.76	2.75[c]	0.55	2.46[d]	3-3-17-y	976	6	4.54	0.84	1.50	0.87	0.92
N-Acetyl-β-Glucosaminidase (nmol g^{-1} h^{-1})	0-0-0-n	992	9	7.25	0.64	1.34	0.61	1.42	0-0-0-y	992	5	25.45	0.27	0.32	0.29	0.18
β-Glucosidase (nmol g^{-1} h^{-1})	3-1-5-y	988	14	11.67	0.38	0.59	-0.09	0.96	2-2-5-y	988	9	13.77	0.64	0.52	0.45	0.17
β-Cellobiosidase (nmol g^{-1} h^{-1})	3-3-11-y	486	6	5.22	0.35	0.53	-24.0	0.24	3-3-11-y	486	7	1.88	0.60	1.54	0.60	1.07
Sulfatase (nmol g^{-1} h^{-1})	0-0-0-n	992	11	1.57	0.89	0.64[d]	0.83	2.10[d]	3-3-23-y	474	14	7.61	0.87	0.69	0.73	0.45
Phosphatase (nmol g^{-1} h^{-1})	0-0-0-n	992	15	35.06	0.88	2.53[d]	0.90	1.65	3-1-23-y	474	14	45.89	0.91	2.23[d]	0.65	1.06
Tyrosine-Aminopeptidase (nmol g^{-1} h^{-1})	2-1-17-y	480	9	1.81	0.90	1.83	0.57	1.52	3-3-23-y	474	15	5.38	0.88	1.53	0.67	0.62
Arginine-Aminopeptidase (nmol g^{-1} h^{-1})	0-0-0-n	992	12	7.62	0.78	1.53	0.40	1.55	2-2-5-y	492	15	10.21	0.61	1.82	0.31	0.59

[a] Excellent: RPIQ > 4.05

[b] Good: RPIQ: 4.05-3.37

[c] Approximate quantitative: RPIQ: 3.37-2.70

[d] High and low distinction: RPIQ: 2.70-2.02

[e] Polynom degree, derivative, detrending

The independent validation for Grinderwald and Rüdershausen using transect T3 gave less accurate estimates for some properties. Soil organic C and N were successfully estimated in independent transects estimated using near infrared data at both sites, indicating the well-established usefulness of vis-NIRS for quantitative estimations for these spectrally active soil properties. The low precision of the N estimation for Grinderwald may be due to a very low range of N content, where also laboratory results are less reliable (Figure 4.2). Besides the confirmation of the usefulness of NIRS for an independent estimation of C and N contents on the field scale, a detailed comparison with literature data is hampered for two reasons: (i) As Stenberg et al. (2010) summarized, in the literature suspected pseudo-independent validation samples are fairly common for vis-NIRS studies, which may result in overoptimistic performance data. (ii) A focus in the literature (see e.g., summarizing reviews by Kuang et al. (2012) and Soriano-Disla et al. (2014)) has not yet been put on estimation accuracies for different scales in dependence of soil texture, soil type and management. For instance, it may not be meaningful to compare vis-NIRS performances for soils that have similar mineralogical background with soils with heterogeneous mineralogical compositions. Soils with sandy texture may be less useful for SOC estimations than finer soils (Stenberg, 2010), and studies which employ fields with different fertilization treatments (e.g., manure vs. control soils) may have large RPD and RPIQ values simply because of increased ranges of SOC contents.

At Grinderwald, the plot of measured against estimated pH (Figure 4.2) of transect 3 showed considerable scatter and the estimation was not usable according to $RPIQ_V$ (1.98, Table 4.2). At Rüdershausen, estimation accuracy for pH was poor and a large bias is visible (Figure 4.2). Similarly, Wetterlind and Stenberg (2010) reported for four farms where 25 local samples were used for the respective calibrations that validation RPD values ranged only from 1.1 to 1.4 for pH.

Estimation accuracies for texture data of transect 3 ranged from poor to excellent depending on the site (Rüdershausen or Grinderwald). The vis-NIRS performances for estimation of texture data depended markedly on the ranges of measured data – in cases of rather small ranges of measured data (maximum minus minimum, Table 4.1) of <10 % for either sand, silt or clay, accuracies according to RPIQ were either poor or allowed distinguishing between high and low values (Table 4.2, Figure 4.2). In cases where the measured range was large – 42.8 % for silt at Grinderwald and 51.8 % for sand at Grinderwald – RPIQ indicated an excellent estimation accuracy. Overall and in contrast to SOC and N a usefulness of vis-NIRS for estimations of soil texture for an unknown field may not be guaranteed.
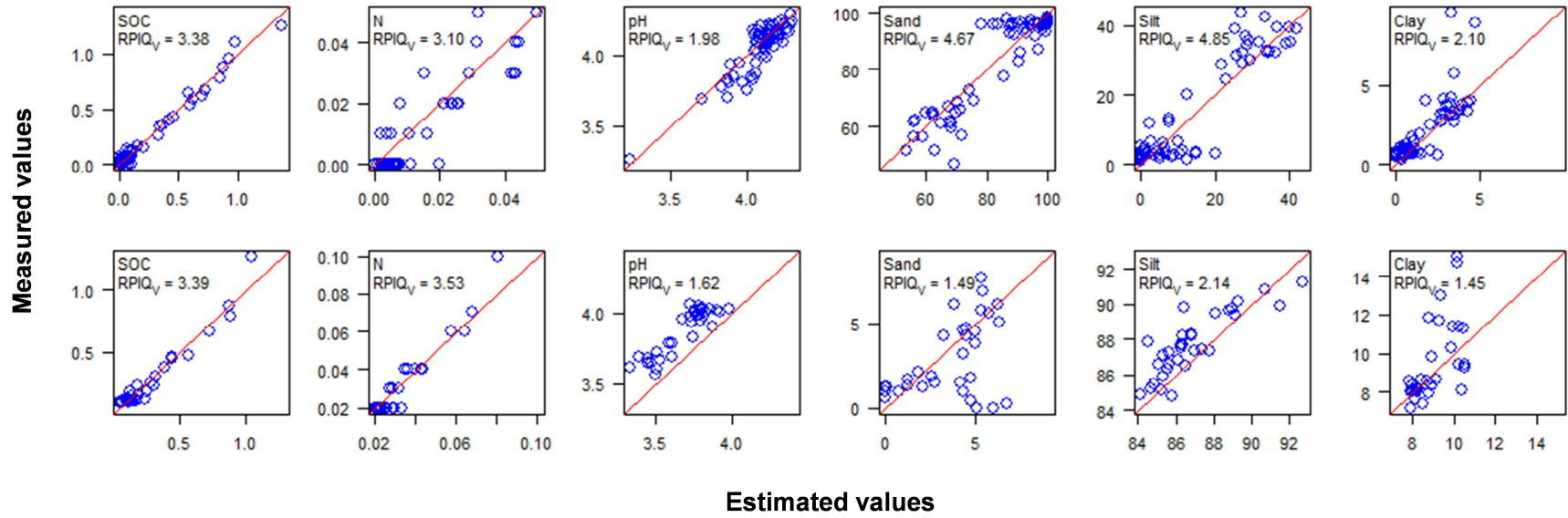
Figure 4.2: Measured against estimated values for contents of SOC and N, pH and soil texture for the validation samples Grinderwald (transect T3, top) and Rüdershausen (transect T3, bottom). Units are given in Table 4.1. Estimates refer to PLS regression with infrared data. RPIQ$_V$ values are also shown.

The use of GA-PLS for variable selection reduced the number of spectral data markedly for the main soil properties SOC, N, soil texture and pH. For Grinderwald and Rüdershausen, the number of spectral data for the main properties ranged from 28 to 48 compared to 992 of the original spectra. All estimation accuracies were increased in the cross-validation procedure (Tables 4.2, 4.3).

Unfortunately, the benefit of the GA-PLS regression did not generally hold for the independent validation transects T3. At Grinderwald, for example, a marked improvement of the estimation accuracy was noted only for N: $RPIQ_V$ for N increased from 3.10 (PLS) to 4.12 (GA-PLS). For the other five properties accuracies decreased, while this decrease was very small for pH and clay. At Rüdershausen, GA-PLS resulted in an increase of the $RPIQ_V$ for SOC from 3.39 (PLS) to 3.60. For the other five properties GA-PLS resulted in a decrease of $RPIQ_V$ compared to PLS regression (Table 4.3). Overall, all results show that LOO-cross validation results alone might result in an overoptimistic appraisal for both PLS and, even more distinctly, for GA-PLS. One has to keep in mind that approaches without a strictly independent validation sample (e.g., random splitting of all data) may achieve higher RPIQ values when using variable selection procedures such as GA-PLS. The reason for the decrease of accuracies in the validation transects using GA-PLS compared to PLS regression may in part be due to the implementation of the GA in this study, as only the one model with the best $RPIQ_{CV}$ results was selected from all 1500 GA runs and then applied to the validation set. However, additional tests which checked all 1500 independent validations for the 1500 GA runs for each property of the Rüdershausen site still showed poor estimation accuracies for sand and silt, poor accuracies or a distinction between high and low for clay and poor or approximate quantitative accuracies for pH. Nevertheless, it should be kept in mind that different selection strategies may be implemented. For instance, Vohland and Emmerling (2011) proposed that all selections from all GA runs first be pooled and then the final model (with the finally selected spectral variables) be derived in a stepwise procedure from the pooled selection frequencies. Overall, for heterogeneous soils, the variables preselected based on the calibration set might not be representative of the effective variables in future prediction process due to the large variability among soils (Jia et al., 2016). Additionally, it should be taken into consideration that the performance of the GA-PLS approach may decrease when N200 variables are used (Leardi et al., 2002).

Table 4.3: Statistics of cross-validation for the soil samples Grinderwald (transects T1 & T2) and Rüdershausen (transects T1 & T2) using genetic algorithms (package ChemometricsWithR) in R and validation statistics for respective samples transect T3; shown are the mathematical treatments, the number of spectral data points, the number of factors used in the final PLS models, the standard error of cross-validation (SECV, the unit is given in the 1st column), 1 – the variance ratio for the cross-validation (1-VR_CV) and validation (1-VR_V), and the ratio of the interquartile range to SECV and SEP (RPIQ_CV and RPIQ_V).

| Property (unit) | Grinderwald | | | | | | Transect T3 | | Rüdershausen | | | | | | Transect T3 | |
| | Transects T1 & T2 | | | | | | | | Transects T1 & T2 | | | | | | | |
	Math Treatment[e]	Data points	Factors	SECV	1 - VR_CV	RPIQ_CV	1 - VR_V	RPIQ_V	Math Treatment[e]	Data points	Factors	SECV	1 - VR_CV	RPIQ_CV	1 - VR_V	RPIQ_V
pH (CaCl$_2$)	3-1-11-y	46	15	0.06	0.96	6.15[a]	0.74	1.94	3-1-11-y	46	14	0.03	0.98	10.80[a]	-0.64	1.53
SOC (%)	3-1-11-y	44	15	0.03	0.99	8.00[a]	0.97	2.75[c]	3-3-17-y	43	15	0.01	1.00	12.13[a]	0.96	3.60[b]
N (%)	3-3-23-y	28	14	0	0.94	4.52[a]	0.93	4.12[a]	3-1-11-y	36	15	0.00	0.98	3.90[b]	0.75	2.13[d]
Sand (%)[a]	0-0-0-n	36	15	7.35	0.87	3.46[b]	0.68	3.31[c]	3-1-5-y	40	15	0.91	0.92	5.02[a]	-0.44	1.27
Silt (%)[a]	0-0-0-n	36	15	6.58	0.87	3.68[b]	0.81	4.45[a]	3-1-5-y	48	15	1.04	0.91	5.00[a]	-18.83	0.36
Clay (%)[a]	0-0-0-n	41	15	0.68	0.86	2.60d	0.60	2.08[d]	2-2-17-y	31	15	0.64	0.79	2.59[d]	0.31	1.41
α-Glucosidase (nmol g^{-1} h^{-1})	3-1-11-y	35	15	1.29	0.62	2.40[d]	-0.15	1.08	3-3-17-y	42	15	2.54	0.82	1.76	-0.40	0.78
β-Xylosidase (nmol g^{-1} h^{-1})	3-1-11-y	30	15	1.48	0.84	3.39[b]	0.48	2.29[d]	3-3-17-y	43	14	2.08	0.97	3.27[c]	0.79	0.72
N-Acetyl-β-Glucosaminidase (nmol g^{-1} h^{-1})	3-1-11-y	28	15	5.79	0.77	1.68	0.45	1.18	3-1-11-y	35	15	12.9	0.81	0.63	0.45	0.20
β-Glucosidase (nmol g^{-1} h^{-1})	3-1-5-y	37	15	8.84	0.64	0.77	-0.03	0.98	2-2-5-y	39	15	5.56	0.94	1.29	0.27	0.15
β-Cellobiosidase (nmol g^{-1} h^{-1})	3-1-11-y	30	15	4.46	0.52	0.62	-25.8	0.23	3-3-11-y	45	15	1.08	0.86	2.67[d]	0.39	0.86
Sulfatase (nmol g^{-1} h^{-1})	3-1-11-y	31	15	1.30	0.93	3.19[c]	0.69	1.57	3-3-23-y	33	14	2.97	0.98	1.77	0.73	0.46
Phosphatase (nmol g^{-1} h^{-1})	0-0-0-n	39	15	22.8	0.95	3.88[b]	0.86	1.36	3-1-11-y	47	14	22.6	0.98	4.55[a]	0.70	1.15
Tyrosine-Aminopeptidase (nmol g^{-1} h^{-1})	3-1-11-y	35	14	1.39	0.94	2.39[d]	0.47	1.37	3-3-23-y	38	15	2.68	0.97	3.06[c]	0.53	0.53
Arginine-Aminopeptidase (nmol g^{-1} h^{-1})	3-1-11-y	39	14	5.94	0.87	1.96	-0.08	1.15	2-2-5-y	37	15	6.02	0.86	3.07[c]	0.16	0.53

[a] Excellent: RPIQ > 4.05

[b] Good: RPIQ: 4.05-3.37

[c] Approximate quantitative: RPIQ: 3.37-2.70

[d] High and low distinction: RPIQ: 2.70-2.02

[e] Polynom degree, derivative, detrending

4.4.2   Estimations of biological properties using vis-NIRS

The evaluation of the performance of vis-NIRS for estimations of enzyme activities may depend on several conditions. An apparent marked usefulness of vis-NIRS for an estimation of enzyme activities may be obtained by using the optimistic cross-validation and by refining the results with a variable selection procedure: the use of GA-PLS resulted in the cross-validation in an apparent usefulness of vis-NIRS for an estimation of five (out of nine tested) enzyme activities for Grinderwald and also for Rüdershausen (Table 4.3). However, the employment of independent validation samples (transects T3) revealed the limitations of vis-NIRS for an estimation of properties which are likely simply estimated due to correlations with absorbing properties or do not have a sufficiently strong impact on the measured signals. At Grinderwald, independent validation revealed that $RPIQ_V$ for all enzyme activities ranged from 0.23 to 2.29 and that only one enzyme activity could be estimated β-xylosidase). At Rüdershausen, not even one of the enzyme activities was successfully estimated using the validation sample transect T3 and GA-PLS with $RPIQ_V$ ranging from 0.15 to 1.15 (Table 4.3).

The use of standard PLS regression instead of GA-PLS indicated that only few enzyme activities could be estimated in independent transects using near infrared data (Table 4.2, Figures 4.3 a and 4.3 b). Overall the data of the independent validation indicated that for the field scale estimations of enzyme activities – outside a closed population – may most likely be inaccurate.
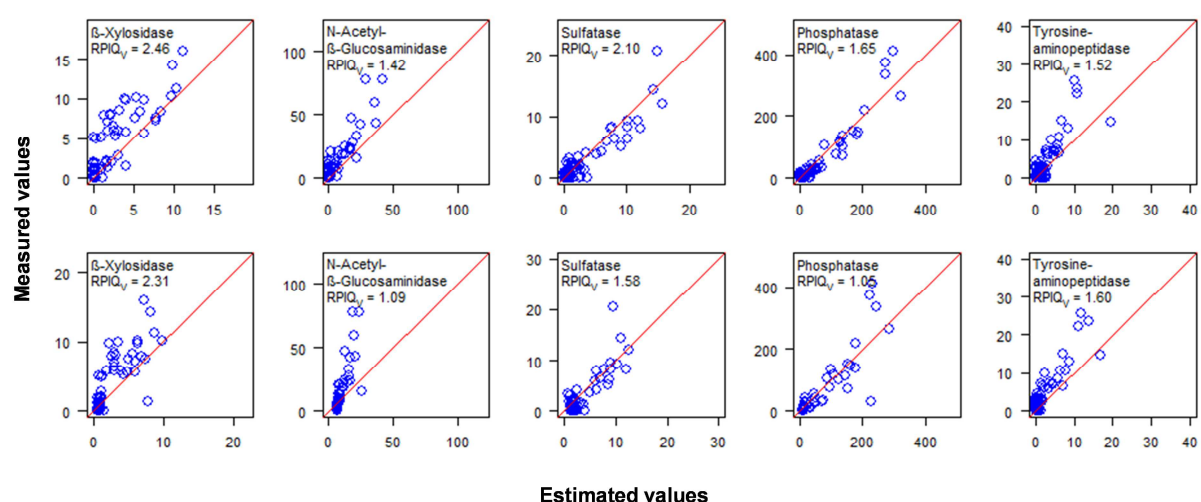

Figure 4.3 a: Measured against estimated values for five enzyme activities for the validation sample Grinderwald (transect T3). Units are given in Table 4.1. Top: Estimates refer to PLS regression with infrared data. Bottom: Estimates refer to multiple linear regressions using the main properties (variables are given in Table 4.4) without infrared data. $RPIQ_V$ values are also shown.
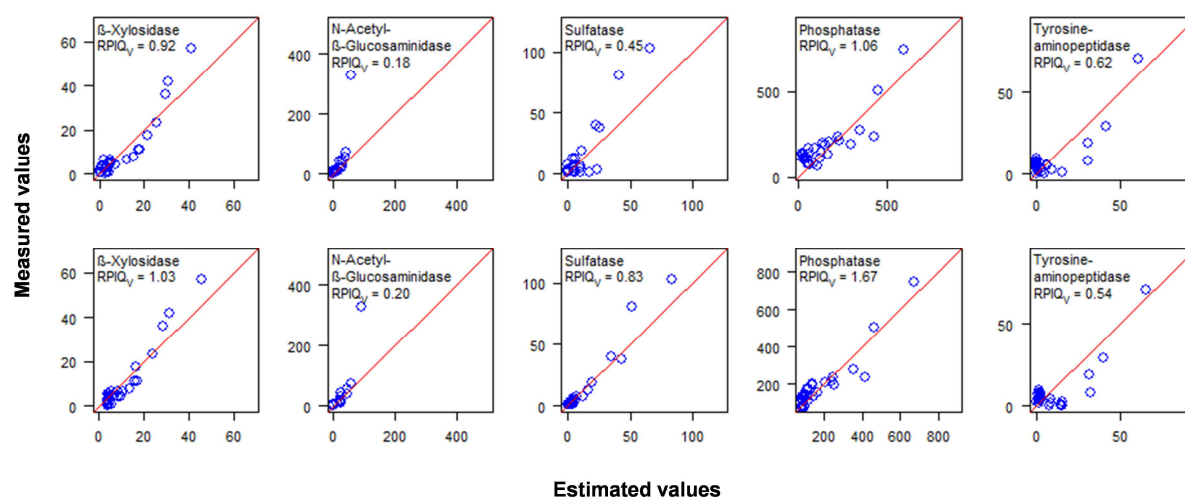
Figure 4.3 b: Measured against estimated values for five enzyme activities for the validation sample Rüdershausen (transect T3). Units are given in Table 4.1. Top: Estimates refer to PLS regression with infrared data. Bottom: Estimates refer to multiple linear regressions using the main properties (variables are given in Table 4.4) without infrared data. RPIQ$_V$ values are also shown.

4.4.3   Estimations of biological properties using the general properties - without NIRS

We hypothesized – in contrast to other studies, which reported a usefulness of vis-NIRS (see the review by Soriano-Disla et al. (2014)) – that vis-NIRS may not be the method of choice for a direct estimation of enzyme activities in soils, since (i) there may be no important absorbances due to specific vibrations for enzyme activities, (ii) the absorbances due to specific vibrations (if present) may be masked by absorbances of other compounds and/or (iii) the absorptions responsible for enzyme activities may be too low. Multiple linear regression analysis indicated for Grinderwald and Rüdershausen that besides SOC contents also clay, silt and N contents and pH may be used for the modelling of enzyme activities (Table 4.4). Using validation sample T3 and RPIQ as an indicator showed that β-xylosidase could be estimated by multiple linear regression at Grinderwald with a possible distinction between high and low values (RPIQ$_V$ = 2.31, Table 4.4).

Table 4.4: Statistics of cross-validation for the soil samples Grinderwald (transects T1 & T2) and Rüdershausen (transects T1 & T2) and validation statistics for respective samples transect T3 using multiple linear regression (MLR) without infrared data; shown are the factors used in the MLR models, the standard error of cross-validation (SECV, the unit is given in the 1st column), 1 – the variance ratio for the cross-validation ($1–VR_{CV}$) and validation ($1–VR_V$), and the ratio of the interquartile range to SECV and SEP ($RPIQ_{CV}$ and $RPIQ_V$).

| Property (unit) | Grinderwald | | | | | Rüdershausen | | | | | |
| | Transects T1 & T2 | | | Transect T3 | | Transects T1 & T2 | | | | Transect T3 | |
	Factors	SECV	$1-VR_{CV}$	$RPIQ_{CV}$	$1-VR_V$	$RPIQ_V$	Factors	SECV	$1-VR_{CV}$	$RPIQ_{CV}$	$1-VR_V$	$RPIQ_V$
α-Glucosidase (nmol g^{-1} h^{-1})	SOC, clay	1.88	0.30	1.86	0.03	1.24	clay	6.06	0.02	0.72	0.54	1.36
β-Xylosidase (nmol g^{-1} h^{-1})	SOC, clay	2.57	0.57	2.10[c]	0.50	2.31[c]	SOC	4.46	0.86	0.54	0.90	1.03
N-Acetyl-β-Glucosaminidase (nmol g^{-1} h^{-1})	SOC, clay	12.2	0.56	1.48	0.34	1.09	N	23.7	0.39	0.35	0.48	0.20
β-Glucosidase (nmol g^{-1} h^{-1})	SOC, pH	16.9	0.06	1.01	-0.05	0.98	N, pH	11.9	0.74	0.69	0.46	0.17
β-Cellobiosidase (nmol g^{-1} h^{-1})	pH	8.12	0.09	0.40	-19.1	0.27	pH	2.82	0.09	0.99	0.08	0.70
Sulfatase (nmol g^{-1} h^{-1})	SOC, pH	2.57	0.77	3.60[a]	0.69	1.58	SOC, pH	8.44	0.85	0.67	0.92	0.83
Phosphatase (nmol g^{-1} h^{-1})	SOC, N	51.6	0.80	2.87[b]	0.76	1.05	SOC, pH	38.9	0.94	2.74[b]	0.86	1.67
Tyrosine-Aminopeptidase (nmol g^{-1} h^{-1})	SOC, pH	2.59	0.87	3.16[b]	0.61	1.60	N, pH	5.39	0.89	1.47	0.55	0.54
Arginine-Aminopeptidase (nmol g^{-1} h^{-1})	SOC. pH, clay	12.0	0.67	0.37	0.37	1.41	SOC, pH, silt	13.3	0.36	1.34	0.51	0.70

[a] Good: RPIQ: 4.05-3.37
[b] Approximate quantitative: RPIQ: 3.37-2.70
[c] High and low distinction: RPIQ: 2.70-2.02

Overall, enzyme activities were estimated with similar accuracy from laboratory data, infrared data were not required (Figure 4.3 a and 4.3 b): At Grinderwald, $RPIQ_V$ values for vis-NIRS were generally slightly higher than for multiple linear regression, but not sufficiently high to recommend that vis-NIRS may be the better choice for estimating enzyme activities (Tables 4.2 and 4.4, Figure 4.3 a). At Rüdershausen, both approaches showed poor performances, with multiple linear regression results having generally even higher $RPIQ_V$ values than vis-NIRS PLS regressions (Tables 4.2 and 4.4, Figure 4.3 b). Nevertheless, one has to keep in mind that the predictor variables used in our multiple linear regressions may be estimated with vis-NIRS with varying accuracies depending on the sites and scale considered (Soriano-Disla et al., 2014).

4.5   Conclusions

This study indicated that use of cross-validation instead of independent validation may result in a highly overoptimistic appraisal of vis-NIRS for estimations, which is especially problematic for those properties such as enzyme activities, where the specific vibrations are not known. We recommend for properties with unknown specific vibrations that the use of independent validation be mandatory, i.e. no cross-validation and no random-splitting of dependent samples, in order to avoid unrealistic expectations of the applicability of vis-NIRS

in soil science.

In contrast to other studies cited in Soriano-Disla et al. (2014), which reported a usefulness of vis-NIRS for an estimation of enzyme activities, independent validation at two sites indicated no benefit of vis-NIRS for an estimation of these properties for the following reasons: (i) only two out of nine activities could be estimated at one site and none at the second and (ii) enzyme activities were estimated with similar accuracy from laboratory data, vis-NIR data did not provide an additional benefit.

For the spectrally active main properties (SOC, N, pH and soil texture) GA-PLS markedly improved estimation accuracies compared to PLS in the cross-validation, but generally not in the validation transects. Future studies may focus on GA-PLS for spectrally active main properties with a strictly independent validation sample as in this study but with different selection strategies so as to gain further insights into the benefits and limitations of GA-PLS.

4.6 Acknowledgements

5   General conclusion

Within the present thesis, the influence of amount and composition of OM and soil mineral characteristics on C mineralization as well as stabilization in different soil depths was analyzed. Additionally, the estimation accuracies of vis-NIRS for general soil properties (SOC, N, pH, texture) and nine enzyme activities with two different methods (GA-PLS and PLS regressions) for two forest sites, along three transects were determined. The results of the research presented above provided some novel insights and contributed to a better understanding of the subsoil C dynamics. The main conclusions according to the specific objectives (chapter 1.4) are as followed:

(i)   The C mineralization in a sandy Cambisol was significantly affected by the rate of root application at both sampling depths (topsoil: 2 – 10 cm and subsoil: 145 – 153 cm). The root distribution had a significant (but small) effect in all topsoil treatments with root application, but in the subsoil only in the treatments with the larger roots. Additionally the data indicated a significant effect of interactions between root size and distribution together with root size and rate of application for the subsoil treatments.

(ii)   Not only the direct effects such as root size and distribution seem to control the decomposition of fine roots at different depths of the sandy soil studied, but also the indirect abiotic effects that affect the living conditions of the microbial community. Independent of soil depth and root distribution, an increase in C turnover with an increase in microbial biomass could be assumed, but for the topsoil this interaction was more evident if the roots were concentrated locally. Our data also suggest that the supply of Ca and K might have had an effect on microbial activity and C turnover that was independent of soil depth for the localized fine root concentrations. Therefore, the supply of Ca and K, affecting the microbial biomass C positively, seems to be important for the plant nutrient and C dynamics in both the top- and subsoil if the fine beech roots are heterogeneously distributed.

(iii)   A higher proportion of the bulk SOC is stabilized against microbial decomposition in the analyzed forest subsoil compared to topsoil because an increasing relative amount of OM associated with highly stable aggregates (<53 µm) and/or the mineral phase was found with increasing soil depth. Furthermore, an increase in the relative proportion of labile OM with increasing soil depth was found, which suggests a stronger separation into a labile and a stable OM pool in the subsoil compared to the topsoil on the cost of the intermediate OM pool.

(iv) For both top- and subsoil the infrared analyses revealed relatively higher C=O groups amounts for the OM associated to the heavy fraction compared to the OM associated to the aggregate size fractions, indicating that the OM within the HF is more microbially processed. The microbial imprint on the composition of the OM seems also to increase with increasing soil depth.

(v) The use of cross-validation instead of independent validation may lead to highly overoptimistic appraisal of vis-NIRS for estimations, which is especially problematic for those properties where the specific vibrations are unknown (e.g., enzyme activities). To avoid unrealistic expectations of the applicability of vis-NIRS in soil science, the mandatory use of independent validation for properties with unknown specific vibrations is recommended.

(vi) The independent validation at two sites indicated no benefit of vis-NIR for an estimation of enzyme activities. Only two out of nine activities could be estimated at one site and none at the second site. Since the estimation of enzyme activities from laboratory data were estimated with similar accuracy, vis-NIR data did not provide an additional benefit.

(vii) For the spectrally active main properties like SOC, N, pH and soil texture GA-PLS markedly improved estimation accuracies compared to PLS in the cross-validation, but generally not in the validation transects.

6 Future research needs

Based on the results of the first study, for a better understanding of the effects of size and distribution of fine tree roots and their interactions on the mineralization kinetics in the subsoil further research is required. Here, different types of forest (specie composition, stand age) and larger variations in root size and distribution will extend the knowledge about their interactive effects on their decomposition in relation to differences in litter chemistry. In a further step, the research should be extended to more sites, which are different in soil mineral characteristics, but rather similar in climate and vegetation conditions, so that a combined effect of substrate quality and soil mineral characteristics can be clarified.

In the second study a relative higher portion of labile OM was found in the subsoil compared to the topsoil. With the date from the OM fractions revealed in this study the main source of the labile OM is less explainable. A fractionation scheme with the opportunity to separate the free light fraction (flF) in various sub-fractions with different characteristics or particle sizes could be a useful approach for further research. These data might provide a more specific differentiation regarding the decomposability of the organic particles. Additionally, further analyses regarding the composition of the microbial community and the quality and amount of dissolved OM might provide explanations for the increase in the relative amount of labile OM with increasing soil depth.

The results of the third study showed markedly improved estimation accuracies of the GA-PLS in the cross-validation compared to the PLS for spectrally active main soil properties, but generally not in the validation transects. To gain further insights into the benefits and limitations of GA-PLS future studies might focus on GA-PLS for spectrally active main properties with a strictly independent validation sample thereby using different selection strategies.

7 Acknowledgements

First of all, I would like to thank my supervisor, Prof. Dr. Bernard Ludwig, who gave me the opportunity to work on this extremely interesting project. His support, advice and encouragement enabled me to prepare this dissertation.

I also thank my second supervisor, Prof. Dr. Rainer Jörgensen, for providing profound advice as well as critical and helpful comments.

I am grateful to Dr. Michael Kaiser for his continuous support, scientific guidance and patience throughout the preparation of my dissertation.

Many thanks to Anja Sawallisch for her support and guidance in the laboratory and field work, as well as for helpful discussions and suggestions. These thanks are also extended to Gabriele Dormann and Sabine Ahlers, who assisted me with advice and technical equipment.

I would also like to thank my former colleagues, Dr. Deborah Linsler, Dennis Grunwald, Anja Nüsse and Dr. Johanna Pinggera, for their helpful advice as well as for spending relaxing and amusing coffee breaks together. I would like to extend these thanks to my student assistances for their help with field work and sample preparation.

I thank the Deutsche Forschungsgemeinschaft for funding this thesis as part of the Research Group 1806 'The Forgotten Part of Carbon Cycling: Organic Matter Storage and Turnover in Subsoils (SUBSOM)'.

Last but not least, I would like to thank my family for their continuous love, support, and encouragement during the completion of this work. They accompanied me through all the ups and downs.

8 References

Agnelli, A., Ascher, J., Corti, G., Ceccherini, M.T., Nannipieri, P., Pietramellara, G., 2004. Distribution of microbial communities in a forest soil profile investigated by microbial biomass, soil respiration and DGGE of total and extracellular DNA. Soil Biology and Biochemistry, 36, 859-868.

Anderson, J.P.E. and Domsch K.H., 1975. Measurement of bacterial and fungal contributions to respiration of selected agricultural and forest soils. Canadian Journal of Microbiology, 21, 314-322.

Angst, G., Kögel-Knabner, I., Kirfel, K., Hertel. D., Mueller, C.W., 2016. Spatial distribution and chemical composition of soil organic matter fractions in rhizosphere and non-rhizosphere soil under European beech (*Fagus sylvatica L.*). Geoderma, 264, 179-187.

Baldock, J.A. and Skjemstad, J.O., 2000. Role of the soil matrix and minerals in protecting natural organic materials against biological attack. Organic Geochemistry, 31, 697-710.

Balesdent, J., 1996. The significance of organic separates to carbon dynamics and its modelling in some cultivated soils. European Journal of Soil Science, 47, 485-493.

Bandick, A.K. and Dick, R.P., 1999. Field management effects on enzyme activities. Soil Biology and Biochemistry, 31, 1471-1479.

Batjes, N.H., 1996. Total carbon and nitrogen in the soils of the world. European Journal of Soil Science, 47, 151-163.

Baumgardner, M.F., Silva, L.F., Biehl, L.L., Stoner, E.R., 1985. Reflectance properties of soils. Advances in Agronomy, 38, 2-44.

Bearden, B.N., 2001. Influence of arbuscular mycorrhizal fungi on soil structure and soil water characteristics of vertisols. Plant and Soil, 229, 245-258.

Bellon-Maurel, V., Fernandez-Ahumada, E., Palagos, B., Roger, J.M., McBratney, A., 2010. Critical reviews of chemometric indicators commonly used for assessing the quality of the prediction of soil attributes by NIR spectroscopy. TrAC Trends in Analytical Chemistry, 29, 1073-1081.

Bodner, G., Leitner,D., Kaul, H.-P., 2014. Coarse and fine root plants affect pore size distributions differently. Plant and Soil, 380, 133-151.

Breland, T.A., 1994. Enhanced mineralization and denitrification as a result of heterogeneous distribution of clover residues in soil. Plant and Soil, 166, 1-12.

Brookes, P.C., Landman, A., Pruden, G., Jenkinson, D.S., 1985. Chloroform fumigation and the release of soil nitrogen: a rapid direct extraction method to measure microbial biomass nitrogen in soil. Soil Biology and Biochemistry, 17, 837-842

Brown, D.J., Bricklemyer, R.S., Miller, P.R., 2005. Validation requirements for diffuse reflectance soil characterization models with a case study of VNIR soil C prediction in Montana. Geoderma, 129, 251-267.

Cambardella, C.A. and Elliott, E.T., 1993. Carbon and nitrogen distribution in aggregates from cultivated and native grassland soils. Soil Science Society of America Journal, 57, 1071-1076.

Capriel, P., Beck, T., Borchert, H., Gronholz, J., Zachmann, G., 1995. Hydrophobicity of the organic matter in arable soils. Soil Biology and Biochemistry, 27, 1453-1458.

Cerli, C., Celi, L., Kalbitz, K., Guggenberger, G., Kaiser, K., 2012. Separation of light and heavy organic matter fractions in soil – testing for proper density cut-off and dispersion level. Geoderma, 170, 403-416.

Chabbi, A., Kögel-Knabner, I., Rumpel, C., 2009. Stabilised carbon in subsoil horizons is located in spatially distinct parts of the soil profile. Soil Biology and Biochemistry 41, 256-261.

Chang, C.W., Laird, D.A., Mausbach, M.J., Hurburgh Jr., C.R., 2001. Near-infrared reflectance spectroscopy – principal components regression analyses of soil properties. Soil Science Society of America Journal, 65, 480-490.

Christensen, B.T., 2001. Physical fractionation of soil and structural and functional complexity in organic matter turnover. European Journal of Soil Science, 52, 345-353.

Clark, R.N., 1999. Spectroscopy of rocks and minerals and principles of spectroscopy. In: Rencz, A.N. (Ed.), Remote Sensing for the Earth Sciences. Wiley, Chichester, pp. 3-58.

Cosack, E., Heinz, J., 1980. Erläuterungen zu Blatt Nr. Neustadt am Rübenberge. NLfB, Hannover, Germany, p. 3422.

De Gryze, S., Jassogne, L., Six, J., Bossuyt, H., Wevers, M., Merckx, R., 2006. Pore structure changes during decomposition of fresh residue: X-ray tomography analyses. Geoderma, 134, 82-96.

Dick, R.P., 1994. Soil enzyme activity as an indicator of soil quality. In: Doran, J.W., Coleman, D.C., Bezdicek, D.F., Stewart, B.A. (Eds.), Defining soil quality for a sustainable environment. SSSA Special Publication Number 35, Madison, WI, pp. 107-124.

Dick, W.A., Thavamani, B., Conley, S., Blaisdell, R., Sengupta, A., 2013. Prediction of β glucosidase and β-glucosaminidase activities, soil organic C, and amino sugar N in a diverse population of soils using near infrared reflectance spectroscopy. Soil Biology and Biochemistry, 56, 99-104.

DIN 19684-6, 1997. Bodenuntersuchungsverfahren im Landwirtschaftlichen Wasserbau - Chemische Laboruntersuchungen - Teil 6: Bestimmung des Gehaltes an oxalatlöslichem Eisen. DIN 19684-6: 1997-12, Beuth Verlag, Berlin.

DIN ISO 11277, 2002. Bodenbeschaffenheit - Bestimmung der Partikelgrößenverteilung in Mineralböden - Verfahren mittels Siebung und Sedimentation. ISO 11277: 1998/Cor.1:2002, Beuth Verlag Berlin, Germany.

Djajakirana, G., Joergensen, R.G., Meyer, B., 1996. Ergosterol and microbial biomass relationship in soil. Biology and Fertility of Soils 22, 299-304.

Dorioz, J.M., Robert, M., Chenu, C., 1993. The role of roots, fungi and bacteria on clay particle organization. An experimental approach. Geoderma, 56, 179-194.

Ellerbrock, R.H. and Gerke, H.H., 2013. Characterization of organic matter composition of soil and flow path surfaces based on physiochemical principles – A review. In: D.L. Sparks, editor, Advances in agronomy 121. Elsevier Academic Press, San Diego, CA. pp. 117-177.

Emerson, W.W. and McGarry, D., 2003. Organic carbon and soil porosity. Australian Journal of Soil Research, 41, 107-118.

European Medicines Agency, 2014. Guideline on the use of near infrared spectroscopy by the pharmaceutical industry and the data requirements for new submissions and variations EMEA/CHMP/CVMP/QWP/17760/2009 Rev2.

Eusterhues, K., Rumpel, C., Kleber, M., Kögel-Knabner, I., 2003. Stabilisation of soil organic matter by interactions with minerals as revealed by mineral dissolution and oxidative degradation. Organic Geochemistry 34, 1591-1600.

Eusterhues, K., Rumpel, C., Kögel-Knabner, I., 2005. Organo-mineral associations in sandy acid forest soils: importance of specific surface area, iron oxides and micropores. European Journal of Soil Science, 56, 753-763.

Fierer, N., Allen, A.S., Schimel, J.P., Holden, P.A., 2003. Controls on microbial CO_2 production: a comparison of surface and subsurface soil horizons. Global Change Biology, 9, 1322-1332.

Giacomini, S.J., Rescous, S., Mary, B., Aita, C., 2007. Simulating the effects of N availability, straw particle size and location in soil on C and N mineralization. Plant and Soil, 301, 289-301.

Gillabel, J., Cebrian-Lopez, B., Six, J., Merckx, R., 2010. Experimental evidence for the attenuating effect of SOM protection on temperature sensitivity of SOM decomposition. Global Change Biology, 16, 2789-2798.

Gobrecht, A., Roger, J.-M., Bellon-Maurel, V., 2014. Major issues of diffuse reflectance nir spectroscopy in the specific context of soil carbon content estimation: a review. Advances in Agronomy, 123, 145-175.

Golchin, A., Oades, J.M., Skjemstad, J.O., Clarke, P., 1994. Study of free and occluded particulate organic matter in soils by solid state ^{13}C CP-MAS NMR spectroscopy and scanning electron microscopy. Australian Journal of Soil Research, 32, 285-309.

Grave, R.A., Nicoloso, R.D., Cassol, P.C., Aita, C., Corrêa, J.C., Dalla Costa, M., Fritz, D.D., 2015. Short-term carbon dioxide emission under contrasting soil disturbance levels and organic amendments. Soil and Tillage Research, 146, 184-192.

Gregorich, E.G., Beare, M.H., McKim, U.F., Skjemstad, J.O., 2006. Chemical and biological characteristics of physically uncomplexed organic matter. Soil Science Society of America Journal, 70, 975-985.

Guirard, B.M., 1958. Microbial nutrition. Annual Review of Microbiology, 12, 247-278.

Hatton, P.-J., Kleber, M., Zeller, B., Moni, C., Plante, A.F., Townsend, K., Gelhaye, L., Derrien, K.L.D., 2012. Transfer of litter-derived N to soil mineral-organic associations: Evidence from decadal ^{15}N tracer experiments. Organic Geochemistry, 42, 1489-1501.

Hastie, T., Tibshirani, R., Friedman, J., 2009. The Elements of Statistical Learning. 2nd Ed. Springer.

Heinze, S., Oltmanns, M., Joergensen, R.G. and Raupp, J., 2011. Changes in microbial biomass indices after 10 years of farmyard manure and vegetal fertilizer application to a sandy soil under organic management. Plant and Soil, 343, 221-234.

Heinze, S., Vohland, M., Joergensen, R.G., Ludwig, B., 2013. Usefulness of near infrared spectroscopy for the prediction of chemical and biological soil properties in different long-term experiments. Journal of Plant Nutrition and Soil Sciences, 176, 520-528.

Hertel, D., Strecker, T., Müller-Haubold, H., Leuschner, C., 2013. Fine root biomass and dynamics in beech forests across a precipitation gradient – is optimal resource partitioning theory applicable to water-limited mature trees? Journal of Ecology, 101, 1183-1200.

Iqbal, A., Garnier, P., Lashermes, G., Recous, S., 2014. A new equation to simulate the contact between soil and maize residues of different sizes during their decomposition. Biology and Fertility of Soils, 50, 645-655.

Isermeyer, H., 1952. Eine einfache Methode zur Bestimmung der Bodenatmung und der Karbonate im Boden. Zeitschrift für Pflanzenernährung, Düngung, Bodenkunde, 56, 26-38.

IUSS Working Group WRB 2006. World Reference Base for Soil Resources 2006. World Soil Resources Reports No 103. FAO, Rome.

IUSS Working Group WRB, 2015. World reference base for soil resources 2014, update 2015. International soil classification system for naming soils and creating legends for soil maps. FAO, Rome World Soil Resources Reports No. 106.

Jacobs, A., Rauber, R., Ludwig, B., 2009. Impact of reduced tillage on carbon and nitrogen storage of two Haplic Luvisols after 40 years. Soil and Tillage Research, 102, 158-164.

Jacobs, A., Helfrich, M., Hanisch, S., Quendt, U., Rauber, R., Ludwig, B., 2010. Effect of conventional and minimum tillage on physical and biochemical stabilization of soil organic matter. Biology and Fertility of Soils, 46, 671-680.

Janzen, H.H., 2004. Carbon cycling in earth systems – a soil science perspective. Agriculture, Ecosystems & Environment, 104, 399-417.

Jia, S., Li, H., Wang, Y., Tong, R., Li, Q., 2016. Recursive variable selection to update nearinfrared spectroscopy model for the determination of soil nitrogen and organic carbon. Geoderma, 268, 92-99.

Jobbágy, E.G. and Jackson, R.B., 2000. The vertical distribution of soil organic carbon and its relation to climate and vegetation. Ecological Applications, 10, 423-436.

Joergensen, R.G. and Mueller, T., 1996. The fumigation- extraction method to estimate soil microbial biomass: calibration of the kEN value. Soil Biology & Biochemistry 28, 33-37

Joergensen, R.G., Raubuch, M., Brandt, M., 2002. Soil microbial properties down the profile of a black earth burie by colluvium. Journal of Plant Nutrition and Soil Science, 165, 274-280.

John, B., Yamashita, T., Ludwig, B., Flessa, H., 2005. Storage of organic carbon in aggregate and density fractions of silty soils under different types of land use. Geoderma 128, 63-79.

Kaiser, K., Eusterhues, K., Rumpel, C., Guggenberger, G., Kögel-Knabner, I., 2002. Stabilization of organic matter by soil minerals – investigations of density and particle-size fractions from two acid forest soils. Journal of Plant Nutrition and Soil Science 165, 451-459.

Kaiser, K. and Kalbitz, K., 2012. Cycling downwards - dissolved organic matter in soils. Soil Biology and Biochemistry, 52, 29-32.

Kaiser, M., Ellerbrock, R.H., Gerke, H.H., 2008. Cation exchange capacity and composition of soluble soil organic matter fractions. Soil Science Society of America Journal, 72, 1278-1285.

Kaiser, M., Ellerbrock, R.H., Wulf, M., Dultz, S., Hierath, C., Sommer, M., 2012. The influence of mineral characteristics on organic matter content, composition, and stability of topsoils under long-term arable and forest land use. Journal of Geophysical Research, 117, G02018.

Kaiser, M., Ghezzehei, T.A., Kleber, M., Myrold, D.D., Berhe, A.A., 2014. Influence of Calcium Carbonate and Charcoal Applications on Organic Matter Storage in Silt-Sized Aggregates Formed during a Microcosm Experiment. Soil Science Society of America Journal, 78, 1624-1631.

Kalbitz, K., Schwesig, D., Rethemeyer, J., Matzner, E., 2005. Stabilization of dissolved organic matter by sorption to the mineral soil. Soil Biology and Biochemistry, 37, 1319-1331.

Keiluweit, M., Bougoure, J.J., Nico, P.S., Pett-Ridge, J., Weber, P.K., Kleber, M., 2015. Mineral protection of soil carbon counteracted by root exudates. Nature Climate Change, 5, 588-595.

Kleber, M., Sollins, P., Sutton, R., 2007. A conceptual model of organo-mineral interactions in soils: Self-assembly of organic molecular fragments into zonal structures on mineral surfaces. Biogeochemistry, 85, 9-24.

Kleber, M., Eusterhues, K., Keiluweit, M., Mikutta, C., Mikutta, R., Nico, P.S., 2015. Mineral-organic associations: Formation, properties, and relevance in soil environments. Advances in Agronomy, 130, 1-140.

Kögel-Knabner, I., Guggenberger, G., Kleber, M., Kandeler, E., Kalbitz, K., Scheu, S., Eusterhues, K., Leinweber, P., 2008. Organo-mineral associations in temperate soils: integrating biology, mineralogy and organic matter chemistry. Journal of Plant Nutrition and Soil Science, 171, 61-82.

König, N. and Fortmann, H., 1996. Probenvorbereitungs-, Untersuchungs- und Elementbestimmungs-Methoden des Umweltanalytik-Labors der Niedersächsischen Forstlichen Versuchsanstalt und des Zentrallabors II des Forschungszentrums Waldökosysteme, Teil 4: Probenvorbereitungs- und Untersuchungsmethoden, Qualitätskontrolle und Datenverarbeitung; In: Berichte des Forschungszentrums Waldökosysteme der Universität Göttingen, Reihe B, Band 49, Göttingen.

Kuang, B., Mahmood, H.S., Quraishi, M.Z., Hoogmoed, W.B., Mouazen, A.M., van Hentent, E.J., 2012. Sensing soil properties in the laboratory, in situ, and on-line: a review. Advances in Agronomy, 114, 155-223.

Leardi, R., Seasholtz, M.B., Pell, R.J., 2002. Variable selection for multivariate calibration using a genetic algorithm: prediction of additive concentrations in polymer films from Fourier transform-infrared spectral data. Analytica Chimica Acta, 461, 189-200.

Lehmann, J., Kinyangi, J., Solomon, D., 2007. Organic matter stabilization in soil microaggregates: implications from spatial heterogeneity of organic carbon contents and carbon forms. Biogeochemistry, 85, 45-77.

Leuschner, C. and Hertel, D., 2003. Fine root biomass of temperate forests in relation to soil acidity and fertility, climate, age and species. Ecology, 64, 405-438.

Liao, J.D., Boutton, T.W., Jastrow, J.D., 2006. Organic matter turnover in soil physical fractions following woody plant invasion of grassland: Evidence from natural ^{13}C and ^{15}N. Soil Biology and Biochemistry, 38, 3197-3210.

Lichstein, H.C., 1960. Microbial nutrition. Annual Review of Microbiology, 14, 17-42.

Loecke, T.D. and Robertson, G.P., 2009. Soil resource in terms of litter aggregation promotes nitrous oxide fluxes and slows decomposition. Soil Biology & Biochemistry, 41, 228-235.

Ludwig, B., Linsler, D., Höper, H., Schmidt, H., Piepho, H.-P., Vohland, M., 2016. Pitfalls in the use of middle-infrared spectroscopy: representativeness and ranking criteria for the estimation of soil properties. Geoderma, 268, 165-175.

Madigan, M.T., Martinko, J.M., Stahl, D.A., Clark, D.P., 2012. Brock Biology of Microorganisms, 13th edn. Pearson Education, Inc./Benjamin Cummings, San Francisco, CA.

Magid, J., De Neergaard, A., Brandt,M., 2006. Heterogeneous distribution may substantially decrease initial decomposition, long-term microbial growth and N-immobilization from high C-to-N-ratio resources. European Journal of Soil Science, 57, 517-529.

Marx, M.C., Wood, M., Jarvis, S.C., 2001. A microplate fluorimetric assay for the study of enzyme diversity in soils. Soil Biology and Biochemistry, 33, 1633-1640.

Mathieu, J.A., Hatté, C., Balesdent, J., Parent, E., 2015. Deep soil carbon dynamics are driven more by soil type than by climate: a worldwide meta-analysis of radiocarbon profiles. Global Change Biology, 21, 4278-4292.

McCormack, M.L., Dickie, I.A., Eissenstat, D.M., Fahey, T.J., Fernandez, C.W., Guo, D., Helmisaari, H.S., Hobbie, E.A., Iversen, C.M., Jackson, R.B., Leppälammi-Kujansuu, J., Norbym R.J., Phillips, R.P., Pregitzer, K.S., Pritchard, S.G., Zadworny, M., 2015. Redefining fine roots improves understanding of below-ground contributions to terrestrial biosphere processes. New Phytologist, 207, 505-518.

Mehra, O.P. and Jackson, M.L., 1960. Iron oxide removal from soils and clays by a dithionite-citrate system buffered with sodium bicarbonate. Clays and Clay Minerals, 7th national conference on clays and clay minerals, Washington, D.C. 7 : 317-327.

Mikutta, R., Kleber, M., Jahn., R., 2005. Poorly crystalline minerals protect organic carbon in clay subfractions from acid horizons. Geoderma, 128, 106-115.

Mikutta, R., Kleber, M., Torn M.S., Jahn, R., 2006. Stabilization of Soil Organic Matter: Association with Minerals or Chemical Recalcitrance? Biogeochemistry, 77, 25-56.

Mikutta, R., Mikutta, C., Kalbitz, K., Scheel, T., Kaiser, K., and Jahn, R., 2007. Biodegradation of forest floor organic matter bound to minerals via different binding mechanisms. Geochemica et Cosmochimica Acta, 71, 2569-2590.

Mikutta, R. and Kaiser, K., 2011. Organic matter bound to mineral surfaces: Resistance to chemical and biological oxidation. Soil Biology and Biochemistry, 43, 1738-1741.

North, P.F., 1976. Towards an absolute measurement of soil structural stability using ultrasound. European Journal of Soil Science, 27, 451-459.

Paul, E.A., Collins, H.P., Leavitt, S.W., 2001. Dynamics of resistant soil carbon of midwestern agricultural soils measured by naturally occurring C-14 abundance. Geoderma, 104, 239-256.

Piepho, H.P., 2009. Data transformation in statistical analysis of field trials with changing treatment variance. Agronomy Journal, 101, 865-869.

Prieto, I., Stokes, A., Roumet, C., 2016. Root functional parameters predict fine root decomposability at the community level. Journal of Ecology, 104, 725-733.

Pronk, G.J., Heister, K., Ding, G.-C., Smalla, K., Kögel-Knabner, I., 2012. Development of biogeochemical interfaces in an artificial soil incubation experiment; aggregation and formation of organo-mineral associations. Geoderma, 189-190, 585-594.

R Core Team 2015. R: A Language and Environment for Statistical Computing., R Foundation for Statistical Computing, Vienna, Austria.
URL https://www.R-project.org/ [accessed on January 2017].

Rasmussen, C., Torn, M.S., Southard, R.J., 2005. Mineral assemblage and aggregates control carbon dynamics in a California conifer forest. Soil Science Society of America Journal 69, 1711-1721.

Rasse, D.P., Rumpel, C., Dignac, M.-F., 2005. Is soil carbon mostly root carbon? Mechanisms for a specific stabilization. Plant and Soil, 269, 341-356.

Rasse, D.P., Mulder, J., Moni, C., Chenu, C., 2006. Carbon Turnover Kinetics with Depth in a French Loamy Soil. Soil Science Society of America Journal, 70, 2097-2105.

Reeves III, J.B., McCarty, G.W., Meisinger, J.J., 2000. Near infrared reflectance spectroscopy for the determination of biological activity in agricultural soils. Journal of Near Infrared Spectroscopy, 8, 161-170.

Reeves III, J.B., 2010. Near- versus mid-infrared diffuse reflectance spectroscopy for soil analysis emphasizing carbon and laboratory versus on-site analysis: where are we and what needs to be done? Geoderma, 158, 3-14.

Rovira, P. and Vallejo, V.R., 2002. Mineralization of carbon and nitrogen from plant debris, as affected by debris size and depth of burial. Soil Biology and Biochemistry, 34, 327-339.

Rumpel, C., Kögel-Knabner, I., Bruhn, F., 2002. Vertical distribution, age, and chemical composition of organic carbon in two forest soils of different pedogenesis. Organic Geochemistry, 33, 1131-1142.

Rumpel, C., Eusterhues, K., Kögel-Knabner, I., 2004. Location and chemical composition of stabilized organic carbon in topsoil and subsoil horizons of two acid forest soils. Soil Biology and Biochemistry 36, 177-190.

Rumpel, C. and Kögel-Knabner, I., 2011. Deep soil organic matter – a key but poorly understood component of terrestrial C cycle. Plant and Soil, 338, 143-158.

Saeys, W., Mouazen, A.M., Ramon, H., 2005. Potential for onsite and online analysis of pig manure using visible and near infrared reflectance spectroscopy. Biosystems Engineering, 91, 393-402.

Saidy, A.R., Smernik, R.J., Baldock, J.A., Kaiser, K., Sanderman J., 2013. The sorption of organic carbon onto differing clay minerals in the presence and absence of hydrous iron oxide. Geoderma 209-210, 15-21.

Salomé, C., Nunan, N., Pouteau, V., Lerch, T.Z., Chenu, C., 2010. Carbon dynamics in topsoil and in subsoil may be controlled by different regulatory mechanisms. Globale Change Biology, 16, 416-426.

Sanaullah, M., Chabbi, A., Leifeld, J., Bardoux, G., Billou, D., Rumpel, C., 2011. Decomposition and stabilization of root litter in top- and subsoil horizons: what is the difference? Plant and Soil, 338, 127-141.

Santos, F., Nadelhoffer, K., Bird, J.A., 2016. Rapid fine root C and N mineralization in a nothern temperate forest soil. Biogeochemistry, 128, 187-200.

SAS Institute Inc. 2014. SAS/STAT® 13.2 User's Guide: High-Performance Procedures. SAS Institute Inc., Cary, NC, USA.

Schmidt, M.W.I., Torn, M.S., Abiven, S., Dittmar, T., Guggenberger, G., Janssens, I.A., Kleber, M., Kögel-Knabner, I., Lehmann, J., Manning, D.A.C., Nannipieri, P., Rasse, D.P., Weiner, S., Trumbore, S.E., 2011. Persistence of soil organic matter as an ecosystem property. Nature, 478, 49-56.

Schneider, M.P.W., Scheel, T., Mikutta R., van Hees, P., Kaiser, K., Kalbitz, K., 2010. Sorptive stabilization of organic matter by amorphous Al hydroxide. Geochimica et Cosmochimica Acta74, 1606-1619.

Schrumpf, M., Schulze, E.D., Kaiser, K., Schumacher, J., 2011. How accurately can soil organic carbon stocks and stock changes be quantified by soil inventories? Biogeosciences, 8, 1193-1212.

Schrumpf, M., Kaiser, K., Guggenberger, G., Persson, T., Kögel-Knabner, I., Schulze, E.-D., 2013. Storage and stability of organic carbon in soils as related to depth, occlusion within aggregates, and attachment to minerals. Biogeosciences, 10, 1675-1691.

Schrumpf, M. and Kaiser, K., 2015. Large differences in estimates of soil organic carbon turnover in density fractions by using single and repeated radiocarbon inventories. Geoderma, 239, 168-178.

Shepherd, K.D., Walsh, M.G., 2002. Development of reflectance spectral libraries for characterization of soil properties. Soil Science Society of America Journal, soil., 66, 988-998.

Shi, T.Z., Chen, Y.Y., Liu, H.Z., Wang, J.J., Wu, G.F., 2014. Soil organic carbon content estimation with laboratory-based visible-near-infrared reflectance spectroscopy: feature selection. Applied Spectroscopy, 68, 831-837.

Silver, W.L. and Miya, R.K., 2001. Global patterns in root decomposition: comparisons of climate and litter quality effects. Oecologia, 129, 407-419.

Six, J., Feller, C., Denef, K., Ogle, S., Carlos de Moraes Sa, J., Albrecht, A., 2002. Soil organic matter, biota and aggregation in temperate and tropical soils - Effects of no-tillage. Agronomie, 22, 755-775.

Skjemstad, J.O., Janik, L.J., Head, M.J., and McClure, S.G., 1993. High energy ultraviolet Photo-oxidation: a novel technique for studying physically protected organic matter in clay and silt-sized aggregates. Journal of Soil Science, 44, 485-499.

Smith, S., House, J.I., Bustamante, M., Sobocká, J., Harper, R., Pan, G., 2016. Global change pressures on soils from land use and management. Global Change Biology, 22, 1008-1028.

Sollins, P., Swantson, C., Kleber, M., Filleyd, T., Kramere, M., Crowa, S., Caldwella, B.A., Lajtha, K., Bowden, R., 2006. Organic C and N stabilization in a forest soil: Evidence from sequential density fractionation. Soil Biology and Biochemistry, 38, 3313-3324.

Sollins, P., Kramer, M.G., Swantson, C., Lajtha, K., Filley, T., Aufdenkampe, A.K., Wagai, R., Bowden, R.D., 2009. Sequential density fractionation across soils of contrasting mineralogy: evidence for both microbial- and mineral-controlled soil organic matter stabilization. Biogeochemistry, 96, 209-231.

Solly, E.F., Schöning, I., Boch, S., Kandeler, E., Marhan, S., Michalzik, B., Müller, J., Zscheischler, J., Trumbore, S.E., Schrumpf, M., 2014. Factors controlling decomposition rates of fine root litter in temperate forests and grasslands. Plant and Soil, 382, 203-218.

Soriano-Disla, J.M., Janik, L.J., Viscarra Rossel, R.A., Macdonald, L.M., McLaughlin, M.J., 2014. The performance of visible near- and mid-infrared reflectance spectroscopy for prediction of soil physical, chemical and biological properties. Applied Spectroscopy Reviews, 49, 139-186.

Stenberg, B., 2010. Effects of soil sample pretreatments and standardised rewetting as interacted with sand classes on Vis-NIR predictions of clay and soil organic carbon. Geoderma, 158, 15-22.

Stenberg, B., Rossel, R.A.V., Mouazen, A.M., Wetterlind, J., 2010. Visible and near infrared spectroscopy in soil science. Advances in Agronomy, 107, 163-215.

Stevens, A., Nocita,M., Tóth, G., Montanarella, L., van Wesemael, B., 2013. Prediction of soil organic carbon at the European scale by visible and near infrared reflectance spectroscopy. PLOS One 8, 1-13.

Tisdall, J.M., and Oades, J.M., 1982. Organic matter and water-stable aggregates in soils. Journal of Soil Science, 33, 141-163.

Toenshoff, C., Joergensen, R.G., Stuelpnagel, R., Wachendorf, C., 2014. Initial decomposition of post-harvest crown and root residues of poplars as affected by N availability and particle size. Biology and Fertility of Soils, 50, 675-683.

Torn, M.S., Kleber, M., Zavaleta, E.S., Zhu, B., Field, C.B., Trumbore, S.E., 2013. A dual isotope approach to isolate soil carbon pools of different turnover times. Biogeosciences, 10, 8067-8081.

Vancampenhout, K., De Vos, B., Wouters, K., Swennen, R., Buurman, P., and Deckers, J., 2012. Organic matter of subsoil horizons under broadleaved forest: Highly processed or labile and plant-derived? Soil Biology and Biochemistry, 50, 40-46.

Vance, E.D., Brookes, P.C., Jenkinson D.S., 1987. An extraction method for measuring soil microbial biomass C. Soil Biology and Biochemistry 19, 703-707

Vestergaard, P., Rønn, R., Christensen, S., 2001. Reduced particle size of plant material does not stimulate decomposition, but affects the microbivorous microfauna. Soil Biology and Biochemistry, 33, 1805-1810.

Viscarra Rossel, R.A., Behrens, T., 2010. Using data mining to model and interpret soil diffuse reflectance spectra. Geoderma, 158, 46-54.

Vohland, M. and Emmerling, C., 2011. Determination of total soil organic C and hot water extractable C from VIS-NIR soil reflectance with partial least squares regression and spectral feature selection techniques. European Journal of Soil Science, 62, 598-606.

von Lützow, M., Kögel-Knabner, I., Ekschmitt, K., Matzner, E., Guggenberger, G., Marschner, B., Flessa, H., 2006. Stabilization of organic matter in temperate soils: mechanisms and their relevance under different soil conditions – a review. European Journal of Soil Science, 57, 426-445.

von Lützow, M., Kögel-Knabner, I., Ludwig, B., Matzner, E., Flessa, H., Ekschmitt, K., Guggenberger, G., Marschner, B., Kalbitz, K., 2008. Stabilization mechanisms of organic matter in four temperate soils: Development and application of a conceptual model. Journal of Plant Nutrition and Soil Science, 171, 111-124.

Wagai, R., Mayer, L.M., and Kitayama, K., 2009. Nature of the "occluded" low-density fraction in soil organic matter studies: A critical review. Soil Science & Plant Nutrition, 55, 13-25.

Weber, K.A., Achenbach, L.A., Coates, J.D., 2006. Microorganisms pumping iron: anaerobis microbial iron oxidation and reduction. Nature Reviews Microbiology, 4, 752-764.

Wehrens, R., 2011. Chemometrics with R. Springer, Heidelberg, Germany.

Wetterlind, J., Stenberg, B., 2010. Near-infrared spectroscopy for within-field soil characterization: small local calibrations compared with national libraries spiked with local samples. European Journal of Soil Science, 61, 823-843.

Williams, R.J.P., 1970. The biochemistry of sodium, potassium, magnesium, and calcium. Quarterly Reviews, Chemical Society, 24, 331-365.

Wiseman, C.L.S. and Püttmann, W., 2006. Interactions between mineral phases in the preservation of soil organic matter. Geoderma, 134, 109-118.

Wolf, A.M. and Beegle, D.B., 1995. Recommended soil tests for macronutrients: phosphorus, potassium, calcium and magnesium. In: Recommended Soil Testing Procedures for the Northeastern United States (eds J.T. Sims & A. Wolf), Northeast Regional Bulletin No 493, Agricultural Experiment Station, pp. 25-43. University of Delaware, Newark, NY.

Wordell-Dietrich, P., Don, A., Helfrich, M., 2016. Controlling factors for the stability of subsoil carbon in a Dystric Cambisol. Geoderma, http://dx.doi.org/10.1016/j.geoderma.2016.08.023

WorldClim Global Climate Data. Free Climate Data for Ecological Modelling and GIS. http://www.worldclim.org/download [accessed on 04 February 2016].

Wu, J., Joergensen, R.G., Pommerening, B., Chaussod, R., Brookes, P.C., 1990. Measurement of soil microbial biomass C by fumigation-extraction - an automated procedure. Soil Biology and Biochemistry 22, 1167-1169

Zhao, Q., Poulson, S.R., Obrist, D., Sumaila, S., Dynes, J.J., McBeth, J.M., Yang, Y., 2016. Iron-bound organic carbon in forest soils: quantification and characterization. Biogeosciences, 13, 4777-4788.

Zornoza, R., Guerrero, C., Mataix-Solera, J., Scow, K.M., Arcenegui, V., Mataix-Beneyto, J., 2008. Near infrared spectroscopy for determination of various physical, chemical and biochemical properties in Mediterranean soils. Soil Biology and Biochemistry, 40, 1923-1930.

Eidesstattliche Erklärung

Hiermit versichere ich, dass ich die vorliegende Dissertation selbstständig und ohne unerlaubte Hilfe angefertigt und andere als die in der Dissertation angegebenen Hilfsmittel nicht benutzt habe. Alle Stellen, die wörtlich oder sinngemäß aus veröffentlichten oder unveröffentlichten Schriften entnommen sind, habe ich als solche kenntlich gemacht. Kein Teil dieser Arbeit ist in einem anderen Promotions- oder Habilitationsverfahren verwendet worden.

Witzenhausen, Mai 2017

_____

(Svendja Vormstein)